Average wave overtopping discharges for complex geometry

A case study for the prediction of average wave overtopping discharges with stepped revetment in the cross-section

B. Scheurwater

May 2022

TU Delft Delft University of Technology

Witteveen+Bos

Casino Middelkerke

A case study for the prediction of average wave overtopping discharges with stepped revetment in the cross-section

by

B. Scheurwater

In partial fulfillment of the degree of Master of Science
at the Delft University of Technology.

Student number:	4279654	
Thesis committee:	Prof. dr. ir. S. G. J. Aarninkhof	TU Delft
	Ing. C. Kuiper	TU Delft
	Dr. ir. B. Hofland	TU Delft
	Ir. B. van den Berg	Witteveen+Bos, daily supervisor

TU Delft

Witteveen + Bos

Abstract

Witteveen+Bos as part of construction consortium Nautilus, has prepared the design of a sea defence system in Middelkerke. The very shallow water conditions (h/H_{m0} = 0.3) and complex geometry of the structure, i.e. a high berm and stepped revetment, caused uncertainties in the usage of the empirical equations from the EurOtop Manual (2018) for wave overtopping discharges. Therefore, small-scale experiments have been performed to asses the overtopping discharges.
Physical model experiments can be used to determine wave overtopping discharges, but can be expensive and time consuming. Recent studies show promising results for the use of SWASH as tool to predict overtopping discharges for relative simple geometries, but SWASH is suspected to be less accurate for more complex cross-sections. Two methods (SWASH, EurOtop) are used to predict wave overtopping discharges for the new boulevard Middelkerke and the results are compared with measurements from small-scale experiments conducted in Ghent. The goal is to asses the feasibility of using both methods for this complex structure with stepped revetment in shallow water conditions.

The EurOtop Manual (2018) uses influence factors to account for roughness at the slope and the presence of a berm in the structure. To use the empirical formula to determine the average overtopping discharge for this specific complex cross-section, a berm influence factor was added to the equation for shallow water conditions developed by Altomare et al. (2016). Recent studies of Schoonees et al. (2021) found that the influence of the roughness of a stepped revetment on overtopping discharge mainly depends on: a characteristic step height, relative overtopping discharge and the wave period at the toe of the structure. Using their research as guideline, a roughness influence factor of γ_f = 0.75-0.9 was estimated for the stepped revetment for this case study. Although not validated for this specific configuration, using the (adjusted) equation resulted in very comparable average overtopping discharges compared to the physical experiments in Ghent.

In this case study, the usability of SWASH to predict the average wave overtopping discharges has been evaluated. First, the SWASH model was calibrated based on the incident wave conditions at the toe of the structure (H_{m0}, $T_{m-1,0}$) with the data the physical experiment in Ghent. This were the target wave conditions of this study since they are generally used to determine the average wave overtopping discharges (e.g. EurOtop) and to exclude the wave-structure interactions. Thereafter, the structure was added to the bathymetry with a smooth slope and local friction was added to represent the stepped revetment, as resolving the small steps would require an overly fine grid.
SWASH was able to reproduce the target incident wave conditions of the physical experiment very well (H_{m0}<3%,$T_{m-1,0}$<5%). However, when the structure was added to the bathymetry, larger differences were seen for the wave conditions at the toe compared to the physical experiment, for which no explicit explanation was found. Contrarily, H_{m0} and $T_{m-1,0}$ include the full wave field, primary waves and infragravity waves, and the limited number of overtopping waves made it difficult to asses the influence of the difference in wave spectrum on the overtopping discharges.
The overtopping reduction due the added roughness/friction compared to a smooth slope reference test, was eventually related to a Nikuradse roughness height for the stepped revetment. A Nikuradse roughness of 1-1.5 times the characteristic step height of the stepped revetment, resulted in very similar average overtopping discharges compared to measurements from the Ghent experiment.

Both the EurOtop Manual (2018) and SWASH were able to reproduce the average wave overtopping discharges from physical experiments, but the results need a wide confidence band since the number of overtopping waves were limited and discharges small (q < 1 l/s/m). Each method has their own benefits and limitations. The EurOtop Manual (2018) is easy to use, but the validity of the empirical equations are uncertain for more complex geometries. SWASH gives more detailed information than only an average q: spatially and temporarily varying surface elevations and velocities along the domain, by which direct attack on the slope and structures (extreme values of u and F) can be calculated. SWASH could also be used as a 'numerical laboratory' to further parameterize the influence of roughness on wave overtopping for a wide range of boundary conditions and structural configurations.

Acknowledgements

This report is the final episode of my Master Hydraulic Engineering at the University of Technology in Delft. It became quite a journey, first starting with a different thesis subject, during a global COVID outbreak in 2020 and eventually becoming sick for a long time. Now almost 2 years later, I can proudly say that I will graduate! This could not have been possible with the help of my committee members and family/friends.

I would like to thank my committee members, who helped me a lot in the process of finishing this thesis. First, I would like to thank Stefan Aarninkhof, who helped me to get back on track to finish my master's at the TU Delft. I will always remember our first phone call, where I did not know how to fix the situation, but you were so understanding and immediately started thinking of practical solutions. This really meant a lot to me.
Next, I would really like to thank Bert van den Berg and Coen Kuiper. During my thesis, Witteveen+Bos has always offered me great guidance and facilities at the office. The first phone call for a possible graduation project at Witteveen+Bos was in April 2020 and now almost 2 years later, I am writing these thank notes as final conclusion of my thesis. Both of you really helped me to finish what we started and it is fair to say that without your help, this would have taken much longer. Coen, I will never forget your enthusiasm. I have always experienced the meetings that we had as very enjoyable. Often I came to you with a lot of questions and you were always very patient and capable of helping to get my thoughts straight again. The same holds for you Bert, looking back to the meetings and conversations we had, you were always capable to nuance my sometimes chaotic approaches/questions. Looking at the practical side of my findings and results is something that I will definitely keep in mind. Lastly, I would like to thank Bas Hofland, who during my masters, I have always admired and hopefully I will find a job which I can do with such passion as you do yours.

I also want to give a shout out to Luuk and Melanie, working at Witteveen+Bos, who helped me to get acquainted with SWASH and were always very interested in the progress that I made.

Finally, I would like to finish my thankings with a big hug to my family and friends, without your support the past 2 years would be a lot harder.

This report concludes my time at the Delft University of Technology, I am ready for new adventures. I hope you enjoy reading this report!

Bart Scheurwater Delft, May 2022

Contents

Nomenclature

α	Slope angle	$^\circ$
γ_b	Berm reduction factor	–
γ_f	Friction reduction factor	–
γ_β	Oblique incident wave reduction factor	–
γ_n	Reduction factor crest wall	–
ν	Viscosity	$\mathrm{m^2\,s^{-1}}$
ρ_w	Water density	kg/m^3
ξ	Breaker parameter	–
Z	Surface elevation	m
B	Berm width	m
d	Water depth below plane of reference	m
Fr	Froude number	–
g	Gravity constant	$\mathrm{m\,s^{-2}}$
h	Water depth	m
h_b	Water depth at berm	m
H_i	Incoming wave height	m
H_r	Reflected wave height	m
H_s	significant wave height	m
h_t	Water depth at toe	m
$H_{2\%}$	Exceedance wave height by the two percent highest waves	m
H_{m0}	Spectral significant wave height	m
k	Wave number	–
K_r	Reflection coefficient	–
L	Length	m
L_0	Deep water wave length	m
L_{berm}	Berm length	m
q	Average overtopping discharge	$\mathrm{L\,s^{-1}\,m^{-1}}$
r_b	influence of berm width	–
R_c	Crest freeboard	m
r_{db}	Vertical difference between still water line and middle of berm	–
$R_{u2\%}$	Two percent run up height	m

Re	Reynolds number	kg/m^3
s	Wave steepness	–
S_h	Step height	m
$s_{m-1,0}$	Local wave steepness	–
T_p	Wave peak period	s
$T_{m-1,0}$	Spectral wave period	s
u	Velocity	m s^{-1}
SWL	Still water level	m

1 Introduction

1.1. Background

Wave overtopping is one of the key parameters for designing coastal structures: the crest level is usually determined using admissible overtopping discharges (Altomare et al., 2016). Empirical methods, e.g. EurOtop Manual (2018), are used to asses the overtopping discharges, mostly averaged over time. Several formulae already exist for the prediction of average wave overtopping discharges per meter width of the coastal defense, which are generally applicable for deep or intermediate water depths at the toe of the dike. However, for more complex the geometry of structures, the validity of the empirical formulas in EurOtop manual (2018) is questionable.

Witteveen+Bos as part of construction consortium Nautilus, has prepared the design of the coastal protection around the new casino in Middelkerke, which is planned to be part of the sea defence system. The coastal protection is designed with curved lines, includes various non-standard overtopping reducing measures, e.g. stilling wave basin, stepped revetments and crest walls. The geometry of the coastal protection with complex elements is therefore outside the range of validity of the EurOtop Manual formulas. Furthermore, the shallow water provides challenging hydraulic conditions. Small scale physical mode tests have been performed at the wave flume in Ghent to determine the amount of average overtopping at the crest of the design. This thesis describes how SWASH can be used as design tool to design the crest level of a sea defence structure with regard to wave overtopping for stepped revetments. The obstacles of using the EurOtop Manual (2018) for a complex geometry are analysed, including recent insights in stepped revetments. The results of both methods will be compared with the measurements from small-scale physical model tests in Ghent.

Figure 1.1: Aerial photograph of newly designed casino complex at Middelkerke a project from Witteveen+Bos

1.2. Problem statement

Average overtopping discharges are generally accepted as reliable quantities to be used for the wave overtopping assessment (Altomare et al., 2016). Individual volume of overtopping waves is also suspected to be important, since averaged overtopping discharge consist either out of a couple of waves with large overtopping volumes or a large number of waves with relatively smaller volumes (Schoonees et al., 2021). This study focuses on average overtopping discharges at the crest of the structure, as no individual overtopping volumes were measured during the physical experiment.
Not only the geometry of the coastal sea defence structure itself influences the amount of wave overtopping, but the bathymetry of the foreshore and therewith changing wave properties are also crucial (Veale, 2012). The presence of the foreshore influences the wave processes that occur from offshore to the shoreline such as wave propagation, frequency dispersion, shoaling, breaking and wave overtopping. The most intensive study on wave run-up and wave overtopping with shallow foreshores has been conducted by Van Gent (van Gent, 1999).

For complex geometrical structures, empirical design methods are in many cases outside the range of validity and the geometry usually needs to be simplified. The designed sea structure at Middelkerke consists of two complex elements in the structure: a berm and a staircase, henceforth stepped revetment. The EurOtop Manual (2018) uses influence factors to include the effect of roughness (steps) on the slope and a berm in relation to overtopping volumes at the crest of the structure. Physical model experiments help to reduce the inaccuracies but have their own limitations with regard to flexibility, time and costs. Numerical modelling might be used as an alternative for non-standard geometries (Suzuki et al., 2011).
SWASH is such a numerical model which is under constant development at Delft University of Technology (Zijlema et al., 2011). The usage of a hydrodynamic model for the estimation of wave overtopping is a complex and advanced approach. There are limits to the accuracy of numerical models for a complex topographic cross-section, since the results depend on many input parameters (bathymetry, mesh size, wave spectrum etc.) and numerical limits (computational time, vertical discretization, numerical stability etc.).
Suzuki et al. (2011) concluded that SWASH reproduces wave transformation and wave overtopping very well, even in shallow water conditions. However, large differences were seen with rapidly changing topographic features (e.g. structure of a dike) and for small overtopping volumes. Gruwez et al. (2020b) investigated the performance of several commonly used numerical models in estimating the wave overtopping and action of smooth uniform sloped coastal structures. This research concluded that OpenFOAM performed best but that SWASH performed reasonable well, considering the required calculation time for these type of structures. It was suggested to investigate whether SWASH provides the same promising results for a cross-section with more complex geometries.

1.3. Research Objective

There are different design methods to design a sea defense structure and different versions of empirical formulae appear. The height of the represented safety level and probability of failure becomes unclear for a stepped revetment in sea defence structures. Besides, the process of wave overtopping on sea dikes with shallow and very shallow foreshore is not yet fully understood. The combination of a stepped revetment in sea defences in shallow water conditions causes difficulties in practical engineering.
In this thesis, SWASH will be used as a design tool to predict average wave overtopping discharges for a geometry including a stepped revetment. The steps of the stepped revetment create slope roughness, resulting in overtopping reduction at the crest of the structure. The EurOtop Manual (2018) uses influence factors in the design formulae to account for roughness at the slope of the structure. This same principle will be used in SWASH: local friction is added on the slope of the structure to represent the stepped revetment in the cross-section. The extra roughness on the slope will lead to smaller overtopping discharges at the crest of the sea defence structure and will be related to a Nikuradse roughness height for the stepped revetment.

Research question:

How to use SWASH and the EurOtop to reproduce average wave overtopping discharges measured in small scale physical model tests, for the new boulevard Middelkerke with a stepped revetment in shallow water conditions?

Sub-questions:

- What are the difficulties of using the EurOtop Manual and recent studies with respect to stepped revetments for the case study Middelkerke?
- Is SWASH capable of reproducing the wave conditions at the toe of the structure for cross-section of the new boulevard in Middelkerke?
- How can SWASH be used to assess the roughness of a stepped revetment?
- To what extend is SWASH capable of predicting average wave overtopping discharges for a complex geometry with stepped revetment?

To answer these research questions a case study is conducted on the Belgium coastline, the development of a new sea defence complex at Middelkerke.

1.4. Research scope

The full design of the new coastal protection structure in Middelkerke consists of several cross-sections. The focus of this research is limited to the assessment of the (average) wave overtopping discharges of a cross-section with a stepped revetment. The stability of the structure itself is therefore out of scope. The simulations are performed with SWASH version 7.01A.

1.5. Outline of the report

In Chapter 2 an overview is given for the case study of the sea defence design at Middelkerke from Construction Team Nautilus. The relevant literature is discussed, giving an overview of important hydraulic- and design parameters of the sea defence structure related to wave overtopping discharge. A comparison between different numerical models is made and the reason for the use of SWASH for this case study is elaborated. Based on recent studies of Schoonees et al. (2021) a roughness influence factor is estimated for the stepped revetment in the structure of this case study. The setup of the physical experiment used as reference test and the numerical setup is presented in Chapter 3. For the physical experiment this includes the layout of the flume, scaling parameters, and the results of wave conditions and overtopping discharges. For the SWASH model, the most important parameters and aspects that caused difficulties in the calibration of the model are discussed. Chapter 4, describes the calibration of the model and the analysis of the wave conditions in SWASH. The wave conditions measured in both deep water and at the toe of the structure are compared to the measurement from the experiments in Ghent. Thereafter, in Chapter 5, the average wave overtopping discharges are calculated using the empirical formulas from the EurOtop Manual (2018) and using the measurements in SWASH simulations. A study is performed to determine the roughness of a stepped revetment in the structure with SWASH and relate this to a friction factor / roughness height. An overview is given of the measured/calculated overtopping discharges for both methods, and the results are compared to the overtopping discharges from the physical experiments in Ghent. Chapter 6, discusses the differences and uncertainties in using these methods as a design tool to predict overtopping discharges. The final conclusions with regard to the research objective and research questions is presented in Chapter 7. The last Chapter, 8, describes suggestions for future research to predict the average wave overtopping discharge using the EurOtop and SWASH more accurately.

In this thesis, “overtopping reduction” describes the reduction in wave overtopping rate between a stepped revetment and a smooth slope with the same boundary conditions.

2
Theoretical background

This chapter provides the theoretical background needed to answer the research questions. Section 2.1 gives a brief overview for the case study of a new sea defence design at Middelkerke from Construction Team Nautilus (CIRIL NV), where Witteveen+Bos is part of. Section 2.2 gives an overview of the boundary conditions and discusses the hydraulic loading of the waves and the design parameters of the sea defence structure, related to wave overtopping discharge. Section 2.3 discusses three different design methods used in this thesis to determine wave overtopping for sea defence structures: a physical experiment, the EurOtop and SWASH. In Section 2.3.4, a comparison is made between different numerical models and the reasoning of using SWASH for this case study is highlighted.

2.1. Case study casino Middelkerke

2.1.1. Location

The municipality of Middelkerke in West Flanders wants to redevelop the location of the old casino, including a new casino, an event hall, a restaurant, an underground parking lot and a new hotel. Witteveen+Bos is collaborating with this new design on behalf of CIRIL NV. Part of the plan is the construction of a seawall seaward from the casino building. Figure 2.1 shows that the full plan has a smooth arched cross-coastal coastline, meaning no cross-section is exactly the same. The total sea defence structure has therefore been divided into 10 design cross-sections to represent the full design defence structure. 'Cross-section 2b' will be use as case study in this thesis, since for this cross-section physical model tests were performed to verify the design, see Figure 2.3.

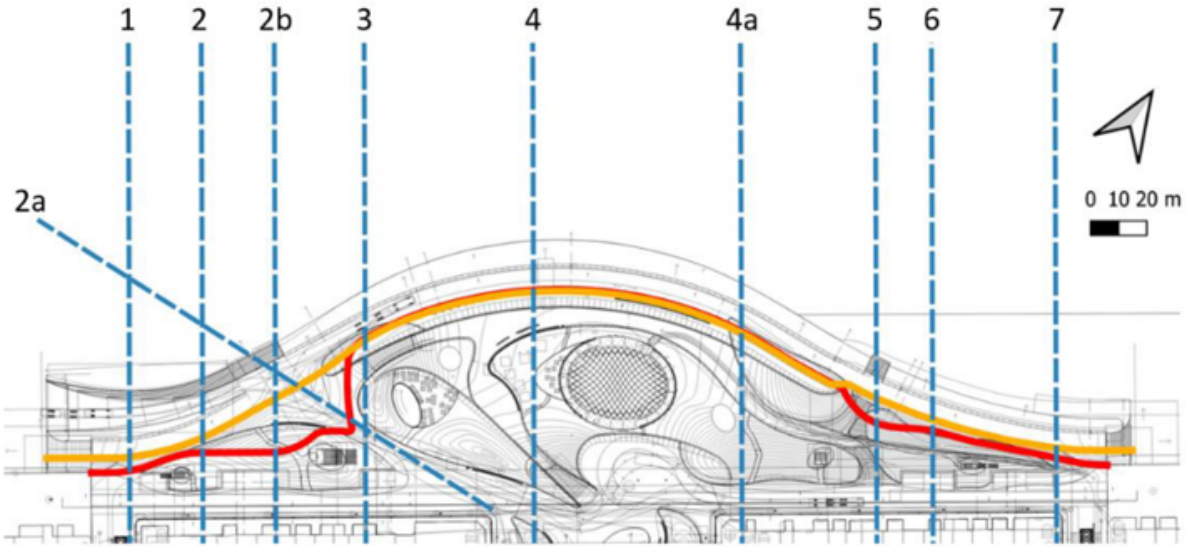

Figure 2.1: The red line shows the location of the safety line along the sea wall. The safety line coincides with the storm wall for most of the route (section 1-4, 7). At the 'gully' along the building (section 2a) and the northern beach entrance (section 5), where no transfer element and storm wall are present, the safety line is located at the highest point of the profile

2.1.2. Bathymetry

The schematization of cross-section 2b is a combination of the cross-coastal profile after the storm calculated with XBeach and the designed dike profile. The position of the toe of the structure is the point where the slope becomes steeper than 1/10, see Figure 2.2. The slope is 1:35 from the -5 m TAW depth line up to -15 m TAW. From -15 TAW, the profile is horizontally extended 100 m, to prevent numerical errors, see Section 3.2.4. The bathymetry of the foreshore seaward of the sea defence structure is characterized as wide and shallow, which is the case for most Northern European Countries. This combination of a gentle foreshore and (very) shallow water may lead to heavy wave breaking and rapid changing wave spectra for waves travelling towards the toe of the structure (Altomare et al., 2016).

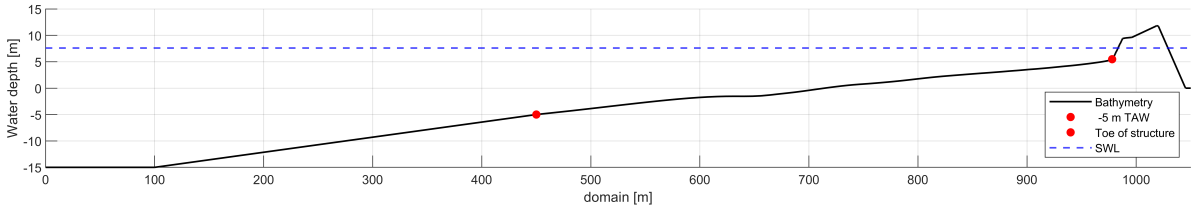

Figure 2.2: Schematization cross-section 2b in Middelkerke.

2.1.3. Cross-section

Cross-section 2b consists of a stepped revetment and a varying upper slope. Both the stepped revetment and the upper slope of the structure are made of prefab concrete. The top of the dike has a small dune path with vegetation, but this change in roughness is considered to be small and is therefore not considered in the design limits. The design scenario has the sea water level at + 7.42 TAW, see Figure 2.3. The wave overtopping will be predicted at the height of the safety line, which is at the highest point of the dike profile. The sea defence structure has a total length of +/- 90 meters and the crest height is located at + 11 TAW. In Figure 2.1 and Figure 2.3 the safety line of the design is displayed by a red line, this is where the average overtopping volume needs to be smaller than 1 l/s/m to met the design criteria.

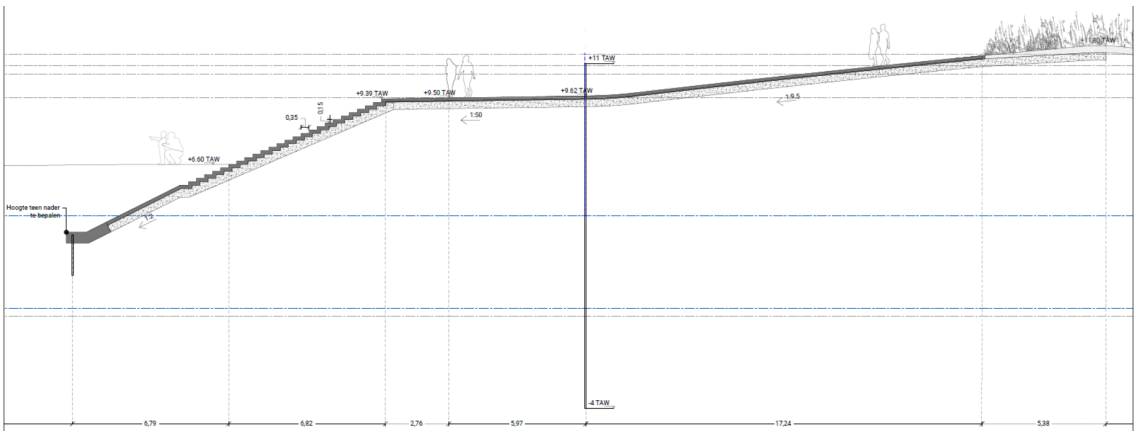

Figure 2.3: Design cross-section 2b, Witteveen+Bos. This cross-section is tested in the laboratory at Ghent University.

2.2. Boundary conditions and design methods

Functional requirements

A full SWASH-2D calculation is performed by Witteveen+Bos in which the geometry varied in the longitudinal direction of the coast. The SWASH-2D calculations resulted in the target wave conditions used for the physical experiments in Ghent: the significant wave height (H_{m0}), the spectral wave period ($T_{m-1,0}$) and the water level (h) at the toe of the dike. The physical scale model tests in the fluid laboratory of the Ghent University were used to verify the designed cross-section against the design conditions. The sea defense structure of the casino building in Middelkerke must withstand wave conditions that occur with a return time of 1,000 years in 2070. To met the design criteria, the average overtopping volume for the chosen dimensions of the structure must smaller than 1 l/s/m.

	2020	**2070**
H_{m0} [m]	4.82	4.99
T_p [s]	11.2	11.2
SWL [m+TAW]	7.00	7.42

Table 2.1: Hydraulic boundary conditions at -5 m TAW design cross section 2b (Figure 2.2), for reference year 2020 and 2070.

2.2.1. Hydraulic loading

Wave properties will change for waves travelling from deep water towards the toe of the structure. The change of these wave properties are important factors for the wave overtopping discharges over the structure (The EurOtop Manual, 2018).

Offshore wave conditions

Deep water is classified with $h/H_{m0,deep} > 4$, meaning a water depth of 4 times the deep water wave height. In deep water, waves follow a Rayleigh distribution, which results in a constant $H_{2\%}/H_s$ ratio of approximately 1.4. However, this is valid for fully developed sea states, but may will be different for scale model experiments, as will be elaborated in Section 4.1.4. For the scale experiments in Ghent, preliminary numerical simulations were used to identify the offshore boundary wave conditions (at the wave paddle location) that lead to the target wave conditions at the toe of the dike. In this report, the wave paddle or wave generation boundary is considered as the 'offshore boundary'.

Definition shallow foreshore

In coastal research different definitions are used for a shallow foreshore. Depth-induced wave processes, such as depth-induced wave breaking are characterizing this part of the bathymetry until the toe of the structure. In the EurOtop manual (2018), the foreshore is defined as the section in front of the dike/structure and it "can be horizontal or up to a maximum slope of 1:10 [...] having a minimum length of one wavelength" . The validity of most design formulae for the calculation for e.g. wave overtopping or wave impact forces depend on the type of wave motion (Hofland et al., 2017). A classification of foreshore depths has been made, based on the water depth at the toe of the structure, see Figure 2.4. With an offshore wave height $H_{m0,o}$ = 4.99 and a water depth at the toe of structure h = 2.1, the conditions for the case study in Middelkerke are very shallow according to Hofland et al. (2017).

Classification	**Limits**
Deep water	$\frac{h}{H_{m0,deep}} > 4$
Shallow water	$1 < \frac{h}{H_{m0,deep}} < 4$
Very shallow water	$0.3 < \frac{h}{H_{m0,deep}} < 1$
Extremely shallow water	$\frac{h}{H_{m0,deep}} < 0.3$

Figure 2.4: Consistent classification of foreshore depths, based on the water depth at toe of structure h_0, normalized by the offshore wave height $H_{m0,0}$ (Hofland et al., 2017)

Water levels
The water level at the structure is an extremely important parameter to predict the wave overtopping over a structure (The EurOtop Manual, 2018). For the design waver level at the structure, four water levels are important: mean still water level, surge, sea level rise and wave set-up. Storm surge is a rise of the water level due to a storm offshore that is added to the predicted astronomical tide. Waves start to break travelling shorewards, causing an increased water level, this is called wave set-up. For the case study a 1000 year storm event added with the predicted sea level rise (year 2070), resulted in the design water level used for the physical experiments and for the calculations with the EurOtop and SWASH simulations.

Shoaling
The wave frequency remains the same for waves travelling from deep water to shallow(er) water. The wave length is related to its frequency by means of a dispersion relation. Therefore, the phase- or group velocity of a wave field can be calculated as a function of the frequency. Hence, the wave length and wave velocity decrease when the water depth decreases. A decrease of the group velocity, increases the wave amplitudes. With an increasing wave amplitude and a decrease of the wave length, waves will become steeper as they travel towards the shore. Triad wave-wave interactions enhance wave shoaling, which results in larger peaks and flatter troughs. The wave spectrum looks similar as the deep water wave spectrum, but now higher and lower frequencies appear because of second order effects (Bosboom and Stive, 2021).

Wave breaking
In deeper water, waves can break if the wave height becomes too large compared to their wave length, this process is called white-capping. As waves travel towards shallow(er) water, depth-induced wave breaking becomes more and more important. The breaking parameter or surf similarity parameter Eq. 2.1, specifies different type of wave breaking that can occur. Four types of wave breaking are distinguished, namely: surging, collapsing, plunging and spilling (Battjes, 1974).

$$\xi = \frac{\tan(\alpha)}{\sqrt{H_0/L_0}} = \frac{1}{2\pi}\frac{\tan(\alpha)}{\sqrt{H_0/gT^2}} \tag{2.1}$$

Wave reflection
Waves can be reflected to deep water when interacting with the sea defence structure. Also a sudden change in depth or the foreshore it self, can induce wave reflection. The wave motion in front of a reflecting structure is mainly determined by the reflection coefficient K_r, where H_r is the reflected wave height and H_i is the incident wave height (van den Bos and Verhagen, 2018).

$$K_r = \frac{H_r}{H_i} \tag{2.2}$$

Zelt and Skjelbreia (1993) developed method based on linear wave theory to decompose one-dimensional wave fields into the incoming and the reflected waves using an arbitrary number of wave gauges. This method will later be used to compare the numerical model results with the physical experiments in Ghent.

Wave height

Three types of wave heights will be discussed in the research: the significant wave height (H_s), which is calculated based on a spectral analysis and is therefore called H_{m0}. The wave height that is exceeded by the highest two percent of the waves in a wave field, ($H_{2\%}$). The highest measured wave height in the domain is labelled H_{max}. These wave heights will be used to analyse the wave conditions in both SWASH and the physical experiments in Ghent.

Wave period

The peak period, corresponds with the peak frequency in the energy density spectrum at a location. The spectral wave period, can be calculated with the energy density spectrum. The spectral wave period $T_{m-1,0}$ gives more emphasis to the longer waves in the wave field and is is often used in design formulas for sea defence structures. In shallow(er) water the wave energy is redistributed from the peak frequency to lower and higher frequencies. In deep water conditions, the ratio $T_p/T_{m-1,0}$ is approximately 1.1, but in shallower water this ratio decreases, since wave energy is redistributed towards the lower frequencies (Bosboom and Stive, 2021). Physical experiments show that is it better to use the spectral wave period for more accurate calculations, especially in shallow water conditions (van Gent, 1999).

$$T_{m-1,0} = \frac{m_{-1}}{m_0} \tag{2.3}$$

Wavelength

Due to the dispersion relation, the wavelength of gravity wave on the surface can be calculated iteratively with Equation 2.3. With the dispersion relation, the wavelength can be related to the frequency of the waves. This relation is important since the accuracy of the wave conditions in SWASH depends on the ability to solve the dispersion relation, as will be explained in Section 3.2.4.

$$L = \frac{gT^2}{2\pi} \tanh \frac{2\pi h}{L} \tag{2.4}$$

2.3. Determination wave overtopping

In this section, three methods used to determine the overtopping volume for the sea defense structure will be discussed. Section 2.3.1 gives an overview of the empirical formulas used in the EurOtop Manual (2018) and the influence of a berm and stepped revetment on average wave overtopping at the crest of the structure are elaborated. In Section 2.3.3, scale and model effects that may occur during small scale physical experiments are highlighted. Finally in Section 2.3.4, a comparison is made between different numerical models and the reasoning for using SWASH to predict overtopping for this case study is given.

2.3.1. Methodology and approach EurOtop

Due to the stochastic nature of breaking waves and numerous factors influencing the wave propagation, an exact mathematical description for the wave overtopping process for coastal sea defence structures is not possible. Therefore, empirical formulae have been derived based on physical experiments to predict the average wave overtopping discharge for coastal sea defence structures. The EurOtop Manual (2018) is one of the main references in hydraulic engineering and will be used for this thesis. In this section, the basic formulas are described to determine wave overtopping volumes according to the EurOtop manual (2018).

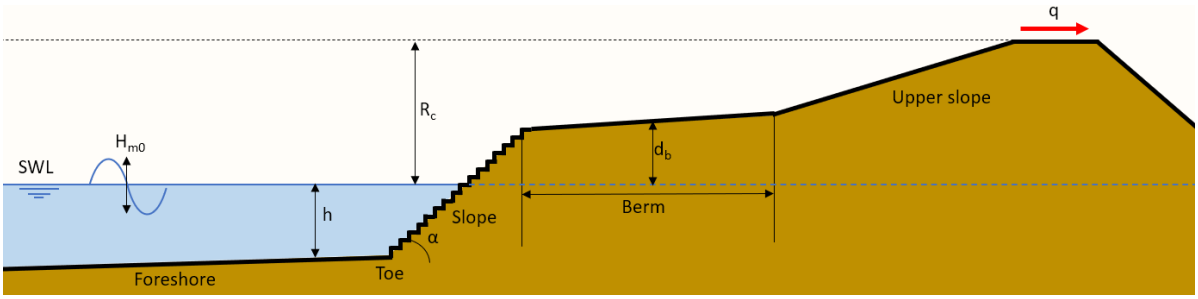

Figure 2.5: Overview of important parameters in design cross-section

In the EurOtop manual a distinction is made between a mean value value and a design approach. The calculated overtopping discharges are one standard deviation higher in the design approach compared to the mean value approach. In this thesis report, the 'mean value approach' is followed as suggested by The EurOtop Manual (2018), since the results will be compared to physical experiments. For non-breaking waves, the overtopping discharge can be determined with Equation 2.5, depending on the height of the foreshore. Equation 2.5 is the general formula to calculate wave overtopping for non-breaking waves and is roughly valid for $\xi_{m-1.0}$ < 5.0.

$$\frac{q}{\sqrt{gH_{mo}^3}} = \frac{0.023}{\sqrt{\tan(\alpha)}}\gamma_b\xi_{m-1,0}\exp\left(-2.7\frac{R_c}{H_{m0}}\frac{1}{\xi_{m-1,0}\gamma_b\gamma_f\gamma_\beta\gamma_v}\right)^{1.3} \tag{2.5}$$

With a maximum of:

$$\frac{q}{\sqrt{g\cdot H_{m0}^3}} = 0.09\cdot\exp\left[-\left(1.5\frac{R_c}{H_{m0}\cdot\gamma_f\cdot\gamma_\beta\cdot\gamma*}\right)^{1.3}\right] \tag{2.6}$$

The variables definition according to The EurOtop Manual (2018):

- q: Wave overtopping rate [m^3/s/m]
- g: Gravitational acceleration 9.81 [m/s^2]
- H_{m0}: The significant wave height at the toe calculated from spectral moment [m]
- α: Slope angle [°]
- γ_β,γ_f, γ_b, γ_v and $\gamma*$ are influence factors (-) for the angle of wave attack, roughness of slope, berms, a wall at the end of a slope and a combined factor of all kind of geometrical influences respectively. [-]

- $\xi_{m-1,0}$: Iribarren parameter [-], deep water wavelength
- R_c: Crest height - difference between SWL and crest of structure [m]

Shallow water conditions
van Gent (1999), discovered with physical experiments that for shallow water conditions the values calculated with Eq. 2.5 are far outside the range. This is due to the heavy breaking, the changing (spectral) wave periods and changing spectral shape in shallow water. Also the wave heights at the toe of the structure, become relatively small compared to the long wave periods, introducing very high breaker parameters. Therefore a suggestion was made to treat shallow and very shallow foreshores differently from situations where waves do not break, or only break to some extent (The EurOtop Manual, 2018). van Gent (1999) proposed to use the local wave length for the calculation of the breaker parameter due to the strongly changing wave properties, instead of the deep water wave length ($L_{m-1,0,o}$) used in the EurOtop manual (2018). Eventually Altomare et al. (2016) introduced a new formula, based on the work of (van Gent, 1999), valid for $s_{m-1,0} < 0.01$ and $\xi_{m-1,0} > 7.0$.

$$\frac{q}{\sqrt{gH_{m0}^3}} = 10^{-0.79} \exp\left(-\frac{R_c}{H_{m0}\gamma_f\gamma_\beta\left(0.33 + 0.022\xi_{m-1,0}\right)}\right) \tag{2.7}$$

Adaptation shallow water equation
Altomare et al. (2016) recommended that for shallow water conditions a part of the foreshore should be taken as “belonging” to the structure. It was advised not to take the average slope of the sea defence structure to calculate the breaker parameter $\xi_{m-1,0}$, but the average slope between the point on the foreshore with a depth of $1.5*H_{m0}$ and the wave run-up level $R_{2\%}$. An adjusted breaker parameter $\xi_{m-1,0}$ is calculated, which is then used to predict the average wave overtopping volume with Eq. 2.7. A schematisation is given in Appendix C.1.

The design cross-section has a berm in its slope, which effect the wave run-up and overtopping, see Section 2.3.2. The EurOtop Manual (2018) accounts this effect with a berm influence factor γ_b, which has not yet been added to Equation 2.8. Therefore, an adjusted has been made for this case study and the berm influence factor is added to Equation 2.8.

$$\frac{q}{\sqrt{gH_{m0}^3}} = 10^{-0.79} \exp\left(-\frac{R_c}{H_{m0}\gamma_f\gamma_\beta\gamma_b\left(0.33 + 0.022\xi_{m-1,0}\right)}\right) \tag{2.8}$$

An important note is that adding the berm influence factor in Equation 2.8 has not been validated, but the only reasoning is that this influence factor is also used in Equation 2.5. Therewith, the predicted confidence band for this equation provided by Altomare et al. (2016), can not simply assumed to be valid. However, the influence of a berm on wave overtopping is extensively tested for various wave conditions and structure designs in the EurOtop Manual (2018). Therefore, the suggested confidence interval for Equation 2.8 is still used in this report.

2.3.2. Influence factors

To include obstacles on a structure such as staircases, rocks or different types of material, the EurOtop Manual (2018) uses influence factors in the equations for the prediction of the average wave overtopping at the crest. For the designed sea defence structure in Middelkerke two influence factors need to be determined, a berm influence factor and roughness influence factor for the stepped revetment in the slope.

Berm and promenade

A berm is part of a structure profile and is often situated on a sloping structure like a dike or levee. A berm induces dissipation of wave energy, which reduces the relative amount of wave overtopping and can therefore results in a lower crest level. The effect of the berm expressed with an influence factor γ_b and berm width (B) of the structure is calculated with Formula 2.9.

$$\gamma_b = 1 - r_b(1 - r_{db}) \tag{2.9a}$$

$$r_b = 1 - \frac{2 \cdot H_{m0}/L_{berm}}{2 \cdot H_{m0}/(L_{berm} - B)} \tag{2.9b}$$

With 0.6 ≤γ_b ≤1.0

The parameter r_{db} is used to express the functionality of the berm with respect to the vertical location of the berm in the structure. According to the EurOtop Manual (2018), a berm is most effective when it is located around the still water level. A brief description of the calculation of the berm reduction coefficient for this case study can be found in Appendix C.2.

Stepped revetment- recent studies

Stepped revetment are a good measure to increase the slope roughness (1 - γ_f) of a sea defense structure. The physical processes that influence the efficiency of a stepped in the structure to reduce (average) wave overtopping are not yet fully understood (van Steeg et al., 2018; Kerpen et al., 2019; Schoonees et al., 2021).

van Steeg et al. (2018) were the first to relate a stepped revetment in the structure to a roughness influence factor. They described the influence factor for roughness γ_f as a function of the characteristic step height $(\cos\alpha \cdot S_h/H_{m0})$, with the characteristic step height perpendicular to the slope, and the local wave height.

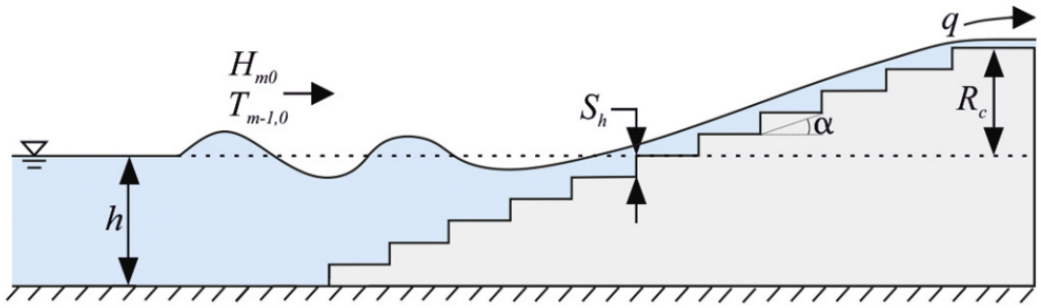

Figure 2.6: Definition figure dimensionless step height of a sea defence structure with a stepped revetment (Schoonees et al., 2021)

They concluded that the roughness influence factor was not constant, but a function of the hydraulic conditions and the geometry of the stepped revetment. The characteristics of the test conditions were limited and more studies followed, see Table 2.2.

Kerpen et al. (2019) performed a broad analysis and combined the data sets of many small scale experiments and proposed an empirical formula to determine wave overtopping for stepped revetments, but strongly advised to study the influence of the wave period on the slope roughness. van Steeg et al. (2018), Kerpen et al. (2019) and David Gallach-Sánchez (2018) each anticipated that small scale experiments are likely affected by scale- and model effects, especially with very low overtopping volumes.

Reference	S_h	$\cot\alpha$	$\xi_{m-1,0}$	$\cos\alpha \cdot S_h/H_{m0}$	γ_f
van Steeg et al., 2018	0.023; 0.046	2; 3	1.7 -3.7	0.13-0.57	0.37-0.65
Kerpen et al., 2019	0.05; 0.30	1; 2; 3	1.5-9.4	0.40-4.82	0.35-0.85
David Gallach-Sánchez, 2018	0.053; 0.106	0.58; 1	4.0-14.7	0.20-1.00	0.57-0.91
Schoonees et al., 2018	0.05	6	0.9-1.5	0.21-0.32	0.54-0.73
Schoonees et al., 2021	0.50;0.17	3	1.80-2.78	0.15-0.61	0.43-0.73

Table 2.2: Studies on (average) wave overtopping with stepped revetments in the structure. The step height(S_h) is given in model values (Schoonees et al., 2021)

These scale effects influencing the slope roughness and overtopping rates will be further elaborated in Section 2.3.3.
Schoonees et al. (2021) performed full-scale experiments to enlarge the current understanding of wave overtopping processes at stepped revetments and refine the proposed empirical formulas. With the data from the experiments in Table 2.2 and full-scale physical model test, Schoonees et al. (2021) concluded that the influence factor for roughness of stepped revetments is certainly not a fixed value and depends on several parameters:

- **Characteristic step height**
  If the characteristic step height is small, the step openings fill up easier with water, leading to a more continuous flow over the steps. With larger step heights (i.e. larger characteristic step height) waves distinctly jumped from step to step, dissipating relatively more energy.
- **Relative overtopping rate**
  With a relatively large overtopping rate, preceding waves leave a layer of water on the stair case more frequently as the next wave approaches. Accordingly, the residual water layer reduces friction between the incident wave and the steps of the stair case.
- **Wave period**
  The physical experiments concluded that the wave length is important, especially for relatively small steps in the revetment. Waves with longer periods, contain more energy and are accordingly less affected by the steps.

A new empirical relation was proposed, valid for conditions by Schoonees et al. (2021) as described in Table 2.2.

$$\gamma_f = 1 - 0.55 \cdot \tanh\left[-31.07 \cdot \ln\left(q_{\gamma_f=1}/\sqrt{g \cdot H_{m0}^3}\right) \cdot \cos\alpha \cdot S_h/L_{m-1,0}\right] \tag{2.10}$$

With $q_{\gamma_f=1}$, the relative average overtopping discharge for a smooth slope, determined with equation 2.6 from the EurOtop Manual (2018), see Section 2.3.1.

Roughness factor case study Middelkerke

In Figure 2.7 the empirical formula as proposed by Schoonees et al. (2021) is plotted. In Appendix C.3 a calculation for the roughness influence factor for this case study is performed following this relation.

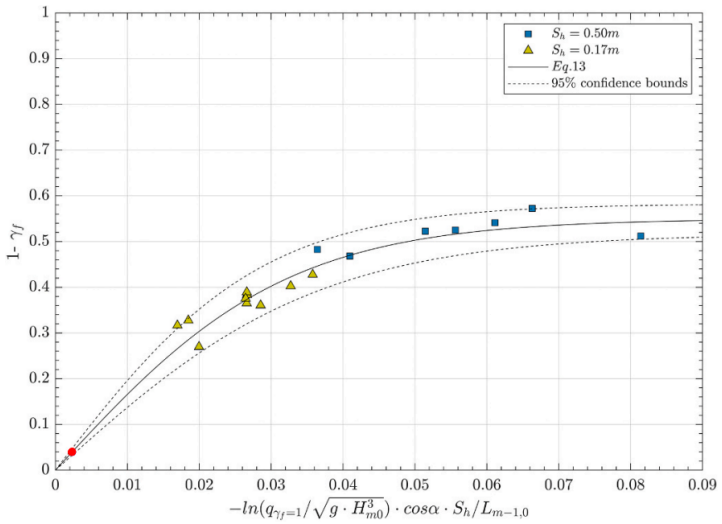

Figure 2.7: Empirical formula for estimating the roughness factor of stepped revetments (Schoonees et al., 2021). The red dot is the result of using the parameters for this case study in the proposed equation.

Using Equation 2.10 for this case study, results in an influence factor γ_f = 0.95, which is close to γ_f = 1 and would imply that for the wave conditions in this case study, the influence of the stepped revetment is almost negligible. This is explained by the very long wave period and thus wave length in this case study.

The roughness influence factor γ_f is always expressed for breaking wave conditions($\xi_{m-1,0} \leq 1.8$), but can be used for non-breaking/surging waves as well. The EurOtop Manual (2018) states that surging waves do not “feel” too much roughness, thus the roughness influence factor increases linearly with the breaker parameter, up to $\xi_{m-1,0}$=10 for surging wave conditions, such that:

$$\gamma_{f,surging} = \gamma_f + \left(\xi_{m-1,0} - 1.8\right) \cdot \left(1 - \gamma_f\right) / 8.2 \tag{2.11}$$

The validity of Eq. 2.10 is restricted to the tested range of boundary conditions in Table 2.2 and the wave period of this case study is far outside the tested conditions. Therefore, two more conservative values are chosen: γ_f = 0.75 - 0.9. The main reasoning for these values:

- Kerpen et al. (2019), developed a formula for stepped revetments based on the characteristic step height, not including the wave period, but valid for more wave conditions. Using this first indication results in a roughness influence factor of γ_f = 0.75 for this case study.
- Using the extreme long wave periods in the proposed formula of Schoonees et al. (2021) for which is it not been validated, causes uncertainties. In addition, the roughness influence factor need to be correct for the extreme long wave periods. Using a wave length outside the range of validity of the proposed formula and correcting it for surging wave conditions, might be a bit redundant. The chosen values, after correction for surging wave conditions, result in a comparable roughness influence factor to the value from proposed formula by Schoonees et al. (2021), see Table 2.3.

	Lower limit	Upper limit
γ_f =	0.75	0.9
$\gamma_{f,corr}$ =	0.95	0.98

Table 2.3: Estimated roughness influence factor case study and corrected with Equation 2.11 according to (The EurOtop Manual, 2018)

2.3.3. Physical model tests

Physical experiments can be a reliable method for the determination of (average) wave overtopping over a structure, as discussed in Section 1.2.

Scale effects

If the physical processes between a model and the prototype can not be represented due to scaling laws, scale effects will occur. In order to correctly reproduce the physical processes in a wave flume, the scaling laws need to be applied in a correct way. For the geometric scaling, all parameters need to be scaled proportionally to the corresponding lengths of the original dimensions. Negligible scale effects are expected for smoother slopes ($\gamma_f \geq 0.9$), provided that critical limits are satisfied (Schoonees et al., 2021). However, for small-scale experiments with rougher slopes, overtopping volumes are quickly underestimated when overtopping rates are low. The EurOtop Manual (2018) proposes an adjustment factor f_q for scale and model effect corrections, which is highlighted in Section 3.1.4 .
A total of four scaling laws are important for scale experiments for coastal sea defence structures:

- **Froude** - ratio between inertia and gravity
- **Reynolds** - ratio between inertia and viscosity
- **Weber** - ratio between inertia and surface tension
- **Cauchy** - ratio between inertia and elasticity

For most physical scale experiments the so-called Froude scaling is used for hydraulic structures under wave load. The Froude's law applies to processes in which gravitational and inertial forces are dominant. It it not possible to fulfill Reynolds law at the same time.Schüttrumpf and Oumeraci (2005) determined critical limits for the influence of viscosity and surface tension, see Table 2.4.

Process	Critical limits
Wave propagation	$Re_w > Re_{w,critical}$ = 1x10^4 T>0.35 s h >2.0 cm
Wave breaking	$Re_w > Re_{w,critical}$ = 1x10^4 T>0.35 s h >2.0 cm
Wave overtopping	$Re_q > Re_{q,critical}$ = 1x10^3 $We > We_{critical}$ = 10

Table 2.4: Scale effects and critical limits according to Schüttrumpf and Oumeraci (2005)

- To avoid the scale effects of surface tension, a minimum water depth of h = 2 and a wave period longer than T = 0.35 s. Both boundary conditions for this case study satisfy this condition and the effect of surface tension is negligible.
- For the wave overtopping discharges, the Reynolds number should be larger than $1x10^3$. Burcharth and Andersen (2009) confirmed that it is unlikely that this definition of a Reynolds number is sufficient related to run-up and overtopping. This is due to the differences in the critical stages of the two phenomena within the wave impact cycle. Due to the scaling with Froude, the Reynolds number is not scaled correctly and scale effects are expected for the physical experiments in Ghent. The measurements from the Ghent experiment will be corrected according to the EurOtop Manual (2018).

Model effects

Model effects can also lead to inaccurate results, since it is not always possible the make an exact reproduction of the prototype in scale models. Model effects can relate to both wave processes and structural effects, which affect the structural properties of the sea defence structure.
Model effects relating to wave processes are for example differences in the wave generation method, methods used to measure wave conditions or implied boundary conditions, such as the negligence of wind. Structural model effects are consequences of using different material properties or making simplifications in the geometry of the structure.

2.3.4. Numerical wave-flow modelling

Wave model comparison

A comparison is given In Table 2.5 between different computational numerical models. With the differences of characteristics and limitations of each numerical model a choice has been made for the model to use for this thesis.

	SWAN	SWASH	OpenFOAM
Category	Phase averaged	Phase resolving	Phase and depth resolving
Operation area	Near shore	untill shore	structure interaction
Shoaling	✓	✓	✓
Wave breaking	Depth-induced	Wave steepness	Depth- & steepnees
Bottom friction	uniform	varying	varying
Computational time	+++	+	-

Table 2.5: Comparison between different numerical computational models

Where SWAN is of good use for modelling wave transformation near shore, it is not developed for predicting the wave physics till shore, but can be used to predict wave conditions near the structure. The computational time needed for the model runs is an important aspect for this case study. OpenFOAM has a considerably higher computational cost compared to SWASH. It would therefore be interesting to look for the limitations of using SWASH for wave overtopping simulations.
Suzuki et al. (2011) concluded with physical model tests, that SWASH reproduces wave transformation and wave overtopping very well, even in shallow water conditions. This is because SWASH includes a non-hydrostatic pressure term. SWASH was able to reproduce the Wave overtopping discharge, but large differences were seen when small overtopping volumes in combination with a rapidly varying topographic features (e.g. sea defense structure) were simulated, which is the case for cross-section 2b. The inability of the depth integrated model to represent the water tongue of the wave overtopping waves was suggested as possible explanation.
Gruwez et al. (2020b) found that SWASH produced comparable results with OpenFOAM and both were capable of modelling the dominant wave transformation (i.e., propagation, shoaling,wave breaking, energy transfer from the SW components to the bound LW via nonlinear wave–wave interactions) and the wave–structure interaction (i.e., individual wave overtopping, bore interactions, and reflection processes). They recommended that if the impulse forces on the structure are less important factors, SWASH is the best numerical model to use, since it was able to predict the maximum horizontal force per impact event relatively accurate, with a significantly reduced computational cost, compared to OpenFOAM. When the force impulse on the structure is an important design, OpenFOAM is recommended, since it is more accurate and capable of predicting wave–dike interactions. Gruwez et al. (2020b) suggests for future work, to investigate whether the same conclusion is valid (particularly regarding applicability of SWASH) in the case of more complex dike geometries.

SWASH

SWASH (Simulating WAves till SHore) (Zijlema et al., 2011) is a freely accessible, time-dependent wave model, which uses the nonlinear shallow water equations (NLSW) with additional non-hydrostatic terms, to accurately calculate the wave transformation under rapidly varying conditions. The Reynolds-averaged Navier-Stokes (RANS) equations are solved with the following statements:

- Shallow water conditions are valid, which means that the horizontal scale size of the model is much wider than the vertical scale size
- SWASH consideres the flow to be incompressible.
- The hydrostatic pressure assumption is valid, which means that the variation in pressure in the vertical is only a function of the height of the water column above a certain point. SWASH is, however, also capable of modelling non-hydrostatic pressures. This is generally important when variations in the vertical are relevant.
- The Boussinesq approximation is applied, which means that density variations are small and a constant reference density is assumed

The governing equations for SWASH are the nonlinear shallow water equations. Swash is also capable of modeling the non-hydrostatic pressures, the simulation of broken waves and wave run-up amounts to the solution of the NLWS equations for free-surface flow in a depth-integrated form. This gives the following Navier-Stokes equations (Zijlema et al., 2011):

$$\frac{\delta\zeta}{\delta t} + \frac{\delta hu}{\delta x} + \frac{\delta hv}{\delta y} = 0 \tag{2.12}$$

$$\frac{\delta u}{\delta t} + u\frac{\delta u}{\delta x} + v\frac{\delta u}{\delta y} + g\frac{\zeta}{x} + \int_{-d}^{\zeta}\frac{\delta q}{\delta x}dz + c_f\frac{u\sqrt{u^2+v^2}}{h} = \frac{1}{h}\left(\frac{\delta h\tau_{xx}}{\delta x} + \frac{\delta h\tau_{xy}}{\delta y}\right) \tag{2.13}$$

$$\frac{\delta v}{\delta t} + u\frac{\delta v}{\delta x} + v\frac{\delta v}{\delta y} + g\frac{\delta\zeta}{\delta y} + \frac{1}{h}\int_{-d}^{\zeta}\frac{\delta q}{\delta y}dz + c_f\frac{u\sqrt{u^2+v^2}}{h} = \frac{1}{h}\left(\frac{\delta h\tau_{yx}}{\delta x} + \frac{\delta h\tau_{yy}}{\delta y}\right) \tag{2.14}$$

The integral of the non-hydrostatic pressure gradient over the water depth is given with Equation 2.15:

$$\int_{-} d\frac{\zeta q}{\delta x}dz = \frac{1}{2}h\frac{\delta q_b}{\delta x} + \frac{1}{2}q_b\frac{\delta(\zeta - d)}{\delta x} \tag{2.15}$$

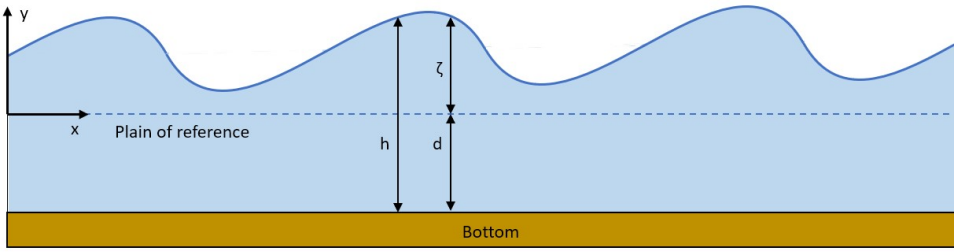

Figure 2.8: Reference frame SWASH equations (Zijlema et al., 2011).

In SWASH, it is possible to define boundary conditions at 3 locations in the domain: the bottom, free surface and at the boundary of the domain, which can be either an open or closed boundary. To numerically solve the equations, SWASH uses four different boundary conditions.

Boundary conditions

- **Bottom:** SWASH is capable of adding an tangential stress, which is the bottom stress in the computational domain. This bottom friction doesn't have to be constant in both time and space. This will be further elaborated in Section 3.2.4
- **Free surface:** At the surface boundary, wind stress can be added. This is not within the scope of this research, thus no windstress at the surface and the pressure at the free surface is therefore zero.
- **Boundaries in SWASH:** At the inflow boundary, a wave maker is used for the wave generation in the computational domain. Besides wave height and period, it is also to define initial conditions such as velocities. At the outflow boundary a so-called sponge layer is inserted, which absorbs the wave energy at the end of the model, so that no reflection occurs at the end of the domain. It is also possible to define the normal velocity and tangential stresses equal to zero, this is called a closed boundary.

SWASH in not a Boussinesq-type wave model, which makes it possible to run it in depth-averaged mode or multiple vertical layers can be added, where the wave celerity is calculated for every layer. By doing this, the wave celerity is modelled more accurately with frequency dispersion relation, because the wave celerity is aloud to vary over depth. SWASH improves its frequency dispersion by increasing this number of layers rather than increasing the order of derivatives of the dependent variables like Boussinesq-type wave model (Zijlema et al., 2011).

3
Model Setup

This chapter discusses the model setup of SWASH and the physical experiments used to determine the average wave overtopping. In Section 3.1 an overview of the setup of the physical model tests performed in the Ghent University Laboratory is given. Section 3.2 describes the input-/output parameter, basic setup settings and highlights sensitive parameters in the settings of the numerical model SWASH.
For readability, all values and results in this report are expressed and scaled to prototype dimensions. Prototype stands for full-scale dimensions, whereas model dimensions are the scale model values.

3.1. Physical model

The goal of the physical model experiments in Ghent were to determine the amount of average wave overtopping over the designed sea defence structure in Middelkerke.

3.1.1. Ghent flume tests

The wave flume at the Department of Civil Engineering at Ghent University has a length of 30.00 m, a width of 1.00 m and a height of 1.20 m. It is a 2D wave flume, therefore only perpendicular incident waves can be tested. The flume is equipped with the state-of-the-art model testing technology including an advanced wave generator system for both regular and irregular waves, solitary waves, second order wave generation, active wave absorption, data acquisition system and wave data analysis software. The wave paddle used 2nd order wave generation to generate irregular sea states using the second order theory (including bound sub and super harmonics).

3.1.2. Bathymetry and structure

In Figure 3.1 an overview is given of the scaled bathymetry that was constructed in the wave flume in Ghent.
The bathymetry of the foreshore in the wave flume is a simplification of the cross-coastal profile after the design storm, as described Section 2.2.1. The bathymetry of the foreshore consists of a 1/47 straight slope up till the toe of the structure. This is a simplification of the curved design bathymetry after the XBeach simulations. The water depth at the toe of the structure is 2.11 m, which corresponds with the design height of the toe of the structure at + 5.46 TAW. The exact length of the foreshore slope has been defined after a first estimation of the breaking position (using preliminary SWASH model runs). This ensures that the waves will break along the foreshore and not on the flat bottom flume part near the wave generation paddle or on the transition slope. The structure was scaled to model dimensions without simplifications, meaning the stepped revetment and varying upper slope were constructed in the flume. Appendix E gives an overview of the scale model constructed in the wave flume.

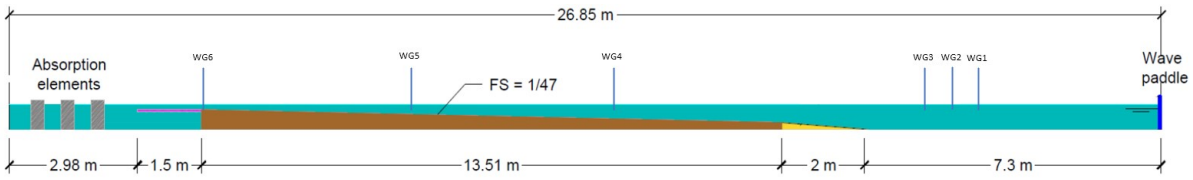

Figure 3.1: Overview of wave flume and test setup at Ghent University (model dimensions).

3.1.3. Scaling parameters

Scaling was achieved using Froude similarity, see Section 2.3.3. The scale selected to perform the hydraulic model tests was 1-to-25. This scale ensures (1) a sufficient water depth to accurately generate the desired wave conditions, (2) an adequate size of the coastal structures (dike, overtopping element, sea wall, etc.), and (3) a large enough foreshore slope extending all the way to deeper water conditions.

Physical parameter	Unit	Scale factor [-]	Scale factor 1-to-25
Length	[m]	$\alpha_L = \frac{L_{proto}}{L_{model}}$	25
Time	[s]	$\alpha_t = \frac{t_{proto}}{t_{model}} = \sqrt{\alpha_L}$	5
Average overtopping rate per running meter	[m^3/s/m]	$\alpha_q = \frac{q_{proto}}{q_{model}} = \alpha_L^{3/2}$	125

Table 3.1: Scale factors based on the Froude scale used during the Ghent laboratory tests

The length, time, overtopping, force and pressure scale factors (α_L, α_t, α_q) are reported in Table 3.1 in which L_{proto} and L_{model} represent the length, t_{proto} and t_{model} the time, q_{proto} and q_{model} the overtopping rate. The indices 'proto' and 'model' stand for the prototype and scale model values respectively. This report describes prototype measures only.

3.1.4. Measurements

Wave conditions

Two model set-ups were tested in the Ghent laboratory: An experiment executed without the dike to capture the incident wave height and a test with structure to determine the amount of wave overtopping over the structure.

A total of 6 wave gauges (WG) was used to record the wave propagation and transformation in the deep (offshore) part of the flume, along the bed profile (foreshore slope) and at the toe location. The first array of three wave gauges was installed in 'deep water' over the horizontal bottom part of the flume (denoted WG1, WG2, and WG3). These wave gauges are placed at a sufficient distance from the wave paddle so the generated wave field can be accurately recorded. The inter-distances between all three wave gauges in deep water was determined according to the spacing proposed by Mansard and Funke (1980). The second array of two wave gauges (WG4, WG5) was placed along the foreshore profile to record the wave transformation triggered by the decrease in water depth. The last wave gauge (WG6) was placed at the toe of the dike to measure and calibrate the incident waves based on the target conditions.

These WG measure the total water surface elevation signal. To minimise the effect of reflection, wave calibration tests have been performed prior to the tests to determine overtopping. These tests were performed with foreshore but without structure. At the end of the wave flume a wave damping slope was installed to minimise the reflections. The (incident) wave conditions from the wave calibration tests have been used for the remainder of this study to compare with the SWASH model results.

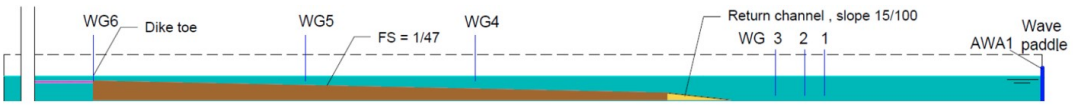

Figure 3.2: Technical drawing of wave gauge positioning Ghent flume. 'WG6' is located at the toe of the structure, which is the target location for the calibration tests for both the physical and numerical model simulations.

The objective of the wave calibration tests in Ghent is to achieve the target wave conditions within the predefined acceptable tolerances (+/- 3% for H_{m0}, +/- 5% for $T_{m-1,0}$, +/- 5 cm for water depth) at the toe of the dike. The target hydraulic conditions are defined at the location of the toe of the dike and are provided by Witteveen+Bos based on preliminary SWASH-2DH calculations.

During the calibration runs in Ghent, the offshore input parameters (H_{m0} and T_p) had to be iteratively adjusted until the toe wave conditions were within the desired tolerances. The target wave conditions

determined with preliminary SWASH simulations at the toe were not achieved during the calibration runs. However, these target conditions were estimated with a relatively simple/robust SWASH model. Therefore, the wave conditions resulting from the final calibration runs in Ghent, are the wave conditions considered in this report. Table 3.2 shows the incident wave conditions at the toe of the structure of the Ghent experiment.

Cross-section	H_{m0} [m]	$T_{m-1,0}$ [s]	Toe level [m TAW]	Water level [m TAW]	Water depth toe [m]
CS2b	1.51	16.68	5.46	7.42	2.11

Table 3.2: Results physical experiments in Ghent and target hydraulic conditions for this report at the toe of dike (WG6) - (prototype dimensions)

Overtopping measurements

The overtopping water volume is collected with a funnel tray located on the crest of the structure (at the safety line) and connected to a reservoir. The average wave overtopping discharge (q) is calculated from the overall volume of water in the reservoir (V [l]) divided by the time in which it is collected (ΔT [s]) and by the width of the funnel tray (b [m]). This has led to a q in [l/s/m] for each test:

$$q = \frac{V}{\Delta T b}[l/s/m] \tag{3.1}$$

The average overtopping discharges for cross-section 2b, the measured volumes and subsequently the calculated average overtopping discharge are much smaller than the limit of 1 l/s/m; with an average value of 0.049 l/s/m.

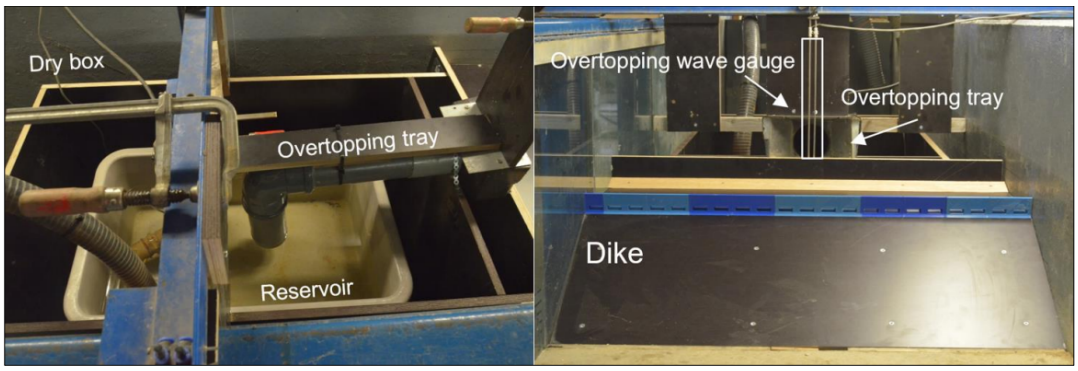

Figure 3.3: In the figure below an schematization is given of the wave flume in Ghent University.

During the tests, different seed numbers resulted into quite significant differences in wave overtopping, as seen in Table 3.3. Therefore multiple tests were performed to asses the variety in wave overtopping at the crest of the dike. It is important to keep in mind that the experiments in Ghent were calibrated based on the target wave conditions at the toe of the structure. To achieve the target wave conditions for different seed numbers, the input wave height at the wave paddle was not always the same. The input (peak) wave period and water depth were kept the same during each test. The values in Table 3.3 are the averaged wave overtopping, but it is important to note that for each test a different number of waves could pass over the structure, with different volumes.

Test ID	O1	O2	O3	O4	O5	O6	O7	O8
H_{m0} [m]	4.5	4.5	5.0	4.5	5.0	4.75	4.5	4.75
q_{prot} [l/s/m]	0.049	0.022	0.043	0.101	0.044	0.078	0.006	0.022

Table 3.3: Average wave overtopping results flume experiments Ghent. q_{prot} is the averaged wave overtopping, H_{m0} is the input wave height at the wave paddle, both in prototype scale.

The different model runs in Ghent showed large differences in wave overtopping volumes for different seed numbers. Only 1 set of data with wave surface elevation measurements across the domain was available for this thesis. Therefore, this thesis focuses only on Test ID-O6. The wave conditions in the SWASH model are calibrated and compared according to the measurements from this test, see Chapter 4.

Correction scale factor

The Eurotop manual (2018) suggests a correction factor for model and scale effects for physical scale experiments. This is based on research conducted in the CLASH (2004) project. The procedure to scale the overtopping results, include the roughness of the structure γ_f [-]; the seaward slope cot$\alpha$of the structure [-]; and the mean overtopping discharge, based on small scale tests or predictions, but up-scaled to prototype with the Froude scaling law, q_{us} [m^3/s/m] (The EurOtop Manual, 2018).
The following formula has been developed to account for scale effects:

$$f_{scale} = 1.0 + \frac{(-\log(q_{us}) - 2)^5}{14} \tag{3.2}$$

The maximum of Eq. 3.2 of the adjustment factor f_{scale}, f_{qmax}, depends on the slope angle $\alpha$and is given by f_{qmax} = 10cotα-9. For this cross-section with a slope angle of cotα= 2, results in f_{qmax} = 11.

In the CLASH (2004)-project no significant scale effects were seen for smooth slopes, in contrast to rubble mound structures. It was therefore proposed to include the roughness influence factor in the correction factor for scale effects. The EurOtop Manual (2018) advises to use this method also for slopes with roughness, e.g. stepped revetments. The estimated roughness influence factor based on research from Kerpen et al. (2019) and Schoonees et al. (2021) are used to calculate the adjustment factor f_{scale}.

$$f_{s,rough} = 5 * \gamma_f * (1 - f_{scale}) + 4.5 * (f_{scale} - 1) + 1 \quad for\ 0.7 \leq \gamma_f \leq 0.9 \tag{3.3}$$

The roughness influence factor for this case study were estimated to range between γ_f = 0.75-0.9, see Section 2.3.2. With the up-scaled overtopping discharge q_{us} in m^3/s/m from test ID-06, Table 3.3, the adjustment factor $f_{s,rough}$ is calculated:

- For γ_f = 0.9, $f_{s,rough}$ = 1
- For γ_f = 0.75, $f_{s,rough}$ = 3.23

The corrected overtopping volumes for the physical scale experiments in Ghent range therefore between:

Test ID	O1	O2	O3	O4	O5	O6	O7	O8
$q_{s,rough=1}$ [l/s/m]	0.049	0.022	0.043	0.101	0.044	0.078	0.006	0.022
$q_{s,rough=3.23}$ [l/s/m]	0.158	0.071	0.139	0.325	0.1417	0.251	0.019	0.071

Table 3.4: Corrected average wave overtopping volumes for the experiments Ghent. q_{prot} is the averaged wave overtopping in l/s/m.

This report focuses only on Test ID-O6, see Table 3.4.

3.2. Computational model

SWASH will be used to reproduce the wave conditions in the domain and the wave overtopping discharges from to the physical experiment in Ghent. First, the geometry, measured parameters and the target wave conditions of the SWASH model will be discused. The most important parameters with respect to the calibration of the SWASH model are highlighted in Section 3.2.4 For readability, all parameters and results are scaled to prototype dimensions.

3.2.1. Geometry

Figure 3.4 gives an overview of the bathymetry of the SWASH numerical model, without structure. The geometry and the measurements locations are an exact copy of the dimensions of the physical models test in the wave flume in Ghent. At the end of the system a so-called sponge layer is added, which absorbs wave energy and prevents wave reflection at the boundary. This bathymetry without structure is used for the calibration of the model and to determine the incident wave conditions at the toe of the structure. In the final SWASH simulations, the structure was added at the 'toe of structure', see Figure 3.4, with identical geometries compared to Gent.

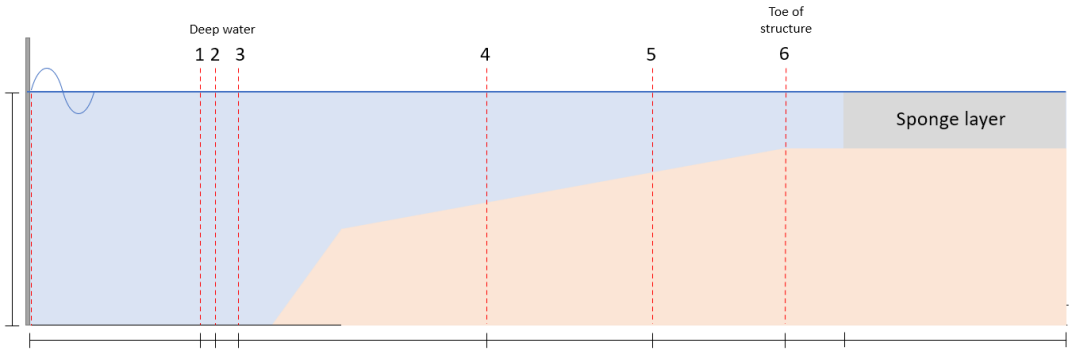

Figure 3.4: Geometry of SWASH model, not according to scale

3.2.2. Measurements and output

The output of the SWASH model runs can be set to 'block' or in a 'table'. The block function gives the chosen parameter value across the entire domain. With the table option, parameters are returned per time step at predefined output locations. These output locations are set to match the location of the surface elevation gauges from the Ghent experiments, as described in Section 3.1.4. SWASH does not have a direct function to calculate the amount of wave overtopping over a structure. Therefore, a method based on the measured velocity at a grid point and the thickness of the water column is used.

The output files were used to calculate the following parameters, which were then compared to the results from the physical model tests in Ghent:

- The significant wave height H_{m0} [m]
- Two percent highest waves $H_{2\%}$ [m]
- The maximum wave height H_{max} [m]
- Peak wave period T_p [s]
- Spectral mean wave energy period $T_{m-1,0}$ [s]
- Average wave overtopping q [l/s/m]

3.2.3. Target wave conditions in system

The wave generation method used in the physical experiments is different than the wave generation method used in the SWASH numerical model. Therefore, the calibration of the model is done based on the deep water wave conditions inside the system and not the input parameters of the wave paddle system (i.e. boundary of system). The measurement locations in the SWASH model are set at the same locations as the physical experiments.
SWASH solves nonlinear shallow water equations to calculate the wave propagation for waves travelling towards the toe of the structure. The goal of the wave calibration is to validate if SWASH can reproduce the wave propagation with foreshore up till the toe of the structure, with the same incident wave conditions in the deep water section of the domain. This study therefore focuses on the deep water section and the wave gauge at the toe of the structure.
For both methods a second order wave generation method is used with a JONSWAP spectrum with a peak-enhancement factor of 3.3. A more extensive description of the steps taken for the calibration of the SWASH model can be found in Appendix A.1.

3.2.4. Important parameters model set-up

This section describes the most important model parameter settings of SWASH. Some input parameters and settings were very sensitive during the calibration and final model runs.

Boundary conditions
The SWASH model runs showed a sudden drop in the wave height at the beginning of the domain. This problem is found in multiple studies and projects, (Witteveen+Bos et al., 2021), (de Wit, 2016), (Jordans, 2019), (Dobrochinski, 2014) and the same practical solution will be used for this thesis. By measuring the wave conditions in the deep water section of the domain, the wave height was increased with a certain amount until the wave conditions in the deep water section were within limits.

Vertical layers and grid size
SWASH is a depth-averaged numerical model, but the domain can be divided into a number of vertical layers. Concerning the wave transformation, the number of layers is determined by the linear frequency dispersion. In particular, the dimensionless depth, kd with k the wave number, decides the number of layers. The higher the value of kd, the more vertical layers needed. The SWASH team (2010) states that for most simulations 2 or 3 layers will be sufficient.
According to the manual, a grid size of 50-100 grid cells per peak wave length is sufficient. For this thesis, lot more grid cells (i.e. 300) were needed to implement the stepped revetment in the cross-section. However, this introduced significant unstable model runs and 'numerical wiggles', as is illustrated in Appendix A.1.3.

Wave breaking
For this study, a maximum of 3 vertical layers is used. This leads to particle velocities near surface being underestimated and waves postponed from getting more asymmetrical and consequently delaying wave breaking (Smit et al., 2013). With a built-in BREAK command, SWASH can control the onset and offset of wave breaking. For this thesis the default threshold values are used according to the The SWASH team (2010).

Seed numbers
In the Ghent experiments, different seed numbers led to differences in wave conditions in the domain and overtopping discharges at the crest of the structure. This was also observed in the SWASH model runs. The wave generation method uses random starting phases resulting in different wave time series, but having the same wave energy spectrum.
The prediction of overtopping discharges inherently involves a scatter of the results for both physical experiment and numerical models (The EurOtop Manual, 2018). This is partly explained with the stochastic nature of the waves in the domain. By generating a random wave field with a certain wave spectrum, the different combinations of wave heights and wave periods, will lead to different volumes of overtopping (Romano et al., 2015).

Friction
Suzuki et al. (2011) and Tuan and Oumeraci (2010) found that the wave overtopping discharges were very sensitive to the value of the bottom friction selected in the SWASH model. Different options are available for the bottom friction in the SWASH model. One can choose for using a constant roughness coefficients, the Manning or Chezy formula's or Nikuradse roughness height. The friction coefficients do not have to be constant and may vary over the spatial domain. The SWASH team (2010) states that numerical experiments have indicated that the Manning formula provides a good representation of wave dynamics in the surf zone. The Manning coefficient is used for open channel flows with a stable velocity profile. In a surf zone, velocity is far from constant and changes direction quick, especially with the wave-structure interaction at the sea defence structure. de Wit (2016) encountered this same problem, leading to unstable simulations. Another problem with using the default Manning friction coefficient was that a friction dominated situation on the slope of the structure originated, preventing waves surging to the crest of the structure. Therefore the Manning coefficient has not been used for the SWASH model runs.
According to the The SWASH team (2010), using more vertical layers with a friction coefficient c_f, increases the possibility of inaccuracies in the vertical structure of the velocity, especially if the depth-averaged velocity is equal to zero. Therefore, the use of a logarithmic wall law function for the friction parameter is advised. In this case, a distinction is made between smooth and rough beds. For rough beds, the user must apply a Nikuradse roughness height. To prevent friction having a dominant effect on the waves surging on the structure, a smooth logarithmic wall function is chosen for the base case model, making the influence of the friction on overtopping discharges almost negligible.

Local friction
The effect between local friction on the slope and overtopping at the crest of the structure was studied. The goal is to use a friction coefficient or roughness height to simulate the roughness of a stepped revetment in the cross-section. Two different friction coefficient are used to asses the influence of an local increase of the friction on the slope of the structure to wave overtopping: the friction coefficient c_f and the Nikuradse roughness height k_s.
These friction formulations, dimensionless friction coefficient and the Nikuradse roughness height, are usually used for quasi-steady flow conditions (e.g. flow in a river). The relation is described with:

$$C = \sqrt{\frac{g}{c_f}} = 18\log(12h/k_s) \tag{3.4}$$

Viscosity
According to the The SWASH team (2010) the use of horizontal eddy viscosity in the model, has a negligible role for far field calculations. However, for near field flows horizontal eddies generated by lateral shear may have an important role in horizontal mixing. The recommended default setting in SWASH assumes the horizontal viscosity to be a constant, but The SWASH team (2010) also states that for near field predictions a constant value for horizontal viscosity is too crude. Especially for the model runs with the structure in the domain showed the importance of this horizontal viscosity value in SWASH. With waves interacting with structure, more turbulence is expected and the model runs became unstable and crashed repeatedly. By removing the constant horizontal eddy viscosity, the numerical calculations became more stable. However, this change in parameters resulted in a slightly different wave spectrum for the calibration runs with the foreshore bathymetry only. Regardless the wave spectrum being slightly different for both options, the significant wave height and spectral period determined with a spectral analysis, were very comparable. This will be discussed in Section 4.3.

Measured overtopping discharge
SWASH showed inconsistencies in the measured velocities and layer thicknesses at various locations in the cross-section. With 2 consecutive grid points, thus a very small horizontal distance, the speed and layer thickness could be very different without a clear explanation. Especially since the layer thickness of the measured water volume at the crest is so small in the particular case study («1 cm in model dimensions), part of the overtopping waves might not be registered. The velocity and water depth are equaled to zero when the water depth is below a value of 0.05 mm within the SWASH model, which is the standard value.

Unstable SWASH runs
SWASH has difficulties if there are sharp angles between grid points in the bathymetry. A rapidly varying topographic cross-section can cause the model to crash, which happened occasionally in preliminary test runs. A different seed number and thus different wave conditions combinations could induce unstable model runs. Especially having a structure in the domain, i.e. complex geometry, inducing heavy wave breaking and highly reflective wave conditions. Besides, as previously explained, some inaccuracies may occur in the vertical structure of the velocity, in particular when the depth-averaged velocity is zero.

4
Calibration SWASH model and validation of wave conditions

This Chapter describes the calibration of the SWASH model, which is performed based on the deep water section of the domain using measurements from the deep water section in the physical experiment, as will elaborated in Section 4.1. The incident wave height at toe of the structure is used for the empirical formulas to predict wave overtopping in the EurOtop Manual (2018). Therefore, SWASH is calibrated based on the incident wave conditions, to first check whether SWASH is capable of reproducing the wave conditions for the bathymetry without structure for this case study compared to the physical experiment.
In Section 4.2, the structure is added in the bathymetry and the effect on the wave conditions in the domain is compared with the data from the physical experiment in Ghent. The dike of the case study make the cross-section complex, for which SWASH is expected to be less accurate (Gruwez et al., 2020b).
As described in Chapter 3.1.4, only one data set from Ghent is used for the comparison between the SWASH model and all dimensions are given in prototype dimensions.

4.1. Calibration incident wave conditions

The SWASH model is calibrated using water surface elevation gauges in the deep water section (WG1, WG2, WG3) placed at the same exact locations as in the physical flume. For WG3 in the Ghent experiment large differences in wave conditions were seen compared to WG1 and WG2. This is expected to be a measurement error during the Ghent experiments, see Section 3.1. The wave conditions at WG1 and WG2 were very similar for each model run for both SWASH and the Ghent tests, therefore only WG1 is used for simplicity during the calibration of the model. In the physical experiment approximately 1400 waves were generated at the deep water boundary. The duration of the SWASH simulation was chosen such that a similar number of waves was generated in the numerical model.
With the surface elevation gauges, the significant wave height (H_{m0}) and the spectral wave period ($T_{m-1,0}$) can be calculated.
The wave generation method in SWASH uses a wave height and a peak period as input parameter. The SWASH model is calibrated by comparing the wave conditions from SWASH to the data sets from the Ghent experiment and check if the wave conditions are within the acceptable tolerances (+/- 3% for H_{m0} and +/- 5% for $T_{m-1,0}$), the same predefined tolerances used in Ghent. As discussed in Section 3.2.4, the input parameters H_s and T_p at the boundary in SWASH were adjusted until the wave conditions at WG1 in SWASH matched the H_{m0} and $T_{m-1,0}$ at WG1 from Ghent. Thereafter, the wave conditions at the toe of the structure (WG6) were analysed to check if they were within the tolerance limits. WG1 and WG6 are therewith the target wave gauges for this thesis. WG2, WG3, WG4 and WG5 will not be used to validate wave conditions in SWASH compared to Ghent and a larger spread is therefore accepted.

4.1.1. Significant wave height

Multiple tests were performed in Ghent, with different seed numbers and the wave conditions at the boundary were adjusted such that both the target H_{m0} and $T_{m-1,0}$ at the toe of structure were achieved. Therefore, different wave input parameters and thus boundary conditions led to the same wave conditions at the toe, see section 3.1.4. Only 1 data set was available with overtopping volumes from the Ghent experiments, thus the model has been calibrated based on this data set. Figure 4.1 displays the significant wave height (H_{m0}) across the domain for the final wave calibration run in SWASH.

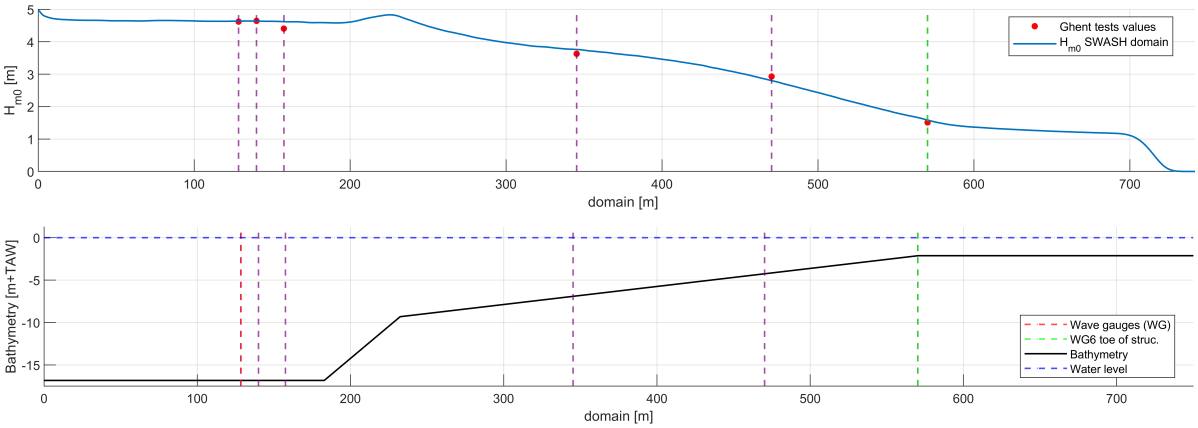

Figure 4.1: Significant wave height over the domain from SWASH results, compared to physical experiments in Ghent

Test	WG1	WG2	WG3	WG4	WG5	WG6
Ghent exp. [H_{m0}]	4.62	4.64	4.41	3.63	2.93	1.51
SWASH [H_{m0}]	4.63	4.63	4.61	3.72	2.76	1.55
Difference [%]	0.24	-0.26	4.69	2.48	-5.70	2.30

Table 4.1: Comparison significant wave heights for the Ghent experiments and the SWASH results at WG in domain. The cut-off frequency used for the calculations is 0.005-0.5 Hz, the same values that were used for the Ghent laboratory experiments.

The influence of the foreshore is seen as waves travel further into the domain, waves start to break and the wave height decreases. In Figure 4.1, the sudden drop at approximately x=700 m in the significant wave height is the result of a wave absorbing sponge layer, absorbing the wave energy and preventing wave reflection at the boundary of the model.

H_{m0} is stable/constant in the deep water part of the domain as is seen in Figure 4.1. This is important, since this means that the influence of the bottom on the waves is negligible in deep water.
Figure 4.1 shows that the SWASH model was able to reproduce the significant wave height at the deep water boundary very accurately, excluding WG3 from Ghent as explained in Section 3.2.3). At the toe of structure (WG6), SWASH the results were also well within the tolerance limits, see Table 4.1.
Larger differences are seen at WG4 and WG5, which is the results of waves starting to break due to the decreasing water depth. The wave conditions at WG4 and WG5 were very sensitive to the viscosity settings chosen within SWASH, which will be highlighted in Section 4.1.2. This study however focuses on the wave conditions at WG1 and the toe of the structure WG6.

4.1.2. Wave spectrum

The wave spectrum is an important parameter to make a good comparison for the wave conditions between the numerical model and the Ghent experiment. This section discusses the energy density spectrum at the deep water boundary (WG1) and at the toe of the structure (WG6), which were used to analyse the performance of the SWASH model.

Deep water

Figure 4.2 shows a similar spectrum shape, but some small differences can be noticed. For the spectral analyses, only the wave energy present within the interval 0.005-0.5 Hz (cut-off frequency) is considered, the same value was used for the physical experiment in Ghent. For the deep water spectrum, a slight increase around the 0.005 Hz frequencies and some inconsistencies around approximately 2 times the peak frequency (f_p) can be seen. In the experimental setup in Ghent bound sub- and superharmonic waves were included as they are considered crucial due to the severe breaking on the foreshore and subsequent release of these bound waves.

An explanation for the overestimation of energy in low frequencies is the imposition of second order bound long waves at the boundary. In addition, for the inconsistency at 2 times the peak frequency: the wave generation method used in the SWASH is a first order wave generation + bound-subharmonics, but bound-superharmonics are not included. Due to the fact that SWASH is trying to generate higher order waves, using first order wave generation, free high order spurious waves occur inside the domain.

For this specific application, this deficiency is assumed to not affect the accuracy of the results significantly. The wave spectra are analysed for each test and for each measurement location. The spectral analysis showed that SWASH was able to reproduce comparable wave spectra for WG1 and WG6, other locations are displayed in Appendix B.

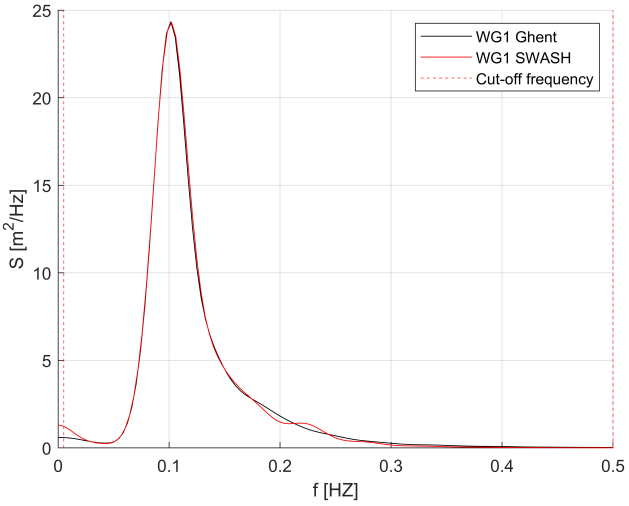

Figure 4.2: This figure shows the calculated wave spectrum at WG1 for both SWASH and the Ghent experiments.

Toe of structure - Horizontal viscosity

Larger differences were seen for the wave spectrum at WG6 at the toe of the structure. As explained in Section 3.2.4, choosing the horizontal viscosity as a constant value for near field predictions is a crude assumption (Zijlema et al., 2011). Based on a stability criterion due to the explicit treatment of the horizontal eddy viscosity term in the momentum equations, a maximum of the eddy viscosity is determined at each time step (The SWASH team, 2010). With a constant horizontal viscosity term most of the runs became unstable or crashed before 1000 waves could be generated, which is assumed to be enough to avoid significant variations in the wave spectrum Van der Meer et al. (2018).
An explanation for the unstable model runs could be the complex cross-section and wave-structure interaction generating horizontal eddies. It was found that by removing the default setting in SWASH, e.g. a constant horizontal viscosity, the numerical model led to more stable runs. This introduced differences in the wave spectrum at the toe of the structure, see Figure 4.3.

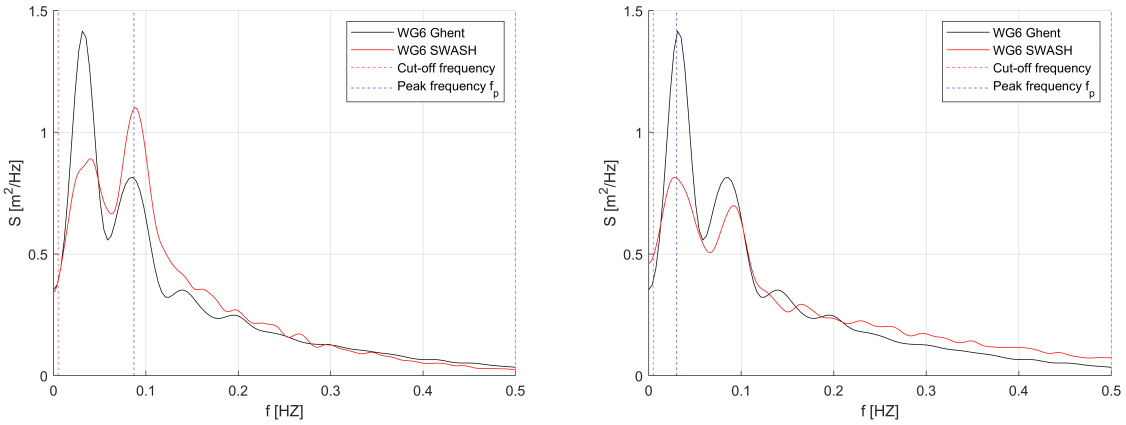

(a) Horizontal viscosity off

(b) Horizontal viscosity constant

Figure 4.3: Difference energy density spectrum at the toe of the structure due to horizontal viscosity setting in SWASH

The wave spectrum at the toe of the structure shows a similar shape compared to the wave spectrum calculated from the physical experiments in Ghent with a constant horizontal viscosity term. However, removing the constant horizontal viscosity results in a shift of the peak frequency as is seen in Figure 4.3.
For the determination of average overtopping discharge, the EurOtop Manual (2018) uses the incident wave height (H_{m0}) and the spectral period ($T_{m-1,0}$) as input parameters. These wave conditions from the spectral analyses were still very similar at both the deep water boundary and at the toe of the structure.

Constant Hor. viscosity		**Hor. viscosity off.**		**Ghent experiment**	
H_{m0} [m]	$T_{m-1,0}$ [s]	H_{m0} [m]	$T_{m-1,0}$ [s]	H_{m0} [m]	$T_{m-1,0}$ [s]
1.48	16.62	1.55	16.48	1.51	16.68

Table 4.2: Spectral wave period $T_{m-1,0}$ at the toe of the structure calculated from energy density spectrum, for model runs with and without constant horizontal viscosity setting in SWASH.

In later model runs with the structure added to the bathymetry, differences were seen in H_{m0} and $T_{m-1,0}$ at the toe compared to the physical experiment. The spectral shape for both model runs with and without a constant horizontal viscosity were still very similar, see Figure B.5 in Appendix B.1.2. However, most of the model runs (with structure) with a constant horizontal viscosity were not long enough to avoid significant variations in statistics (<1000 waves) and crashed, therefore the SWASH simulations were performed without a constant horizontal viscosity.

4.1.3. Wave period

Peak period

The model was able to accurately reproduce the peak period in the deep water section of the model. However, for waves travelling towards the toe of the structure, shoaling and wave breaking change the wave spectrum. The peak period will change as well and has to be checked at the locations of the surface elevation gauges. The peak period can be calculated with the peak frequency f_p determined with the wave spectrum. $T_p = 1 / f_p$. As previously discussed and displayed in Figure 4.3, depending on the horizontal viscosity setting, SWASH was able to reproduce the peak period at the toe of the structure compared to the Ghent experiment.

Spectral wave period

The spectral wave period is calculated with the energy density spectrum, a key parameter in the calculation of wave overtopping since it effects the breaker parameter and the local wave steepness, as discussed in Section 2.2.1. The calculated spectral wave period showed some differences, because of the small inconsistencies discussed in Section 4.1.2.

Test	WG1	WG2	WG3	WG4	WG5	WG6
Ghent exp. [$T_{m-1,0}$]	9.56	9.64	9.86	9.57	10.26	16.68
SWASH [$T_{m-1,0}$]	9.84	9.87	9.90	9.47	10.93	16.48
Difference [%]	2.9	2.3	0.3	1.0	6.6	1.2

Table 4.3: Comparison spectral periods for the Ghent experiments and the SWASH results. The cut-off frequency used for the calculations is 0.005-0.5 Hz, the same values that were used for the Ghent laboratory experiments.

As is seen in Table 4.3 SWASH was able to reproduce the wave conditions at the deep water boundary (WG1) and at the toe of the structure (WG6), within the tolerance limit of 5% for $T_{m-1,0}$.

4.1.4. Characteristic parameters $H_{2\%}$ and H_{max}

It could be argued that the highest waves in the domain are responsible for most of wave overtopping over the structure. Therefore, the highest 2% wave height ($H_{2\%}$) and the maximum wave height (H_{max}) from the numerical SWASH model and the physical experiments in Ghent are compared to one another. Figure 4.4 presents the significant wave height across the domain and $H_{2\%}$ and H_{max}.

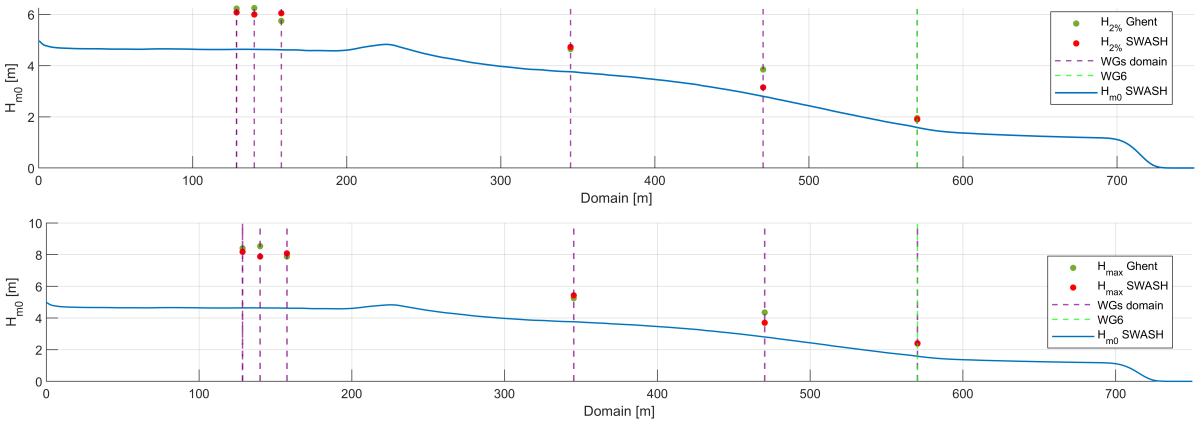

Figure 4.4: Comparison Ghent and SWASH model for characteristic wave heights $H_{2\%}$ and H_{max} over spatial domain

Figure 4.4 shows that the characteristic wave height $H_{2\%}$ and H_{max} for the SWASH model are slightly different from the physical test in Ghent. However, at the locations of interest used for the wave calibration WG1 and WG6, both $H_{2\%}$ and H_{max} are almost equal in value.

In deep water, the probability of exceeding the wave height are following a Rayleigh distribution and a constant relation is found between $H_{2\%}/H_{1/3}$ = 1.4. Figure 4.5 shows the Rayleigh distribution in deep water for the SWASH numerical model and the Ghent experiments.

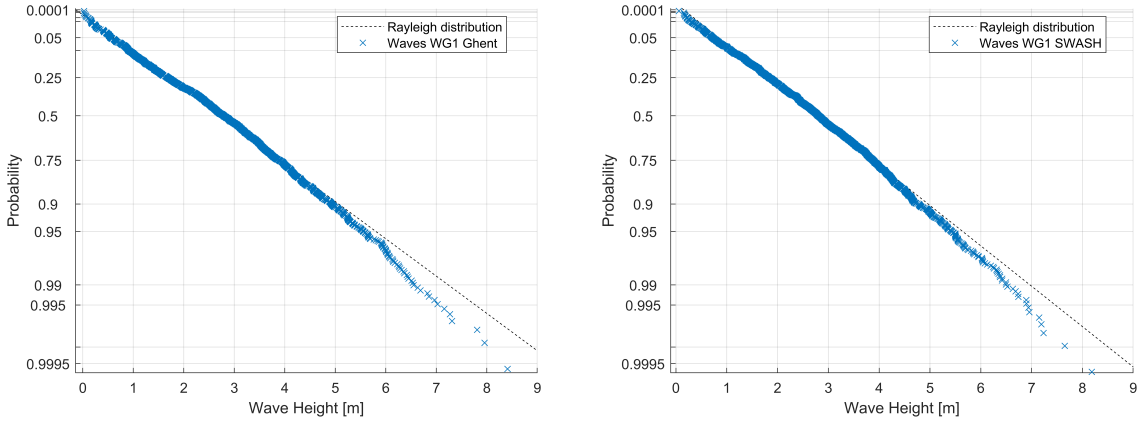

(a) Rayleigh distribution deep water (WG1) Ghent exp.

(b) Rayleigh distribution deep water (WG1) SWASH

Figure 4.5: Rayleigh distribution deep water section of both SWASH model results and the Ghent experiments

As seen in Figure 4.5, the waves waves in deep water did not follow the Rayleigh distribution. This can be explained that this condition ($H_{2\%}/H_{1/3}$ = 1.4) is only valid for a fully developed JONSWAP spectrum and deep water (The EurOtop Manual, 2018). The shallow water conditions in the flume are the reason that waves do not follow the Rayleigh distribution. However, both models showed stable wave conditions in the deep water section of the domain, thus the influence of the bottom on the waves in deep water is assumed to be negligible, as explained in Section 3.2.4.

4.1.5. Wave reflection

The advantage of calibrating the model without structure is that the incident wave height at the toe of structure is easy to determine. Since there is no structure, just a flat part with a wave absorbing sponge layer at the end of the domain, there is no reflection after this point. Therefore, the wave height at the toe of structure is the same as the incident wave height at the toe of the structure.
A abrupt change in the bathymetry can induce wave reflection, since waves feel the bottom. To check if the wave reflection in the domain due to foreshore is comparable for both models, the method developed by Zelt and Skjelbreia (1993) is used. The reflection coefficient in the Ghent experiments calculated with the surface elevation data is 15 % on average. The SWASH surface elevation data resulted in a reflection coefficient of 18 %, which is comparable with the reflection coefficients from Ghent. In Appendix B.1.2 a figure illustrates the separation of the total wave height in an incoming wave height and an reflected wave height.

4.2. Validation wave conditions with structure

The wave conditions in the domain with structure added in the bathymetry are compared to the tests in Ghent. The input wave parameters are the same as for the calibration runs, to asses the influence of structure on the wave parameters in the domain and compare the wave conditions with the physical experiment in Ghent. The comparison of the wave conditions between SWASH and Ghent will later be used to explain possible differences in wave overtopping discharges in Chapter 5.

4.2.1. Spectral analysis deep water and toe of structure

A spectral analysis is performed on the deep water gauge (WG1) and at the toe of the structure (WG6) to determine the significant wave height and spectral wave period, which were used to calibrate the model.

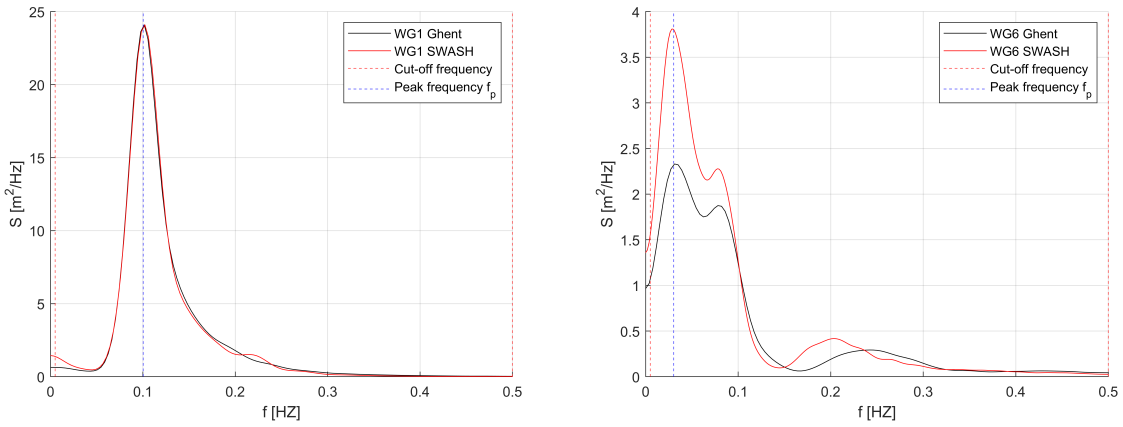

(a) WG1 (b) WG6

Figure 4.6: Wave spectra in deep water conditions (WG1) and at the toe of the structure (WG6). Again cut-off frequency same as Ghent.

H_{m0}

In Figure 4.7 the significant wave height H_{m0} is plotted across the domain for the final wave overtopping runs. As seen in Table 4.4, the wave conditions in the deep water section from SWASH matches the data from the Ghent experiments. Moving closer to the structure and thus in shallower water, the wave height shows larger differences.

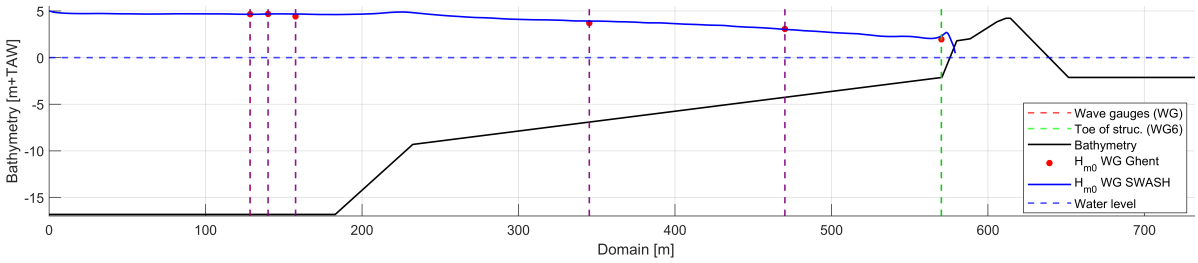

Figure 4.7: Significant wave height over the domain with structure from SWASH results, compared to physical experiments in Ghent

Test	WG1	WG2	WG3	WG4	WG5	WG6
Ghent exp. [H_{m0}]	4.66	4.69	4.42	3.71	3.08	1.97
SWASH [H_{m0}]	4.64	4.68	4.68	3.88	2.98	2.24
Difference [%]	0.4	0.2	5.7	4.5	3.3	13

Table 4.4: Comparison H_{m0} for the Ghent experiments and the SWASH results at WG's in domain with structure. The cut-off frequency used for the calculations is 0.005-0.5 Hz

$T_{m-1,0}$

Test	Period [s]	WG1	WG2	WG3	WG4	WG5	WG6
Gent	$T_{m-1,0}$	9.70	9.70	9.97	9.69	10.28	21.27
SWASH	$T_{m-1,0}$	10.14	10.07	10.26	10.11	12.07	24.45
Difference [%]		4.4	3.7	2.9	4.2	16	14

Table 4.5: Comparison $T_{m-1,0}$ for the Ghent experiments and the SWASH results at WG's in domain with structure. The cut-off frequency used for the calculations is 0.005-0.5 Hz

Possible explanations differences in wave conditions

Compared to the physical experiment, both H_{m0} and $T_{m-1,0}$ show differences at the toe of the structure. At the toe of the structure the spectrum has a similar same shape but the peaks are higher, which was also seen with the higher H_{m0} seen in Table 4.4. Also a clear shift is seen for the 'bulge' around 0.2 Hz. As discussed in Section 4.3, most of the model runs with a constant horizontal viscosity showed numerical instabilities and crashed, as discussed in Section 3.2.4. Not using a constant horizontal viscosity resulted in a slightly different incident wave spectrum, but similar values for H_{m0} and $T_{m-1,0}$. However, this is not a conclusive explanation for the differences in wave conditions at the toe of the structure compared to the Ghent experiment. With structure added to the bathymetry, the model runs with a constant horizontal viscosity setting resulted in a slightly smaller difference in H_{m0} +9.7% vs. +13% without horizontal viscosity (see Table 4.4), but the difference in $T_{m-1,0}$ was even larger +14% vs +24%, see Table B.6 in Appendix B.1.2.

Also, as explained in Section 3.2.4, friction in the model was set to a negligible value. However, using the default values in SWASH for friction factors still resulted in nearly the same differences in the spectrum, it is therefore assumed that the friction is not an explanation for the differences. Other possible explanations for the differences in H_{m0} and $T_{m-1,0}$ at the toe of the structure compared to the physical experiment could be:

- **Reflection of structure: smooth slope vs stepped revetment**
  In SWASH, the stepped revetment was schematized with a smooth slope and increased friction instead of a physical stair case due to numerical limitations, see Section 3.2.4. As waves surge up the structure, the steps of the stepped revetment within the structure dissipate wave energy. Therefore a larger reflection coefficient, and thus higher reflected wave height, was expected for a smooth slope in SWASH compared to the physical experiment with a stepped revetment.
  The reflection coefficient of both model tests is determined with the method proposed by Zelt and Skjelbreia (1993). This resulted in more or less the same reflection coefficient, 0.27 for the Ghent test and 0.26 for SWASH model, See Appendix B.1.2. A comparable reflection coefficient could be explained by the very long wave periods in this case study as they lead to a decreasing effect of the roughness of the steps, as explained in Section 2.3.2. As previously mentioned, no smooth slope reference tests were performed to validate this hypotheses.

- **Numerical limitations**
  van den Bos et al. (2014) found that SWASH performs well to predict the wave-structure interaction with regards to reflection for simple geometries, but is less accurate for more complex structures. The relatively steep slopes and a complex slope of the structure may therefore also be the cause of the differences in wave conditions at the toe of the structure.
  Another reason could be the weakly-reflective wave generation boundary used in SWASH. The weakly reflective wave generation is a wave generation and absorption method in phase-resolving models, based on the assumption that the waves propagating towards the wave generation boundary are small amplitude shallow water waves with direction perpendicular to the boundary (Vasarmidis et al., 2021). This assumption makes the method weakly reflective at the offshore boundary for the reflected dispersive waves in the domain. As a result, resonance may occur in the flume, causing variability in wave spectra and affecting the water level at the toe of the structure. Also, the wave spectrum in SWASH showed an overestimation in the lower energy frequencies. In the surf zone, short waves break, but these infragravity waves propagate ashore as free wave and may cause higher wave heights at the toe of the structure.

4.2.2. Wave conditions and overtopping

It is important to understand that H_{m0} and $T_{m-1,0}$ consider the full wave field in front of the structure, including primary waves and infragravity waves. In Table 4.6 and 4.7, the wave heights, $H_{2\%}$ and H_{max} are given for the SWASH simulations and the Ghent experiment.
The parameter $H_{2\%}$ contains a lot more waves than the number of waves that actually overtopped the structure, which were only a few waves (<5), see Chapter 5. The ten largest waves measured in SWASH and the physical experiments are given in Table B.5 in Appendix 4.2, which were very comparable. An individual waves analysis would be interesting following the hypotheses that the highest waves are responsible for the largest amount of wave overtopping over the structure. Since only a few waves (<5) actually overtopped the structure, it is difficult to asses the consequences of the difference in wave spectrum with respect to actual wave overtopping for this specific case study. Unfortunately, individual overtopping volumes were not measured during the physical experiments, thus a further analysis and comparison was not possible.

Comparing $H_{2\%}$ shows a large difference between both methods, possible explanations for the higher $H_{2\%}$ and H_{m0} are given compared to the physical experiment are discussed in the previous section.

Test	Parameter	WG1	WG6
Gent	$H_{2\%}$ [m]	6.33	2.38
SWASH	$H_{2\%}$ [m]	6.05	2.70
Difference	[%]	4.5	12.6

Table 4.6: Characteristic parameter $H_{2\%}$ at deep water WG1 and at the toe of the structure WG6.

Test	Parameter	WG1	WG6
Gent	H_{max} [m]	8.30	3.35
SWASH	H_{max} [m]	8.30	3.4
Difference	[%]	0	1.5

Table 4.7: Characteristic parameter H_{max} at deep water WG1 and at the toe of the structure WG6.

Figure 4.8 displays the $H_{2\%}$ and H_{max} at various locations along the domain for the SWASH simulations and the Ghent experiment.

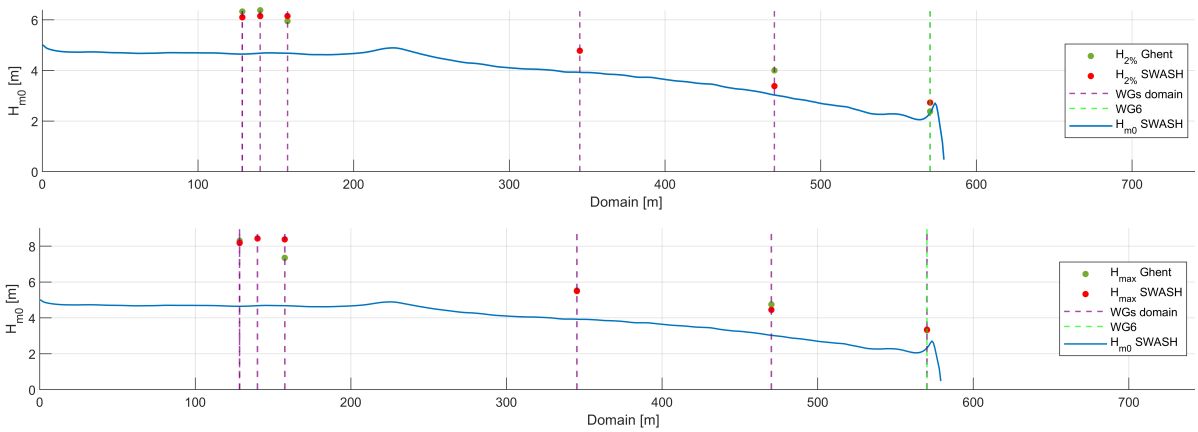

Figure 4.8: Comparison Ghent and SWASH model for characteristic wave heights $H_{2\%}$ and H_{max} over spatial domain

4.3. Overview wave conditions SWASH

It is important to keep in mind that the model was first calibrated to capture the incident wave conditions at the toe of the structure and compare the results with the Ghent experiments. The wave conditions with structure added to the bathymetry were expected to be different compared to the physical experiment because of the wave-structure interaction, varying slope angles, wave breaking, making the numerical calculations complex.

4.3.1. Incident wave conditions

Test	Gauge	H_{m0} [m]	$T_{m-1,0}$ [s]	$H_{2\%}$ [m]	H_{max} [m]
Ghent experiment	WG1	4.62	9.56	6.23	8.3
SWASH	WG1	4.62	9.84	6.08	8.18
Difference [%]		0.24	2.9	2.44	1.46
Ghent experiment	WG6	1.51	16.68	1.95	2.38
SWASH	WG6	1.55	16.46	1.90	2.40
Difference [%]		2.30	1.2	2.60	0.84

Table 4.8: Incident wave conditions SWASH at the deep water section WG1 and at the toe of the structure WG6.

4.3.2. Wave conditions with structure

Test	Gauge	H_{m0} [m]	$T_{m-1,0}$ [s]	$H_{2\%}$ [m]	H_{max} [m]
Ghent experiment	WG1	4.66	9.70	6.33	8.30
SWASH	WG1	4.64	10.14	6.05	8.30
Difference [%]		0.4	4.4	4.5	0.0
Ghent experiment	WG6	1.97	21.27	2.38	3.35
SWASH	WG6	2.24	24.45	2.70	3.40
Difference [%]		12.83	13.9	12.6	1.5

Table 4.9: Wave conditions with structure in SWASH at the deep water section WG1 and at the toe of the structure WG6.

5
Results and analysis: Overtopping

The goal of this chapter is to determine average wave overtopping volumes with the EurOtop Manual (2018) and SWASH, and compare the overtopping results to the physical experiment in Ghent.
In Section 5.2.1, the average overtopping discharge is calculated with the empirical formulas from the EurOtop Manual (2018). The case study includes a stepped revetment in the structure, creating roughness on the slope, for which The EurOtop Manual (2018) uses a roughness influence factor. Based on recent studies by Schoonees et al. (2021), a roughness influence factor has been determined for this particular cross-section. Section 5.2.2 discusses uncertainties for the use of these empirical formulas. The average wave overtopping discharges measured during the SWASH simulations are treated in Section 5.3. Multiple simulations were executed to asses the influence on wave overtopping discharges with different seed numbers to generate random wave fields in the domain. The differences in average overtopping discharge and possible explanations, are elaborated in Section 5.3.1. Thereafter, a stepped revetment is added in SWASH using roughness/friction on the slope of the structure. In Section 5.3.2, the friction/roughness factor is related to the roughness height for the stepped revetment and to an overtopping reduction at the crest of the structure.
Concluding, Section 5.4 shows an overview of the measured/calculated overtopping discharges for both methods compared to the overtopping discharges from the physical experiments in Ghent.

5.1. Schematization of sea defence geometry

The vertical coordinate has to increase per horizontal grid cell in SWASH, which means 2 y-coordinates having the same x-coordinate is not possible. A step with a perpendicular shape can therefore not be defined in the bathymetry in SWASH. Another limiting factor were the number of grid cells, as too much grid cells led to an unstable numerical models and thus inaccurate results in regard to wave conditions and wave overtopping measurements, Section 3.2.4. Therefore, the stepped revetment in the sea defence structure is simulated with a smooth slope in SWASH. As is previously discussed in Section 2.3.2, the EurOtop Manual (2018) uses a roughness reduction factor to add extra friction on the slope of the structure. The procedure, a calculation with the structure being simulated as a smooth slope and adding roughness by means of a friction factor, is therefore more or less similar for both methods.

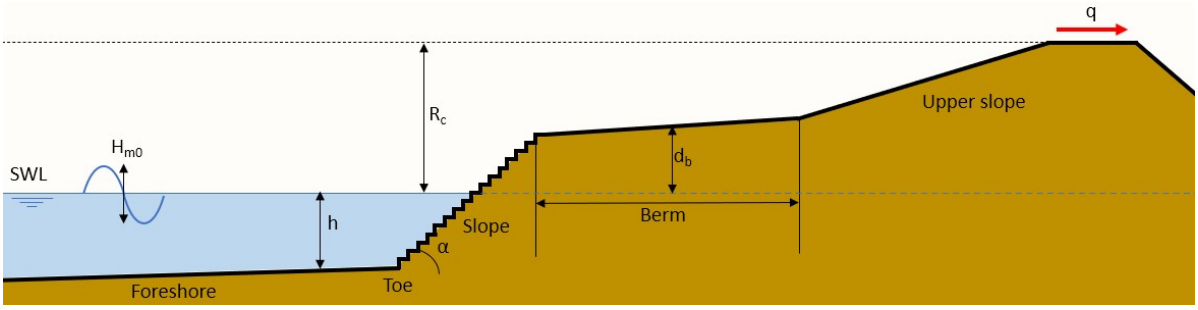

Figure 5.1: Overview of important parameters of cross-section 2b.

5.2. Overtopping with EurOtop Manual

This section uses the determined incident wave conditions from the physical experiment in Ghent to predict the average wave overtopping discharges with formulas from the EurOtop Manual (2018). With recent studies of Schoonees et al. (2021), a roughness influence factor for the stepped revetment has been determined in Section 2.3.2. This estimated roughness influence factor will be used with Eq. 5.15 from the EurOtop manual (mean value approach) to compare the results from the physical model tests with stepped revetment.

5.2.1. Overtopping calculation

As discussed in Section 2.3.1, van Gent (1999), proposed a new formula for shallow water conditions, due to the heavy breaking, the changing (spectral) wave periods and changing spectral shape. The addition of the berm influence factor γ_b in this formula is also explained in Section 2.3.1.

$$\frac{q}{\sqrt{gH_{m0}^3}} = 10^{-0.79} \exp\left(-\frac{R_c}{H_{m0}\gamma_f\gamma_\beta\gamma_b\left(0.33 + 0.022\xi_{m-1,0}\right)}\right) \tag{5.1}$$

In Table 5.1 an overview is given for the input parameters used to calculate the average wave overtopping with formula 5.1. A step by step calculation is given in Appendix C.

H_{m0} [m]	$T_{m-1,0}$ [s]	$\xi_{m-1,0}$ [-]	R_c [m]	γ_f [-]	γ_β [-]	γ_b [-]
1.51	16.68	8.48	4.25	0.75-0.9	1	0.86

Table 5.1: Overview important input parameters for EurOtop Manual (2018) calculations, an overview is given in Figure 5.1.

Using Equation 5.1 and the input parameters from Table 5.1, results in an average overtopping volume for a smooth slope $q_{\gamma_f=1}$ of:

$$q_{\gamma_f=1} = 0.248 \text{ l/s/m}$$

In Section 2.3.2,the roughness reduction factor was estimated and it was explained that a correction was needed for the surging wave conditions. Due to the long wave period for this case study, the corrected roughness influence factor is close to 1. This means a low slope roughness, yet not negligible influence on the average overtopping discharge. This led to the values in Table 5.2. Note that in the remainder of this report, the roughness influence factor γ_f is expressed for breaking wave conditions.

	Lower limit	Upper limit
γ_f =	0.75	0.9
$\gamma_{f,corr}$ =	0.95	0.98

Table 5.2: Estimated roughness influence factor case study and corrected with Equation 2.11 according to (The EurOtop Manual, 2018)

Since the stepped revetment is only located at the lower part of the structure, see Figure 5.7, the roughness along the total structure varies. The EurOtop Manual (2018) suggests for roughness elements on a slope to weigh the various influence factors by including the lengths of the relevant sections of the slope. For three different roughness elements with certain lengths (L), the weighted average roughness influence factor can be calculated with:

$$\gamma_f = \frac{\gamma_{f,1}L_1 + \gamma_{f,2}L_2 + \gamma_{f,3}L_3}{L_1 + L_2 + L_3} \tag{5.2}$$

For this case study, the estimated roughness factors y_f, corrected for the surging wave conditions, are both close to 1, see Table 5.2. Equation 5.2 to estimate the weighted roughness influence factor for various types of roughness elements, is the only available method. Moreover, the proposed formula has not been validated systematically and therefore the accuracy of this formula remains unknown (Chen et al., 2020). Therefore, no weighted roughness influence factor is calculated for this case study.

The average overtopping volumes with the roughness reduction factor in Eq. 5.1 are shown in Table 5.3

Roughness influence factor	γ_f=1	γ_f=0.75	γ_f=0.9
q [l/s/m]	0.248	0.160	0.209
Reduction		- 35.5 %	-15.7 %

Table 5.3: In this Table the roughness influence factors are used in Equation 5.1 to determine the average overtopping discharge q. $\gamma_{y,surg}$ is the corrected roughness factor for surging wave conditions

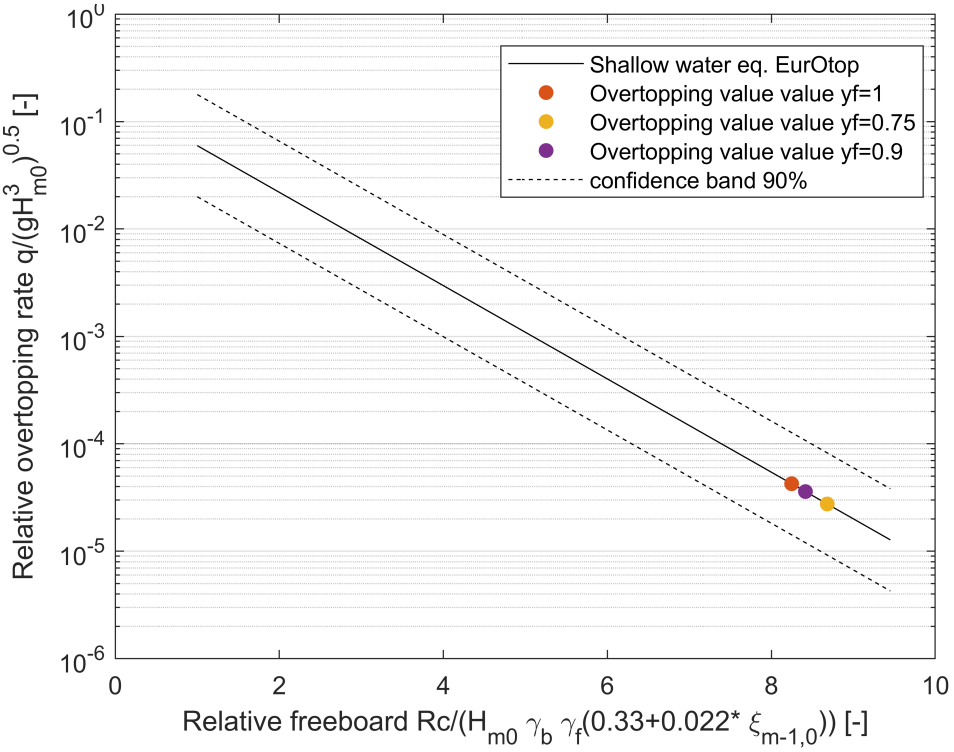

Figure 5.2: Wave overtopping for (very) shallow foreshore conditions, $s_{m-1,0} < 0.01$ and $\xi_{m-1,0} > 5.0$. Altomare et al. (2016) Note that q is displayed in $m^3/s/m$ and the confidence-band of 90% is valid for Equation 5.1 without the added berm factor.

For the estimated roughness influence factor for this case study, an overtopping reduction between 16% and 36% is calculated, as seen in Table 5.3. Altomare et al. (2016) proposed a 90% confidence band for Equation 5.1, which despite the added berm influence factor, is still used in thesis, see Section 2.3.1. The results for calculated average wave overtopping volumes for cross-section 2b with a stepped revetment using the EurOtop Manual (2018), are given in Table 5.4. These values will later be used for further comparison.

Roughness	q [l/s/m]	q_{lower} [l/s/m]	q_{upper} [l/s/m]
γ_f=0.9	0.21	0.07	0.63
γ_f=0.75	0.16	0.05	0.48

Table 5.4: Average wave overtopping discharge for cross-section 2b in Middelkerke according to the EurOtop Manual (2018) and recent studies on the influence of a stepped revetment in slope of the structure. The confidence band of 90% is used as proposed by Altomare et al. (2016).

5.2.2. Uncertainties and sensitivities

Reference tests

The EurOtop Manual uses empirical equations to determine the average wave overtopping at the crest of the structure. Since there is a large spread in the amount of wave overtopping for different wave conditions and structural configurations, the equations are true for a certain confidence interval.
If, during the physical experiments, large difference are seen between the predicted and measured overtopping discharge with a smooth slope, the empirical coefficients can be chosen such that the test results correspond better with Equation 5.1 (van Steeg, 2012). This is than assumed to be the reference case for a smooth slope with a roughness of γ_f = 1. For shallow water conditions this general fitted value is A = -0.79, see Equation 5.1 in Section 5.2.1.

As described in Section 3.1.4, no test runs were performed without the stepped revetment in the structure, i.e. a smooth slope. Therefore, the model test results of the Ghent experiments will be compared with Equation 5.1, using the coefficients for 90%-confidence band as propsed by Altomare et al. (2016).

Berm factor

The formula developed by Altomare et al. (2016) includes a 90%-confidence band, displayed in Figure 5.2. For this case study, the berm influence factor needed to be added to the equation used to predict the average wave overtopping in shallow water conditions. However, the formula has not been verified for shallow water conditions in combination with a berm in the slope of the structure. As described in Section 2.3.2, the berm influence factor depends on the wave conditions in front of the structure. Assuming this confidence band to be valid with a berm influence factor is therefore a bit short-sighted. However, the influence of a berm on wave overtopping is extensively tested for various wave conditions and structure designs in the EurOtop Manual (2018). Therefore, the suggested confidence band of 90%, despite the addition of the berm influence factor, is still used for this case study.

Small overtopping volumes

Especially for low overtopping rates (q< 1 l/s/m), the results are expected to be influenced by scale effects The EurOtop Manual (2018). The relative overtopping rate is an important parameter for the determination of the roughness factor. Schoonees et al. (2021) highlighted that due to the varying overtopping discharges, the roughness influence factor was not a fixed value. Taking the very low overtopping rates for this case study into account, increases the uncertainty with respect to average overtopping discharges. Therefore also a choice has been made for this case study to estimate the roughness factor with a certain range instead of a fixed value.

5.3. Overtopping with numerical model SWASH

Initial model runs showed large differences in overtopping discharges with a smooth slope structure for different seed numbers. Therefore, Section 5.3.1 presents the average wave overtopping discharges measured for the SWASH model runs with different seed numbers. Possible explanations for the large variety in overtopping discharges are discussed in Section 5.3.1 by analysing 3 wave parameters at the toe of the structure: H_{m0}, $T_{m-1,0}$ and $H_{2\%}$.
In Section 5.3.2 a study is performed to determine the roughness of a stepped revetment in the structure with SWASH and relate this to a friction factor/ roughness height.

5.3.1. Average wave overtopping results

During the Ghent experiments, the overtopping discharges showed large differences for different seed numbers. Therefore, also different seed numbers are used to compare the influence of the seed number on wave conditions at the toe resulting in variations in overtopping discharges within SWASH. Figure 5.3 displays a large variety of the averaged overtopping discharges for different seed numbers in SWASH. These are simulations with a constant friction along the slope of the structure, thus the roughness of stepped revetment has not been added yet, to exclude the influence of extra roughness on the wave conditions in front of the structure.
As explained in Chapter 3.2.4, the average wave overtopping results in SWASH are calculated with the layer thickness and average speed of the water column.

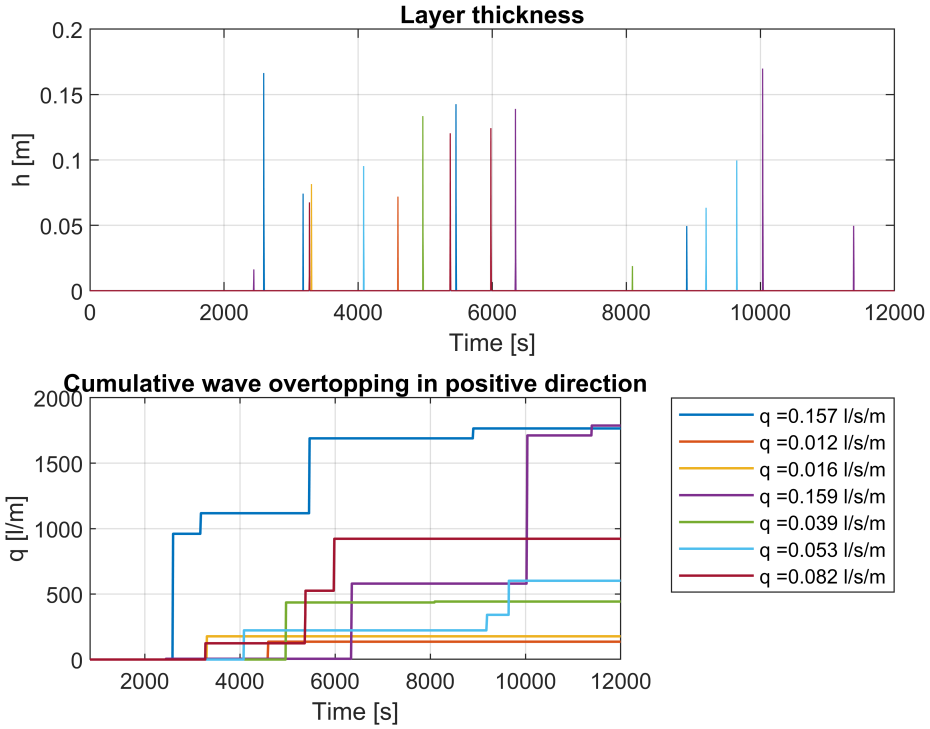

Figure 5.3: Test results for 7 SWASH model runs. The input parameters and boundary conditions are the same for each run, but the seed numbers to generate a random wave field at the boundary are different.

Model run	1	2	3	4	5	6	7
q_{SWASH} [l/s/m]	0.1571	0.0119	0.0158	0.1591	0.0394	0.0535	0.0821

Table 5.5: Measured average overtopping volumes q_{SWASH} for model runs with the same boundary conditions, except for different seed numbers.

5.3.1.1 Explanation differences in overtopping discharges

In Chapter 4, the SWASH model was calibrated based on the deep water gauge (WG1), without structure added to the bathymetry. It was concluded that for both deep water and at the location of the toe of the structure (WG6), SWASH was able to reproduce the incident wave conditions compared to the Ghent experiment within the acceptable tolerances (+/- 3% for H_{m0} and +/- 5% for $T_{m-1,0}$). This is important, because the wave height H_{m0} that is always used in wave overtopping calculations is the incident wave height $H_{m0,i}$ at the toe (The EurOtop Manual, 2018).

To explain the differences in overtopping discharges at the crest with different seed numbers, the wave parameters at the toe of the structure are compared to one another. The most important findings will be highlighted in this section and related to the measured wave overtopping for that particular seed number in SWASH.

The large differences seen for the wave conditions when the structure was added to the bathymetry compared to the Ghent experiments, as discussed in Chapter 4.2, will also be addressed. In Appendix B a full overview is given of all wave parameters in SWASH at deep water (WG1) and at the toe of the structure (WG6), for both the bathymetry with and without structure.

1. **Number of overtopping waves and volumes**
   The overtopping discharges are averaged over time and consist either out of a couple of waves with large overtopping volumes or a larger number of waves with relatively smaller volumes. In Figure 5.3, both appearances occurred, the volume per overtopping wave varied and the number of waves overtopping the crest also showed a range between 1-5 waves. The different number of overtopping waves and volumes causes large variety in averaged overtopping discharges.

2. **Wave height at toe H_{m0} and $H_{2\%}$**
   Changing the seed number resulted in relatively small differences in H_{m0} at the toe for SWASH runs without structure, the incident wave height H_{m0} (<2.6%, see Table 5.6). As displayed in Figure 5.4 a relation is found for both a higher H_{m0} (R^2=0.68) and $H_{2\%}$ (R^2=0.66) resulting in larger average overtopping discharges.
   H_{max} showed no correlation for the average overtopping discharge. An explanation is the different number of overtopping waves that overtopped the structure, which for model runs was limited to only one wave, averaged over a relatively long period of time.

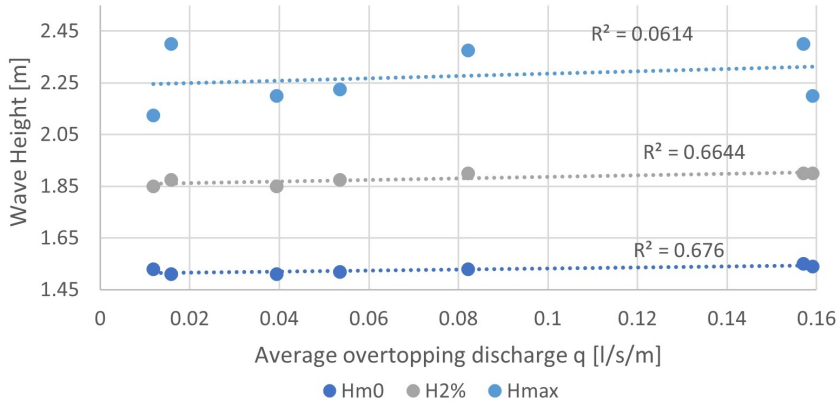

Figure 5.4: Incident wave heights H_{m0}, $H_{2\%}$ and H_{max} at the toe of the structure

Incident		**1**	**2**	**3**	**4**	**5**	**6**	**7**
H_{m0}	[m]	1.55	1.53	1.51	1.54	1.51	1.52	1.53
$H_{2\%}$	[m]	1.9	1.85	1.875	1.9	1.85	1.875	1.9
H_{max}	[m]	2.4	2.125	2.4	2.2	2.2	2.225	2.375
With structure		**1**	**2**	**3**	**4**	**5**	**6**	**7**
H_{m0}	[m]	2.24	2.18	2.13	2.22	2.15	2.16	2.18
q_{SWASH}	[l/s/m]	0.1571	0.0119	0.0158	0.1591	0.0394	0.0535	0.0821

Table 5.6: Average overtopping volumes for different seed numbers in SWASH relative to H_{m0}, $H_{2\%}$ and Hmax at the toe of the structure (WG6).

3. **Spectral wave period at toe $T_{m-1,0}$**
   The largest differences due to a different seed number were seen in spectral wave periods at the toe of the structure. Figure 5.5 shows a positive correlation for an increasing spectral wave period with respect to average overtopping discharges, which is conform with the EurOtop Manual(2018). Again, it is important to note that Model run 1 and 4 have a significantly larger spectral wave period compared to other seed numbers and resulted in the largest average overtopping discharges. The spectral shape at the toe was comparable but there were some differences as well. An overview is given in Appendix B.1.1.

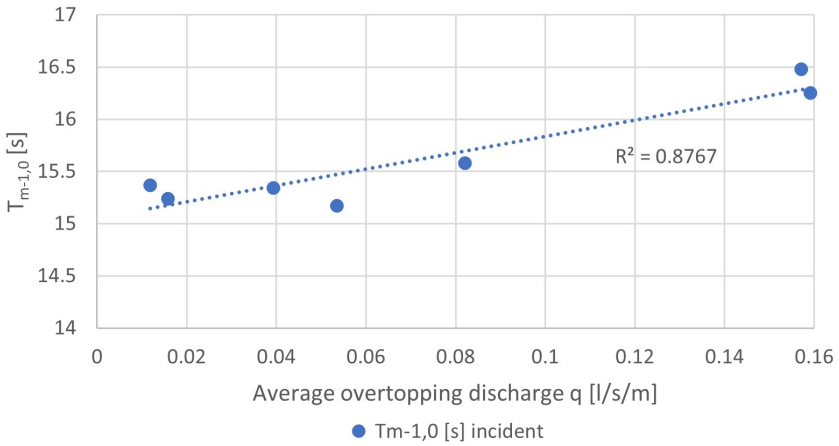

Figure 5.5: Spectral wave period $T_{m-1,0}$ at the toe of the structure, with and without structure added to the bathymetry

Incident		**1**	**2**	**3**	**4**	**5**	**6**	**7**
$T_{m-1,0}$	[s]	16.48	15.37	15.24	16.25	15.34	15.17	15.58
With structure		**1**	**2**	**3**	**4**	**5**	**6**	**7**
$T_{m-1,0}$	[s]	25.45	24.6	24.32	25.73	24.10	24.09	24.81
q_{SWASH}	[l/s/m]	0.1571	0.0119	0.0158	0.1591	0.0394	0.0535	0.0821

Table 5.7: Average overtopping volumes for different seed numbers in SWASH relative to $T_{m-1,0}$ at the toe of the structure (WG6).

Conclusion influence seed number wave overtopping

The results in Table 5.6 and 5.7 show large variabilities in average wave overtopping, but positive relations were found between the average overtopping discharge for H_{m0} and $T_{m-1,0}$ at the toe of the structure. However, $T_{m-1,0}$ was especially long for 2 seed numbers: Model run 1 and Model run 4. The highest H_{m0} was also measured for Model run 1 and 4 compared to the other seed numbers. Both runs resulted in significantly larger overtopping discharges compared to other seed numbers. H_{m0} and $T_{m-1,0}$ at the toe of the structure are key parameters for predicting overtopping discharges (The EurOtop Manual, 2018). Since the difference of $T_{m-1,0}$ at the toe of the structure due to a different seed number is significant (+9%), it is not correct to blindly compare the overtopping discharges from Model run 1 and 4 with the other seed numbers.

If these two model runs are excluded from the data set, the wave conditions at the toe are more comparable and no strong correlations can be found between the measured overtopping discharges and H_{m0} and $T_{m-1,0}$, see Figure 5.6. Which was also seen during the physical experiments in Ghent and confirms that a small number of overtopping waves and small overtopping volumes, increasing the uncertainties with respect to average overtopping discharges (The EurOtop Manual, 2018).

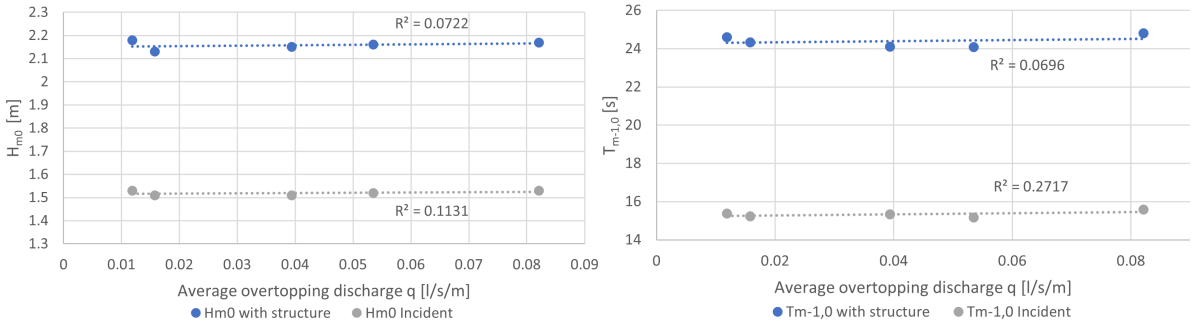

(a) H_{m0} (b) $T_{m-1,0}$

Figure 5.6: Correlation between the average overtopping discharge at the crest of the structure and the wave parameters H_{m0} and $T_{m-1,0}$

However, the goal of this thesis was to reproduce the wave conditions from the physical experiment in Ghent and the target wave conditions were not achieved for most seed numbers, except for model run 1 and 4. $T_{m-1,0}$ at the toe of the structure for the other seed numbers in SWASH was approximately -10% shorter than $T_{m-1,0}$ at the toe in the physical experiments. Also, only 1 data set was available for the overtopping measurement in Ghent. Therefore the SWASH model has been calibrated based on the boundary conditions of that single test, thus only one seed number was used. This is 'Model run 1' in Table 5.6 and 5.7.

It is not correct to determine a root-mean-square error or R^2 for the average overtopping discharges when the incident wave conditions at the toe show such large differences due to a different seed number. Therefore, the average overtopping discharge from 'Model run 1', is considered to be the final result of the SWASH simulations with a smooth slope and will be used to asses the effect of local roughness with SWASH, see Section 5.3.2.

	H_{m0} [m]	$T_{m-1,0}$ [s]	q [l/s/m]
SWASH	1.55	16.48	0.157

Table 5.8: Final results of the SWASH simulation with a smooth slope (Model run 1), no extra roughness for the stepped revetment has been added in this model. H_{m0} and $T_{m-1,0}$ located at the toe of the structure

5.3.2. Prediction roughness influence factor

Chapter 3.2.4 explained that for this case study, 2 different friction coefficients will be used to assess the influence of local friction on the slope of the structure in SWASH on overtopping discharges: the friction coefficient c_f and the Nikuradse roughness height k_s. The goal of this section is to analyse the overtopping reduction at the crest, by adding friction locally at the lower slope of the structure, and relate this reduction to a roughness height/friction coefficient of the stepped revetment.
Initial model runs showed that the overtopping events were very limited and varied a lot depending on the chosen grid point at the crest of the structure. Therefore, the overtopping at the crest varied a lot and especially around sharp angles in the structure, large differences were seen. Therefore, various grid points at the crest of the dike were assessed and the grid cell with the largest discharges was chosen, which was Point 6. Point 5 is also used for the analysis of overtopping reduction, since it is located just below the crest of the dike and will measure more overtopping volumes/events.
Point 1,2,3 and 4 were used to analyse if an increase of the local friction at the lower slope had any effect on the wave volumes and could explain the measured discharges at the crest of the structure, marked in red in Figure 5.7.

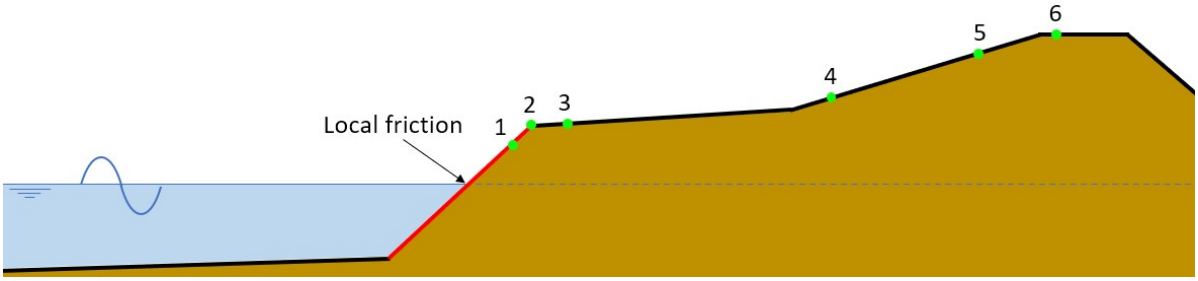

Figure 5.7: This is an overview of the locations were the (overtopping) discharge volumes were measured in the SWASH simulations. Points 1,2, 3 and 4: x = 579 m, x = 580 m, x = 582 m, x=591. Point 5 is located at x = 605. Point 6 is located at the crest of the sea defense structure.

Dimensionless coefficient c_f

Figure 5.8 shows the average wave overtopping discharges at the top of the structure, see Figure 5.7. The dimensionless friction factor c_f was increased up to 0.4. As explained in Section 3.2.4 c_f is related to Chezy and with such high values for c_f, the overtopping volumes were expected to reduce significantly.

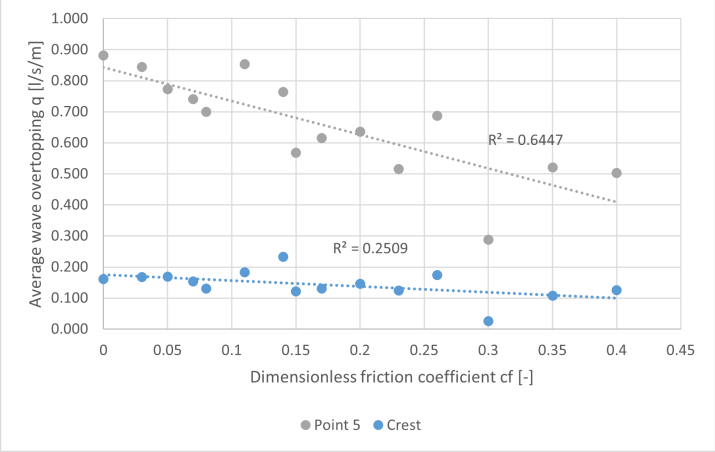

Figure 5.8: Average overtopping discharges in l/s/m for the cross-section at point 5 and the crest (point 6). The x-as displays the increased dimensionless friction factor cf at the lower slope of the structure.

Most of the SWASH simulations crashed, which confirmed the warning from the The SWASH team (2010) that using multiple vertical layers with a dimensionless friction coefficient may result in inaccuracies. The Figure shows a poor relation for the average wave overtopping discharges at the crest of the structure (R^2=0.25). Also, in front of the crest (point 5), a weak linear decrease is found (R^2=0.65).

van Steeg et al. (2018) found that the larger the relative overtopping rate becomes, the less effective the stepped revetment is in reducing overtopping discharges. Waves surging on the slope of the structure, leave a residual layer of water on the structure, making it easier for subsequent waves to run up on. With this hypothesis one could reason that a very large wave is less sensitive to the change in local friction, resulting in no significant effect for the overtopping at the crest of the structure. However, an increase in local friction on the structure, results in energy loss, thus a smaller water layer and/or slower velocity. The influence of the friction may become less effective, but still smaller overtopping volumes at the crest of the dike are expected with an increase in roughness on the slope.
This reduction in discharge was however seen at the other points at the slope of the structure, see Figure 5.9. Confirming that the local friction indeed resulted in small discharges on the slope of the structure. The individual overtopping volumes at the crest however showed no consistencies in the layer thickness and velocity. The use of a dimensionless friction coefficient c_f to asses the influence of roughness at slope on a reduction in overtopping volumes, therefore led to inaccurate results for this case study.

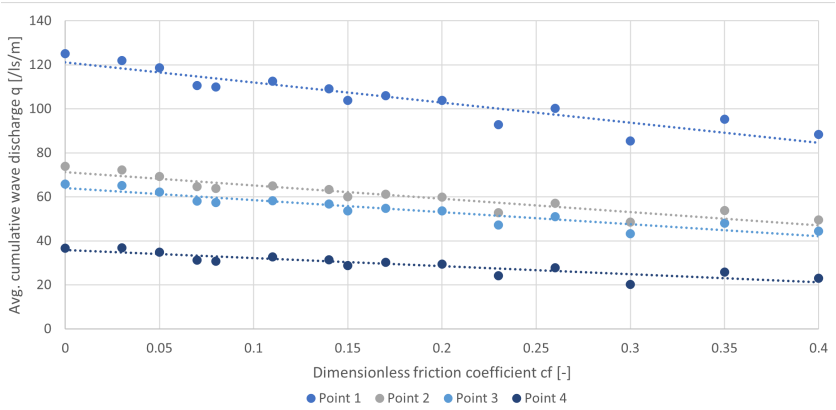

Figure 5.9: Averaged wave discharge volumes in positive direction, measured in the SWASH simulations at point 1,2,3 and 4 from Figure 5.7.

Nikuradse roughness height k_s

The logarithmic wall law was applied for the next model runs using a Nikuradse roughness height as suggested by The SWASH team (2010), see Section 3.2.4. Figure 5.10 shows the results of the overtopping discharges at the crest of the structure.

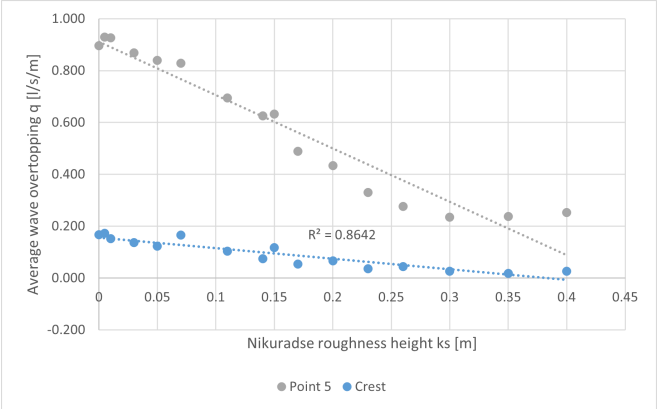

Figure 5.10: Average overtopping discharges in l/s/m for the cross-section at point 5 and the crest (point 6). The x-as displays the increased Nikuradse roughness height k_s at the lower slope of the structure.

Figure 5.10 shows a strong linear fit (R^2 = 0.86) looking at the data at the crest of the structure. For the averaged wave discharges at point 5, a linear decrease is also seen, but for roughness value larger than $\approx k_s$ = 0.25, the effect of friction flattens or even a slight increase is seen. To analyse the cause of this problem, the cumulative discharges at different points (1-4) on the slope of the structure were analysed, see Figure 5.1.

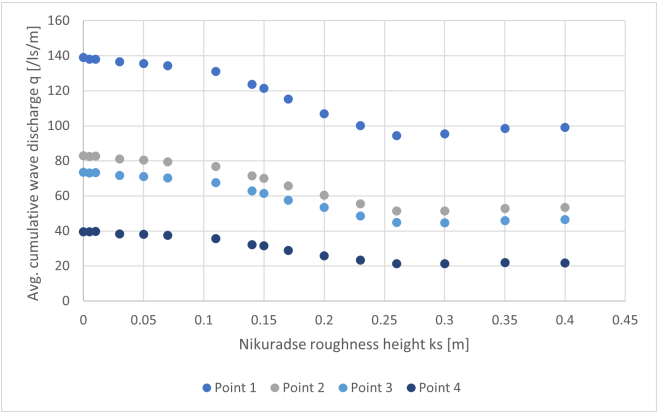

Figure 5.11: Averaged wave discharge volumes in positive direction, measured in the SWASH simulations at point 1,2,3 and 4 from Figure 5.7.

Figure 5.11 shows at approximately k_s=0.25 a sudden increase in the cumulative overtopping volumes with in increasing Nikuradse roughness height. An increase in roughness, results in energy loss and should thus result in smaller discharges. This flattening effect (and slight increase) might be explained with the friction formulation of the Nikuradse roughness height, which usually used for quasi-steady flow conditions, e.g. flow in a river. The calculate the friction coefficient with the Nikuradse roughness height, formula is used:

$$C = \sqrt{\frac{g}{c_f}} = 18\log(12h/k_s) \tag{5.3}$$

With C is Chezy constant, h is water depth and k_s is roughness height. However, for very small water depths, this equation cannot be used. Therefore, Christensen (1972) proposed an equation as a

practical alternative approach (CIRIA, 2007). Note that for $h/k_s>2$, this equation is close to Eq. 5.3

$$C = 18\log(1 + 12h/k_s) \tag{5.4}$$

The layer thickness of the moving water column on top of the structure are within the order of < 5 cm magnitude (model dimensions). The combination of such a small layer of water and relatively high roughness heights, causes the calculated Chezy value to be very small. Using these high values for the Nikuradse roughness height in combination with the small layer thickness of the water column is assumed to be the reason for the flattening of the discharge volumes on the slope. Therefore, the model runs with $k_s> 0.25$ were excluded from the analysis, leading to a linear fit of $R^2 = 0.86$ at the crest of the structure and a linear fit of $R^2 = 0.98$ for point 5, see Figure 5.12.

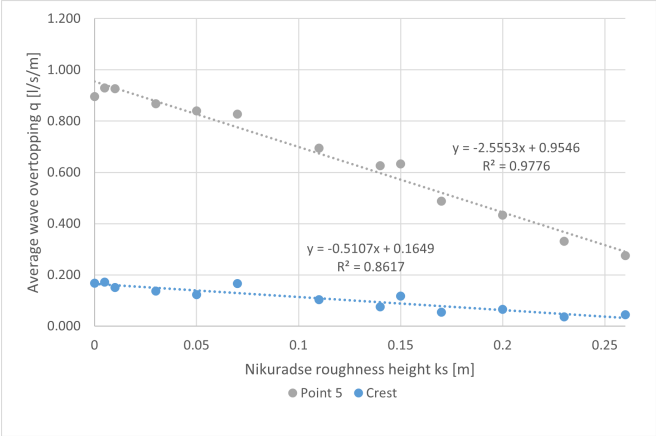

Figure 5.12: Average overtopping discharges in l/s/m for the cross-section at point 5 and the crest (point 6). The x-as displays the increased Nikuradse roughness height k_s at the lower slope of the structure.

Roughness height stepped revetment with SWASH

The estimated roughness influence factor for this case study is between γ_f = 0.75-0.9, as determined in Section 2.3.2. Using the formulas from the EurOtop Manual (2018) and with the determined roughness influence factor γ_f it could be calculated, that γ_f = 0.75 results in an overtopping reduction at the crest of the structure of 36% and γ_f = 0.9 results in an overtopping reduction of 16%.

With the results displayed in Figure 5.12, a roughness height is estimated that leads to these overtopping reduction percentages at the crest of the structure in the SWASH model. As explained before, large differences were measured in discharges at various grid points at the crest of the structure. Therefore, a comparison is made between a lower point at the slope (Point 5) and at the crest of the structure (Point 6), see Figure 5.7. The estimated roughness height with the discharges at Point 5 at the lower part of the slope, were very comparable and thus support the result at the crest of the structure.

The linear correlation (R^2 = 0.86) at the crest and (R^2 = 0.98) at point 5 at the slope obtained from Figure 5.12, lead to the Nikuradse roughness heights in Table 5.9:

Upper slope	k_s [m]	q [l/s/m]	Crest Structure	k_s [m]	q [l/s/m]
Smooth slope	0	0.95	Smooth slope	0	0.16
Overtopping red. 16%	0.06	0.80	Overtopping red. 16%	0.05	0.14
Overtopping red. 36%	0.14	0.61	Overtopping red. 36%	0.12	0.10

Table 5.9: Shows the overtopping reduction (red.) in [l/s/m] compared to the situation with no added friction at the slope of the structure (smooth slope). Upperslope - point 5, Crest - point 6, see Figure 5.7.

The roughness of a bed profile or material can be expressed with a Nikuradse roughness height. In practical engineering, the roughness height in Equation 5.3 is often replaced with the D_{n50} of the material, k_s= $2D_{n50}$, where D_{n50} is median nominal diameter (Schiereck and Verhagen, 2012). The stepped revetment can be schematised as fairly rough bed with rocks of a certain height. Section 2.3.2 explained that the roughness of the stepped revetments (SR) depends on a characteristic step height perpendicular to the slope of the structure: $\cos\alpha^* S_h$ (van Steeg et al., 2018).

The characteristic step height of the stepped revetment for this particular cross-section has a value 0.09, see Section 2.3.2. The results from Table 5.9 would suggest that using 1-1.5 times the characteristic step height for the Nikuradse roughness height, would be a good first estimate for roughness of a stepped revetment for preliminary design calculations.

5.3.3. Scale and model effects

SWASH has no limitations and can capture flow phenomena with spatial scales from centimeters to kilometers and temporal scales from seconds to hours (The SWASH team, 2010). Scale effects come from aspects of resistance scaling which represent the resistance of fluid: the viscosity of the fluid and the bed friction. The influence of both viscosity and bed friction in a small-scale experiment is normally higher than that in the large-scale experiment. For a same viscosity value in the full-scale experiment as in the small-scale experiment, its relative influence decreases if scaling up, as the momentum in the waves increases significantly (Dao et al., 2021). The bottom friction should theoretically increase with a factor of $\alpha_{scale}{}^{1/6}$ for full-scale experiments. The viscosity and bottom friction are therefore both important parameters to consider, since the SWASH model runs are performed in model dimensions.
For the overtopping simulations in SWASH with a smooth slope, thus no extra roughness added for the stepped revetment, the roughness height was set to zero, meaning the bottom is smooth. The influence of the bottom friction is therefore negligible, as discussed in Section 3.2.4. No bed friction effects are expected if the model is scaled up to prototype for the smooth slope runs without roughness added for the stepped revetment.

However, for the prediction of a roughness height with SWASH, the friction value was adjusted and thus may cause differences. Not only the Nikuradse roughness height is an input parameter for the friction value in SWASH, but the water depth or the thickness of the water column (h) is also an input parameter, Eq. 5.5.

$$C = 18\log(12h/k_s) \tag{5.5}$$

In Section 5.3.2, the cumulative overtopping volumes showed a sudden increase in discharge volumes at too high values for the Nikuradse roughness height. It was reasoned that the combination the small layer thickness of the water column and high value of the Nikuradse roughness height probably led to these inaccuracies.
Based on the results in the previous section, it was found that the characteristic step height would be a good first estimate to use as roughness height for a stepped revetment in SWASH. The characteristic step height is a dimensionless number, thus this factor will not change if the model is scaled to prototype dimensions, but the thickness of the water layer will. The influence of the roughness is therefore expected to be relatively large in this case study, compared to a full scale model as will discussed in Chapter 6.

5.4. Comparison SWASH and EurOtop with Ghent experiments

This section gives an overview of the wave overtopping results from SWASH and using the EurOtop Manual (2018) compared to the Ghent experiment. The goal of this thesis was to asses which tool (SWASH, EurOtop) is best to reproduce wave overtopping discharges for the new boulevard Middelkerke containing a stepped revetment, compared to small scale experiments in Ghent. The results are presented in Table 5.10, 5.11 and 5.12, the averaged overtopping discharge for a smooth slope $q_{\gamma_f=1}/q_{k_s=0}$, is also shown as reference.

5.4.1. Ghent Experiment

Only data from one model run was available for this thesis, see Section 3.1.4. For low overtopping rates (q < 1 l/s/m) the results are likely to be effected by scale effects. The Eurotop Manual (2018) therefore suggests to correct the overtopping discharges for physical scale experiments with a scale factor f_{scale}. The roughness of the slope γ_f is an important parameter for this correction and since a range has been proposed in this research, two average overtopping discharges are given.

Influence factor γ_f [-]	**scale factor f_{scale}** [%]	**q** [l/s/m]
1	1	0.078
0.9	1	0.078
0.75	3.23	0.251

Table 5.10: Final overtopping results for the physical scale experiment in Ghent, corrected for scale effects according to the EurOtop Manual (2018).

5.4.2. EurOtop Manual

The predicted of average wave overtopping according to the EurOtop Manual (2018) shows, despite some adjustments of the formula because of the large breaker parameter/shallow water conditions and berm in the slope of the structure, very similar results compared to the physical experiments in Ghent. A range for roughness influence factor for this specific case study has been estimated based on research from Schoonees et al. (2021).

influence factor γ_f [-]	**Overtopping red.** [%]	**q** [l/s/m]	**q_{lower}** [l/s/m]	**q_{upper}** [l/s/m]
1	-	0.248	0.083	0.74
0.9	-16	0.209	0.07	0.63
0.75	-36	0.16	0.054	0.48

Table 5.11: Average overtopping discharges according to the EurOtop Manual (2018). Using the roughness influence factor estimated based on recent studies by (Schoonees et al., 2021).

5.4.3. SWASH

The measured overtopping discharges with the numerical model SWASH are within the same order of magnitude as seen in Table 5.12.

Nikuradse roughness height k_s [m]	**Overtopping red.** [%]	**q** [l/s/m]
0	-	0.16
0.05	-16	0.14
0.12	-36	0.10

Table 5.12: Average overtopping discharge and estimated roughness height and therewith reduction in overtopping for the SWASH simulation.

6
Discussion

Two methods were used in this study to reproduce overtopping discharges measured with a small-scale experiment, for a case study in Middelkerke with a stepped revetment in the geometry: A numerical model SWASH and the empirical formulas according to the EurOtop Manual (2018). The results were compared with data from physical experiments conducted in a small-scale flume in a laboratory of the Ghent University.
Section 6.1 discusses difficulties of using the EurOtop Manual (2018) for this specific case study. In Section 6.2 important findings and uncertainties with respect to the results from the numerical model SWASH are considered. Section 6.3 discusses the uncertainties of small-scale test set-up and measured data of the physical experiment in Ghent.

6.1. EurOtop Manual (2018)

The case study has shallow water conditions, for which a specific empirical formula is proposed by the EurOtop Manual (2018). The formula has been systematically validated for simple geometries, but parameters needed to be adjusted/added for this case study due the complex geometry. This causes uncertainties in the accuracy of the used formula to predict overtopping discharges, since it is has not yet been validated for these adjustments and this specific configuration.

6.1.1. Berm in slope

The EurOtop Manual (2018) uses a berm influence factor for the reducing effect on wave run-up and thus overtopping discharges. A berm is known to reduce the relative amount of wave overtopping and the influence of the berm on overtopping therefore needs to be included in the formula. No tests were performed in the study of Altomare et al. (2016) for shallow foreshores with a berm or varying slope of the structure, and a berm influence factor is therefore not included in the formula. In this study, the berm influence factor was added in the equation for shallow water conditions, but this adaptation has not yet been validated.
Altomare et al. (2016) advised to take a part of the foreshore as 'belonging' to the structure for very shallow foreshores. This results is an adjusted breaker parameter $\xi_{m-1,0}$ to be used as input parameter for the equation. He stated that one should not take the average slope of the sloping structure as proposed by The EurOtop Manual (2018). For this specific case study a berm was present in the structure and not using the average slope resulted in too large overtopping discharges relative to the overtopping discharges measured in the physical experiment in Ghent. Therefore, the average slope of the structure was still used for this case study.

6.1.2. Prediction roughness of a stepped revetment

Research of Schoonees et al. (2021) discovered that the wave period at the toe of the structure was a key parameter for the roughness of the stepped revetment. This case study consists of extreme long wave periods compared to the data sets used to develop the empirical relation. Using the formula outside its range of validity resulted in an influence factor γ_f=0.95, which means that the stepped revetment in this case study has almost no added roughness compared to a smooth slope. The roughness influence factor is expressed for breaking wave conditions and The EurOtop Manual (2018) corrects the roughness influence factors for surging wave conditions, which was also done in the research of Schoonees et al. (2021). For these extreme long wave periods as in this case study, using the wave length in the proposed formula and correcting it for surging wave conditions, might be a bit redundant. Unfortunately, no tests were performed with a smooth slope for the physical experiments in Ghent, to estimate the roughness of the stepped revetment based on the physical experiment.
It is also important to note that a different type of wave field was used in this case study compared to the experiments performed by Schoonees et al. (2021), with both infra-gravity and primary waves, of which only the primary waves are believed to be affected by the roughness of the steps.

6.1.3. Independency influence factors

The influence factors in the EurOtop formulas for the berm and roughness of the stepped revetments, are used as independent and constant values. However, a study of Chen et al. (2020) with roughness elements and a berm, concluded that the roughness value along the structure may vary and the effect of a berm and roughness on wave overtopping are not independent. The water volumes surging on the stepped revetment, lose energy due to friction as they go further up the slope, which results in decreasing water volumes. The influence of the roughness on the volume discharges is therefore not constant along the stepped revetment.
The roughness of the stepped revetment also results in different volumes and water depths on the berm compared to a smooth slope situation. The dependency and varying roughness influence factor along a slope were outside the scope of this research.
Chen et al. (2020) suggests to weigh the roughness influence factors on the slope of the structure with Eq. 6.1. According to The EurOtop Manual (2018) roughness elements outside of the range of SWL – $0.25R_{u2\%,smooth}$ and SWL + $0.5R_{u2\%,smooth}$ have little influence on the overall roughness factor. In this study, this range is mostly covered with the stepped revetment. As previously discussed, the estimated roughness influence factors γ_f corrected for the surging wave conditions, are already close to 1 (γ_f = 1 is smooth slope). Therefore, no weighted roughness influence factor is used in this case study.

$$\gamma_f = \frac{\gamma_{f,1}L_1 + \gamma_{f,2}L_2 + \gamma_{f,3}L_3}{L_1 + L_2 + L_3} \tag{6.1}$$

6.2. SWASH

SWASH was used to reproduce wave overtopping discharges from the small-scale experiment in Ghent. Therewith, local friction on the slope of the structure was added, imitating the roughness of a stepped revetment.

6.2.1. Wave conditions

SWASH was capable of reproducing the incident wave conditions at the toe of the structure of the physical experiment within acceptable limits (+/- 3% for H_{m0} and +/- 5% for $T_{m-1,0}$).
However, with structure added to the bathymetry, H_{m0} and $T_{m-1,0}$ were significantly higher/longer for the SWASH model (+ 13%, 14% respectively) compared to the Ghent experiment. As discussed in Section 4.3, using a constant horizontal viscosity setting in SWASH led to unstable model runs and crashes depending on the seed number. Therefore, it was chosen to not use a constant horizontal viscosity, which resulted in a slightly different incident wave spectrum. However, model runs with structure added to the bathymetry, with and without a horizontal viscosity still resulted in a very similar wave spectrum, see Figure B.5 in Appendix B.1.2.
Also, as explained in Section 3.2.4, to prevent friction having a dominant effect on the waves surging on the structure, friction in the model was set to a negligible value. However, using the larger friction values still resulted in nearly the same differences in the spectrum, meaning friction is not the explanation for the difference in H_{m0} and $T_{m-1,0}$. Thus, no clear explanation was found, but it could be the difference in geometry of the structure or numerical limitations in SWASH:

1. The cross-section in SWASH was schematized with a smooth slope since the stepped revetment could not accurately be implemented in the bathymetry. This could be a reason for the higher H_{m0} for the smooth slope structure in SWASH compared to the physical experiment with a stepped revetment. However, the reflection coefficient was calculated for both models and was approximately the same. Unfortunately, no smooth slope test was conducted during the physical tests to validate the difference in reflection compared to a stepped revetment.

2. van den Bos et al. (2014) found that SWASH performs well predicting the wave-structure interaction with regards to reflection for simple geometries, but is less accurate for more complex structures. The relatively steep slopes and a varying topographic slope of the structure may caused differences in wave conditions at the toe of the structure.
   Another reason could be the inflow boundary in SWASH, which is weakly reflective for dispersive waves (Vasarmidis et al., 2021). It could be that reflected dispersive waves in the domain are not fully absorbed at the inflow boundary and thus re-reflect into the domain.

6.2.2. Overtopping discharges

The results for the average overtopping discharge in SWASH were within the same order of magnitude as the physical experiment in Ghent. However, there are two important notes:

1. Only a limited number of waves (1-5) overtopped the structure, with large variety in volumes. Part of these differences could be explained by the fact that a different seed number, resulted in significant variations in spectral wave periods at the toe (10 %). Still, for different seed numbers resulting in approximately the same incident wave conditions at toe of the structure, the overtopping discharges showed large differences. These differences in average wave overtopping were also seen in the physical experiments in Ghent.

2. Secondly, with the structure added to the bathymetry, large differences were seen for $H_{m-1,0}$ (13%) and $T_{m-1,0}$ (14%) compared to the physical experiment. It might therefore be a bit short-sighted to conclude based on the incident wave conditions alone and the overtopping discharges measured at the crest of the structure, that SWASH was able to produce similar results in overtopping discharges compared to the small-scale experiment in Ghent.
   On the other hand, it is important to note that the for the determination of H_{m0} and $T_{m-1,0}$ the full wave field is used, including primary waves and infragravity waves. Only some of the highest waves will reach the crest and generate wave overtopping. The highest waves in SWASH and the physical experiment were very comparable and only a few waves were large enough to eventually overtop the structure. The limited number of overtopping waves made it difficult to asses the consequences of the difference in wave spectrum at the toe with respect to the actual measured wave overtopping discharges.

Prediction roughness of a stepped revetment

A strong fit was found between an increase of the roughness at the lower slope of the structure and the overtopping reduction at the crest. It was found that using 1-1.5 times the characteristic step height as Nikuradse roughness height, seems to be a valid first estimate for preliminary design calculations.
However, the SWASH model was an exact copy of the physical experiment, thus small scale dimensions. The results from SWASH showed inconsistencies for a Nikuradse roughness height $k_s > 0.25$ m, which is probably caused by the extreme small water depths on the slope for this small-scale model. The characteristic step height is a dimensionless number, thus this factor will not change if the model is scaled to prototype dimensions, but the thickness of the water layer will. The relative influence of the added roughness at the slope on the water volumes is therefore expected to be larger for this SWASH model compared to a full-scale SWASH model. A relatively higher roughness height is expected to be needed to result in the same amount of overtopping reduction at the crest of the structure for a full-scale SWASH model. This is also a very promising expectation for future research, since in practical engineering for rough (rocky) river bed, choosing a roughness height of a couple of times the median nominal diameter of the rock, is a common approach (Schiereck and Verhagen, 2012).

6.3. Uncertainties physical experiment

The test results in Ghent showed large variabilities in average overtopping discharges. As previously discussed, caution should be applied with adopting scale experiment results for design purposes, especially for small overtopping volumes The EurOtop Manual (2018). Some important notes are highlighted regarding the model set-up and test results of the physical experiments in Ghent.

6.3.1. Surface elevation gauges

The SWASH model was calibrated with deep water wave gauges from the Ghent experiments. The third surface elevation gauge showed significant differences compared to the first two gauges. The inter-distances between all three of them is determined according to the spacing proposed by Mansard and Funke (1980). Since WG3 showed such differences compared to WG1 and WG2 for the physical experiments, the surface elevation gauge might be placed to close to the foreshore. This could not be verified and a measurement error could be an explanation as well.

6.3.2. Scale and model effects

Scaling was achieved using Froude similarity for the experiments in Ghent. Therefore, the Reynolds number is not scaled correctly, which might lead to scale effects. According to the EurOtop Manual (2018) overtopping discharges measured at rougher slopes in small scale experiments are often underestimated, especially when overtopping rates are low ($q < 1$ l/s/m). Schoonees et al. (2021) also found that small-scale experiments overestimate the ability of stepped revetments to reduce wave overtopping. The quantification of scale effects is difficult, because it is hard to recreate the same conditions for different scales in order to isolate the scale effects (Burcharth and Andersen, 2009).
Williams et al. (2019) concluded that lower overtopping rates and lower probability of overtopping similarly show greater variability in overtopping, which was also seen in both the physical experiment and SWASH simulations.

Model effects are also important to keep in mind for the accuracy of physical scale experiments. This includes factors such as the negligence of the wind, simplified bathymetry of the foreshore, simplified geometry of structure, no oblique wave attack and the width of the overtopping channel can also cause model effects.

7
Conclusion

The objective of this thesis was to assess the feasibility of a modern-day empirical method (EurOtop) and a process-based numerical model (SWASH), to predict the average wave overtopping discharge for the new boulevard Middelkerke containing a stepped revetment and compare them with measurements from physical scale experiments.
The main research question of this study is:

How to use SWASH and the EurOtop to reproduce average wave overtopping discharges measured in small scale physical model tests, for the new boulevard Middelkerke with a stepped revetment in shallow water conditions?

The equation developed by Altomare et al. (2016) in The EurOtop Manual (2018) to determine the average wave overtopping in shallow water conditions, is only validated for simple geometries. The equation has no influence factor to include the effect of a berm in the structure. Therefore, a berm influence factor was added to the equation, for which it is important to note that the (adjusted) empirical formula is thus used in a configuration for which the equation has not (yet) been validated.
Recent studies by Schoonees et al. (2021) discovered that the influence of the roughness of a stepped revetment on overtopping discharge mainly depends on: the characteristic step height ($\cos \alpha \cdot S_h / H_{m0}$), relative overtopping discharge and the wave period at the toe of the structure. Using the study of Schoonees et al. (2021) as guideline, the roughness influence factor for the stepped revetment in this case study was determined to range between γ_f = 0.75-0.9. With the (adjusted) equation from Altomare et al. (2016), this resulted in average overtopping discharges comparable with the measurements from the physical experiments in Ghent, see Table 7.1.

The model was calibrated based on the incident wave conditions (without structure), which are generally used to determine the average wave overtopping discharges (e.g. EurOtop) and to exclude reflection from the structure in the domain. SWASH was capable to accurately reproduce the target incident H_{m0} and $T_{m-1,0}$ at the toe of the structure for the same deep water wave conditions as in the physical experiment.
Since the model was calibrated based on the incident wave conditions, this inherently means that larger deviations may occur on other points in the domain: differences up to 14% for H_{m0} and $T_{m-1,0}$ were seen with the structure added to bathymetry compared to the physical experiment, for which no explicit reason was found. An explanation could be the difference in geometry of the structure, where for the experiment in Ghent a stepped revetment was present and in SWASH a smooth slope was schematized. Another explanation could be numerical limitations, such as the wave-structure interaction or the weakly reflective offshore boundary in SWASH.
Still, the difference in H_{m0} and $T_{m-1,0}$ does not necessarily mean that the measured overtopping discharges are not comparable with the physical experiment, as for the determination of H_{m0} and $T_{m-1,0}$ the full wave field is used, including primary waves and infragravity waves. Only some of the largest waves will reach the crest and generate wave overtopping. In this case study, the limited number of overtopping waves (1-5) made it difficult to asses the consequences of the difference in wave spectrum at the toe with respect to the measured average wave overtopping discharges.

An overly fine grid was needed to schematize a stepped revetment in the cross-section in SWASH, causing numerical instabilities in the model. The stepped revetment was therefore schematised with a smooth slope and roughness was added at the location of the stepped revetment. Using the Nikuradse roughness height as friction factor resulted in a strong relation between the added roughness at the slope of the structure and the overtopping reduction at the crest. A Nikuradse roughness height of 1-1.5 times the characteristic step height, resulted in average overtopping discharges that were similar to the measured overtopping discharges from the Ghent experiment.
Using roughness/friction at the (smooth) slope of the structure in SWASH to represent the stepped revetment in the cross-section, showed very encouraging results for future studies. SWASH could be used as a 'numerical laboratory' to further parameterize the influence of roughness on wave overtopping for a wide range of boundary conditions and structural configurations. Once systematically validated, the results can be related to Nikuradse roughness heights to be used in practical engineering or influence factors as used in the EurOtop Manual (2018).

The predicted overtopping discharges using the EurOtop and SWASH, compared to the measurements from the physical experiment in Ghent are given in Table 7.1.

q_{Ghent} [l/s/m]	$q_{EurOtop}$ [l/s/m]	q_{SWASH} [l/s/m]
0.08-0.25	0.16-0.21	0.10-0.14

Table 7.1: q_{Ghent} measured and corrected for possible scale effects according to the EurOtop Manual (2018). For q_{SWASH} and $q_{EurOtop}$ a range is given since two roughness factors were assessed.

The EurOtop and SWASH produced a good first estimate of the expected average wave overtopping for this specific case study compared to the physical experiment. Each method has their own benefits and limitations, thus in practical engineering they are often used side by side, to increase the accuracy of the results. Physical experiments are time consuming and expensive, the empirical equations in the EurOtop are quick and much easier to use, but for more complex situations and geometries often outside the range of validity.
This is were SWASH is advantageous and has shown a lot of potential, since it is still relatively easy to use and a quick numerical model. Moreover, it gives more detailed information than only an average q: it gives spatially and temporarily varying surface elevations and velocities along the domain and on the slope of the structure. Extreme values of the velocity and therewith forces on the structure can be calculated and individual (overtopping) waves can easily be assessed with the use of SWASH. The first results of this case study are very promising and confirm the potential of using SWASH to predict overtopping discharges for more complex geometries, supporting the research of Gruwez et al. (2020b).

8
Recommendations

This chapter describes suggestions for future research for the prediction of wave overtopping discharges with the SWASH. The low overtopping discharges caused uncertainties in the results of this case study, but were nevertheless very promising for future research. First, recommendations will be given for using SWASH for the specific conditions regarding this case study. Also suggestions are given for future measurements with physical scale experiments, to make a better comparison for the overtopping volumes in SWASH possible.

8.1. Numerical model: SWASH

8.1.1. Repetition methods used case study

The complex geometry of the dike, limited number of overtopping waves (1-5) and a small average overtopping rate (q « 1 l/s/m), all resulted in uncertainties in the accuracy of the measured overtopping discharges. A systematical approach of the methods used in this case study, using existing experiments with more overtopping waves/volumes and a simple geometry with stepped revetment, would make the results of the average overtopping discharges more reliable, as discussed in Section 5.2.2. The full-scale experiments conducted by Schoonees et al. (2021) would be an interesting case study with a simple cross-section with stepped revetment, a large number of overtopping waves and less complex wave conditions (primary waves, non-shallow water conditions).
An assessment of the individual of overtopping events by means of a cumulative overtopping method could provide useful insight for cases with complex geometry. The study of Schoonees et al. (2021) showed that the individual overtopping volumes at stepped revetment SR also follow a Weibull distribution, consistent with the literature for overtopping volumes without stepped revetment. (Schoonees et al., 2021) also found a linear relation between the maximum measured overtopping volume and the average overtopping rate. Analysing individual overtopping volumes and maximum overtopping volumes could enlarge the understanding of the applicability of SWASH for the prediction of average overtopping volumes for complex cross-sections.

8.1.2. Parameters SWASH

During the calibration of the SWASH model, the wave conditions in the domain were very sensitive to the input parameters. For most of the settings, default values were used, but some parameters could be interesting to evaluate with future model runs.

Settings and Numerical schemes

For the wave transformation in SWASH, different numerical schemes can be selected for the approximation of the non-hydrostatic pressure, space discretisation and time integration (Zijlema et al., 2011). The default schemes are used in the SWASH model based on the amount of vertical layers used in the model, as recommended in The SWASH team (2010). The horizontal viscosity in SWASH was an important parameter, since a constant horizontal viscosity resulted in unstable model runs and crashes. Using different numerical schemes was not within the scope of the thesis.
A sensitivity study using different numerical schemes/settings and vertical layers for a bathymetry with a complex cross-section might give new insights in explanations for the differences seen in wave conditions in this case study and why some model runs crashed.

Bottom friction
To represent a stepped revetment in the structure roughness was added on the slope with a Nikuradse roughness height. The SWASH team (2010) advised to use a logarithmic wall law, since inaccuracies may occur for other friction coefficients in the vertical of the structure of the velocity when multiple vertical layers are used. For this case study three vertical layers were used, since this is considered to be enough for typical wave simulations (Zijlema et al., 2011). It would be interesting to test what would happen when more or less vertical layers are used, since the overtopping wave discharges are turbulent and thus consist of variable velocities over the vertical.

Wave generation method
The surface elevation time series from the physical experiment can be implemented in the wave generating boundary in SWASH. The influence of a random seed number is then excluded from the results. This has not been conducted in this research, since this wave generation method may cause differences as the frequency dispersion and non-linear effects will still lead to differences for the wave propagation in the SWASH model. Suzuki et al. (2011) noticed that for the SWASH simulations a (small) deviation was seen in surface elevations closer towards the structure, compared to data from a physical experiment. However, it would be interesting to see if this time series as wave input would lead to smaller differences in wave conditions compared to the Ghent experiment.
The offshore wave generation boundary in SWASH is weakly reflective for dispersive (and directional) waves. It is possible that the difference in wave spectrum at the toe with structure added to bathymetry could be explained with dispersive waves that re-reflect at the inflow boundary. Recent study of Vasarmidis et al. (2021) showed that using an internal wave generation method leads to a significantly more accurate prediction of the resulting wave field in case of waves reflected back to the numerical boundary.
The duration of the SWASH model runs were chosen such that a comparable number of waves was generated compared to the Ghent experiment. A longer duration would increase the reliability of the averaged overtopping discharge results, as a longer duration leads to more overtopping waves.

8.2. Future scale experiments overtopping discharges

8.2.1. Smooth slope test

Unfortunately, no smooth slope tests were performed for the small scale experiments. Therefore the differences in wave conditions with SWASH at the toe with structure added to the bathymetry compared to the physical experiment, could not be verified. It was speculated that an explanation could be the higher reflective characteristic of a smooth slope compared to a stepped revetment. A smooth slope reference test might have led to explanations for possible differences in wave conditions and overtopping discharges. For future studies and small scale experiment it is therefore recommended to first do a smooth slope reference test, to better asses the influence of the stepped revetment in the (complex) cross-section. This smooth slope test can also be used to calibrate the empirical coefficients such that the test results correspond better with the EurOtop (van Steeg, 2012).

8.2.2. Measurements physical experiment

It is common to asses the average overtopping discharge by dividing the volume that is gathered in a tank behind the structure by the test duration and tank width. However, the wave overtopping discharges showed large varieties in volumes and an assessment of individual overtopping waves would be interesting. Especially for similar conditions as this case study, where only a few waves averaged the crest of the structure during a two hour storm.
It would be interesting the asses the run up height for a structure with varying slope angles and compare this to the run up height that is measured in SWASH simulations. Especially for this case study, were only a limited amount of waves overtopped the crest of the structure, assessing the volume discharges at various points on the slope of the structure, could provide useful insight.
Particle velocities are hard to measure during physical experiments as are small discharges on the slope of the structure. A camera could be placed next to the flume, where the layer thickness of an overtopping wave along the slope of the structure could be captured. With this the speed of the moving water column at various points on the slope of the structure could be analysed. In SWASH the

layer thickness and speed of the water column are easily calculated and processed. The inability of the numerical model to reproduce the water tongue of the waves surging the structure could then be compared with data from the physical experiment.

8.2.3. Overtopping discharges and slope roughness

The roughness influence factor are used as constant values in the formulas in the EurOtop Manual (2018). However, waves surging up to the crest of the structure experience friction, which decreases both the velocity and layer thickness of the water column. The relative overtopping discharge is also very important, since a relatively large overtopping wave is less affected by the roughness of the structure compared to a smaller wave. Besides, an overtopping wave may leave a residual water layer on the steps, making it easier for subsequent waves to run up on Schoonees et al. (2021). More research is needed for the possibility of the varying value of the roughness influence factor along the slope itself. SWASH could be a useful tool to analyse this changing roughness along a slope, since it is possible to vary the friction factor along the slope.

8.3. SWASH vs. OpenFOAM

The main advantage of using SWASH for overtopping calculations is it is quick, robust and recent studies confirm that for simple geometries, the overtopping discharges are predicted relatively well (van den Bos et al., 2014). However, SWASH seems to have difficulties for more complex structures Suzuki et al. (2011). It would be interesting to compare overtopping results for a similar case study with a complex geometry and stepped revetment with a physical experiment, SWASH and with a more advanced numerical model, for example OpenFOAM.
Studies showed that modelling with a Reynolds-averaged Navier–Stokes (RANS) model (i.e. OpenFOAM®) can provide very similar results to large-scale experiments of overtopped wave impacts on coastal dikes with a very shallow foreshores (Gruwez et al., 2020a). Recent studies by Gruwez et al. (2020a); Jacobsen et al. (2015) showed very promising results for the modelling of interaction of waves and structures, even for more complex structures. The study of Gruwez et al. (2020a) also showed reasonable behaviour of the reduction of wave overtopping influenced by a berm and roughness.
For this case study a structured grid is employed where each interior cell is surrounded by the same number of cells. In unstructured grids however, this number can be arbitrarily. For this reason, the level of flexibility with respect to the grid point distribution of unstructured grids is far more optimal compared to structured grids (The SWASH team, 2010). This could be a solution the better schematize the stepped revetment in SWASH and would therewith still be a lot quicker than OpenFOAM.

References

Altomare, C. , Suzuki, T. , Chen, X. , Verwaest, T. , and Kortenhaus, A. (2016). *Wave overtopping of sea dikes with very shallow foreshores*. Coast. Eng. 116, 236–257.

Battjes, J. (1974). *Surf Similarity*. In Proceeding 14th International Conference on Coastal Engineering, pages 466– 480, Copenhagen.

Bosboom, J. and Stive, M.J.F. (2021). *Coastal Dynamics*. Delft University of Technology, Delft, The Netherlands. Revision no. 1269.

Burcharth, Hans F. and Andersen, Thomas Lykke (2009). *Scale Effects Related to Small Physical Modelling of Overtopping of Rubble Mound Breakwaters*.

Chen, W. , Marconi, A. , van Gent, M. R. A. , Warmink, J. J. , and Hulscher, S. J. M. H. (2020). *Experimental Study on the Influence of Berms and Roughness on Wave Overtopping at Rock-Armoured Dikes.* Journal of marine science and engineering, 8(6), 1-21. [446]. https://doi.org/10.3390/jmse8060446.

CIRIA, CETMEF , CUR (2007). *The rock manual : the use of rock in hydraulic engineering.* C683, CIRIA, London.

CLASH (2004). *Crest Level Assessment of coastal Structures by full scale monitoring, neural network prediction and Hazard analysis on permissible wave overtopping*. Fifth Framework Programme of the EU, Contract n. EVK3-CT-2001-00058. www.clash-eu.org.

Dao, T. H. , Hofland, B. , Suzuki, T. , Stive, M. J. F. , Mai, T. , and Tuan, L. X. (2021). *Numerical and Small-scale Physical Modelling of Wave Transmission by Wooden Fences*. Journal of Coastal and Hydraulic Structures, 1. https://doi.org/10.48438/jchs.2021.0004.

David Gallach-Sánchez, Andreas Kortenhaus , Peter Troch (2018). *Average and wave-by-wave overtopping perfomance of stepp low-crested structures*. Coastal Engineering 2018 Vol 36.

de Wit, F. (2016). *Tide-induced currents in a phase-resolving wave model*. Master's thesis, TU Delft, Delft University of Technology.

Dobrochinski, J. P. (2014). *A combination of swash and harberth to compute wave forces on moored ships.* Master's thesis, TU Delft, Delft University of Technology.

Gruwez, V. , Altomare, C. , Suzuki, T. , Streicher, M. , Cappietti, L. , Kortenhaus, A. , and Troch, P (2020a). *Validation of RANS Modelling for Wave Interactions with Sea Dikes on Shallow Foreshores Using a Large-Scale Experimental Dataset*. J. Mar. Sci. Eng. 2020, 8(9), 650; https://doi.org/10.3390/jmse8090650.

Gruwez, Vincent , Altomare, Corrado , Suzuki, Tomohiro , Streicher, Maximilian , Cappietti, Lorenzo , Kortenhaus, Andreas , and Troch, Peter A. (2020b). *An Inter-Model Comparison for Wave Interactions with Sea Dikes on Shallow Foreshores*, volume 8.

Hofland, B. , Chen, X. , Altomare, C. , and Oosterlo, P. (2017). *Prediction formula for the spectral wave period $T_{m-1,0}$ on mildly sloping shallow foreshores*. Coastal Engineering, 123:21–28.

Jacobsen, Niels G. , van Gent, Marcel R.A. , and Wolters, Guido (2015). *Numerical analysis of the interaction of irregular waves with two dimensional permeable coastal structures*, volume 102.

Jordans, L.M.A. (2019). *The average wave overtopping discharge for a composite slope: A case study to the Afsluitdijk rehabilitation project*. Master's thesis, TU Delft, Delft University of Technology.

Kerpen, Nils B. , Schoonees, Talia , and Leibniz, Torsten Schlurmann (2019). *Wave Overtopping of Stepped Revetments*. Journal: Water 2019, 11, 1035.

Mansard, E.P.D. and Funke, E.R. (1980). *The Measurement of Incident and Reflected Spectra Using a Least squares Method*. ASCE - Texas Digital Library, Int. Conf. on Coastal Engineering (ICCE), 1980, Sydney.

Romano, A , Bellotti, G. , Briganti, R. , and Franco, L. (2015). *Uncertainties in the physical modelling of the wave overtopping over a rubble mound breakwater: The role of the seeding number and of the test duration*. Coastal Engineering, Volume 103, 2015, Pages 15-21, ISSN 0378-3839, https://doi.org/10.1016/j.coastaleng.2015.05.005.

Schiereck, G.J. and Verhagen, H.J. (2012). *Introduction to Bed, bank and shore protection: Engineering the interface of soil and water*. VSSD:ISBN 978-90-6562-306-5, NUR 956.

Schoonees, Talia , Kerpen, Nils B. , Liebisch, Sven , and Schlurmann, Torsten (2018). *WAVE OVERTOPPING PREDICTION OF A GENTLE SLOPED STEPPED REVETMENT*. Coastal Engineering Proceedings, 1(36), papers.99. https://doi.org/10.9753/icce.v36.papers.99.

Schoonees, Talia , Kerpen, Nils B. , and Leibniz, Torsten Schlurmann (2021). *Full-scale experimental study on wave reflection and run-up at stepped revetments*. Coastal Engineering November 2021 Vol 167.

Schüttrumpf, H. and Oumeraci, H. (2005). *Layer thicknesses and velocities of wave overtopping flow at seadikes*. Coastal Engineering, 52:473–495.

Smit, Pieter B. , Zijlema, Marcel , and Stelling, G. S. (2013). Depth-induced wave breaking in a non-hydrostatic, near-shore wave model. *Coastal Engineering*, 76:1–16.

Suzuki, T. , Verwaest, T. , Hassan, W. , W., Veale , Reyns, J. , Trouw, K. , Troch, P , and Zijlema, M. (2011). *The applicability of SWASH model for wave transformation and wave overtopping: A case study for the Flemish coast*. Faculty of Civil Engineering and Geosciences, Delft University of Technology.

The SWASH team (2010). *SWASH USER MANUAL: SWASH version 7.01*. Delft University of Technology. Faculty of Civil Engineering and Geosciences. Environmental Fluid Mechanics Section.

Tuan, T.Q. and Oumeraci, H. (2010). *A numerical model of wave overtopping on seadikes.* Coastal Engineering, 57: 757-772, 2010.

van den Bos, J. , Verhagen, H.J. , Zijlema, M. , and Mellink, B. (2014). *TOWARDS A PRACTICAL APPLICATION OF NUMERICAL MODELS TO PREDICT WAVE-STRUCTURE INTERACTION: AN INITIAL VALIDATION*. COASTAL STRUCTURES No 34 (2014) Published October 28, 2014: https://doi.org/10.9753/icce.v34.structures.50.

van den Bos, J.P. and Verhagen, H.J. (2018). *Breakwater design: Lecture notes CIE5308*. Department of Hydraulic Engineering Faculty of Civil Engineering and Geosciences.

Van der Meer, J.W. , Allsop, N.W.H. , Bruce, T. , De Rouck, J. , Kortenhaus, A. , Pullen, T. , and Schüttrump (2018). *Manual on wave overtopping of sea defences and related structures. An overtopping manual largely based on European research, but for worldwide application*. The EurOtop team.

van Gent, M. (1999). *Physical Model Investigations on Coastal Structures with Shallow Foreshores: 2D Model Tests with Single and double-Peaked Wave Energy Spectra.* Delft Hydraulics/Waterbouwkundig Laboratorium.

van Steeg, P. (2012). *Invloedsfactor voor ruwheid van een getrapt talud bij golfoverslag bij dijken Verslag: fysieke modeltesten en analyse*. Deltares, Opdrachtverlening Hoogheemraadschap Hollands Noorderkwartier.

van Steeg, Paul , Joosten, Ruud , and Steendam, Gosse Jan (2018). *Physical model tests to determine the roughness of stairshaped revetments*. 3th International Conference on Protection against Overtopping,UK.

Vasarmidis, Panagiotis , Stratigaki, Vasiliki , Suzuki, Tomohiro , Zijlema, Marcel , and Troch, Peter (2021). On the accuracy of internal wave generation method in a non-hydrostatic wave model to generate and absorb dispersive and directional waves. *Ocean Engineering*, 219:108303. ISSN 0029-8018. doi: https://doi.org/10.1016/j.oceaneng.2020.108303. URL https://www.sciencedirect.com/science/article/pii/S002980182031218X.

Veale, T. S. (2012). *INTEGRATED DESIGN OF COASTAL PROTECTION WORKS.* Santander, Spain: Proceedings of 33rd International Conference on Coastal Engineering, 2012.

Williams, H.E. , Briganti, R. , Romano, A. , and Dodd, N (2019). *Experimental analysis of wave overtopping: a new small scale laboratory dataset for the assessment of uncertainty for smooth sloped and vertical coastal structures*. J. Mar. Sci. Eng. 7, 217. https:// doi.org/10.3390/jmse7070217.

Witteveen+Bos, Schippers, M. , van Bemmelen, C , Jordans, L. , and van den Berg, B. (2021). *Casino Middelkerke: Ontwerprapportage Nota Zeewering*. CIRIL NV and Witteveen+Bos.

Zelt, J. A. and Skjelbreia, James Eric (1993). *ESTIMATING INCIDENT AND REFLECTED WAVE FIELDS USING AN ARBITRARY NUMBER OF WAVE GAUGES*.

Zijlema, M , Stelling, G. , and Smit, P. (2011). *SWASH: An operational public domain code for simulating wave fields and rapidly varied flows in coastal waters.* Coast. Eng. 58, 992–1012.

List of Figures

List of Tables

A
SWASH

A.1. Settings model

Swash is a program without interface and command files are used for the calculation. In this command fill the input parameters and boundary conditions must be written to be able to run start the calculation. With incorrect input parameters, SWASH will return an error file in which the wrong settings are given. The different basic input parameters are discussed in this chapter and a summary of the steps taken in postprocressing of the data is given. An example of such a command file is given in Appendix A.2.

A.1.1. Bottom profile and boundary conditions

The model runs are performed in one dimensional mode and a multi-layered mode, in which the computational domain was divided into 3 vertical layers. By increasing the vertical layers, the frequency dispersion relation is followed more accurately. According to the The SWASH team (2010), using 3 vertical layers, provides a good linear wave dispersion for primary waves up to a wave number (kd) of 16, with a relative error in the normalized wave celerity of 1%. Two bathymetry were used for this thesis to replicate the test conditions of the physical experiment in Ghent, see Figure A.1

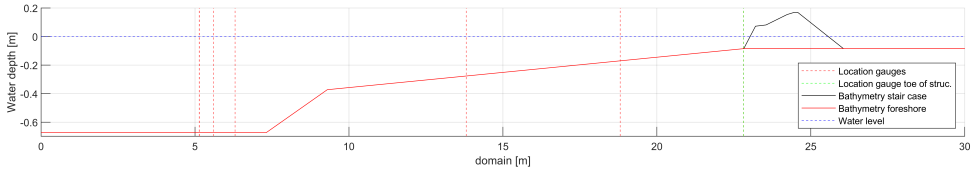

Figure A.1: Bathymetry used for the SWASH simulations

A sponge layer at the end of the domain, absorbs the wave energy and thus prevents wave reflection. The SWASH team (2010) mentions that a sponge layer length of 1-3 times the wave length is sufficient. In Figure A.1, on the left side, the wave input has been defined by means of a wave generator. For the wave conditions a JONSWAP spectrum has been selected with a peak enhancement factor of 3.3, same as for the Gent experiments. From the offshore boundary, a minimum flat bottom distance of approximately 2 wave lengths is advised for the area of interest, since the wave generation method can induce some numerical errors, this will be further explained in Section A.1.3.

Figure A.2 shows an example of a water surface elevation output signal from SWASH that could be used for the time domain analysis.

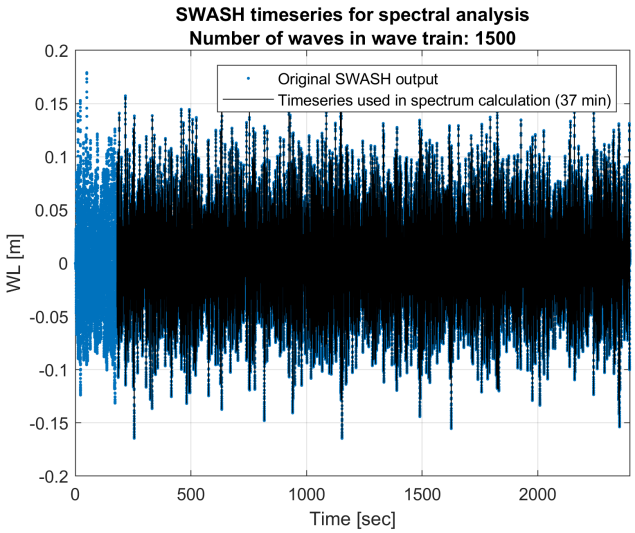

Figure A.2: Example of a time series from SWASH output file

A.1.2. Wave conditions and calibration

The target wave conditions were the wave conditions resulting from the physical experiments in Ghent. The wave generator at the boundary of the domain is different in a numerical model as for the physical experiments. The model has therefore been calibrated based on surface elevation gauges in the deep water section of the domain/flume. Based on a spectral analysis for both the physical experiments and the numerical model runs, the input parameters were calibrated. This has been done by means of trial and error. As can been seen in Figure A.3 as sudden drop can be seen, which is explained in Section A.1.3. The peak period was the same for SWASH compared to the Ghent experiments, therefore only the wave height had to be adjusted to get the right wave conditions in the deep water section of the domain. For both the significant wave height and the peak period, a deviation of 1% was easily achieved. The spectral wave period, showed larger differences, this is further explained in Chapter 4.1.3.

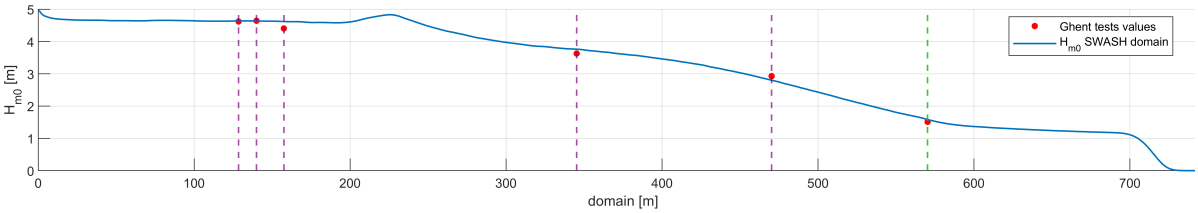

Figure A.3: Significant wave height over the domain from SWASH results, compared to physical experiments in Ghent

A.1.3. Boundary conditions

Input wave height

Although the boundary wave height can be simulated really well by SWASH, a sudden drop in wave height occurs in vicinity of the boundary. Waves are generated by the wave maker by imposing horizontal velocities for every layer according to linear wave theory. The drop at the boundary probably has to do with the fact that waves are not linear and that the assumed vertical orbital velocity profile is not entirely correct. Consequently, within one wave length from the boundary, wave height decreases up to 5%, while the water depth is constant. This error seemed to be very sensitive to changes in number of grid cells, grid size and number of layers. Dobrochinski (2014) encountered the same problem and his practical solution will be applied here as well. The drop has to be quantified after which a certain additional wave height needs be applied in following runs to account for the sudden drop.

Measurement overtopping discharge

The measured overtopping showed large differences depending on the grid cell that was used to asses the volumes. With 2 consecutive grid points, thus a very small horizontal distance, both the speed and layer thickness good vary a lot. Figure A.4 shows an example of two consecutive grid cells at the crest of the slope, which should therefore give similar results. Yet, the average overtopping discharge has a 35% difference. This is the uncertainty caused by the little number of waves that overtopped the crest of the structure.

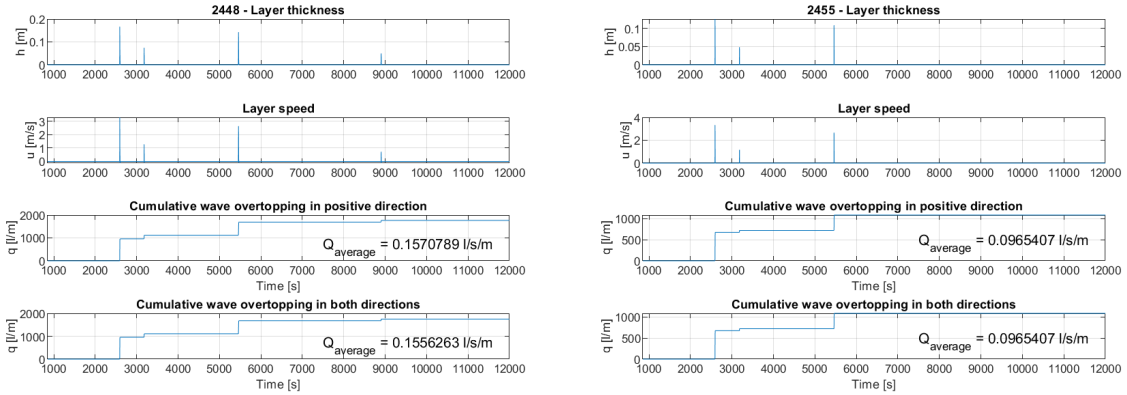

Figure A.4: Example of the difference in overtopping discharges for 2 consecutive grid point at the (flat) crest of the structure.

VERTICAL LAYERS

SWASH is a depth-averaged numerical model, but the domain can be divided in a number of layers over the vertical. The number of layers depends on the linear frequency dispersion relation. The layers needed can be calculated with the dimensionless depth kd, which is the wave number multiplied by the depth of the model. A higher value means more layers are needed over the vertical of the domain. For most simulations 2 or 3 layers are sufficient (Zijlema et al., 2011).
SWASH improves its frequency dispersion by increasing the number of layers. The value of kd usually highest and thus critical at offshore boundary in coastal models, due to the largest water depth. For this location kd should be small enough for the number of layers applied to correctly solve dispersion in the model (Zijlema et al., 2011).

The number of vertical layers showed large differences in both wave height along the domain and the wave spectrum. Figure A.5 shows the differences in predicted H_{m0} along the domain. Figure A.6a and Figure A.6 show the differences in the energy density spectrum due to a different number of vertical layers. The SWASH team (2010) advises to use 2 or 3 vertical layers. The deep water wave conditions showed very similar results, at the toe the wave spectra have a similar shape, but small differences can be seen as well.

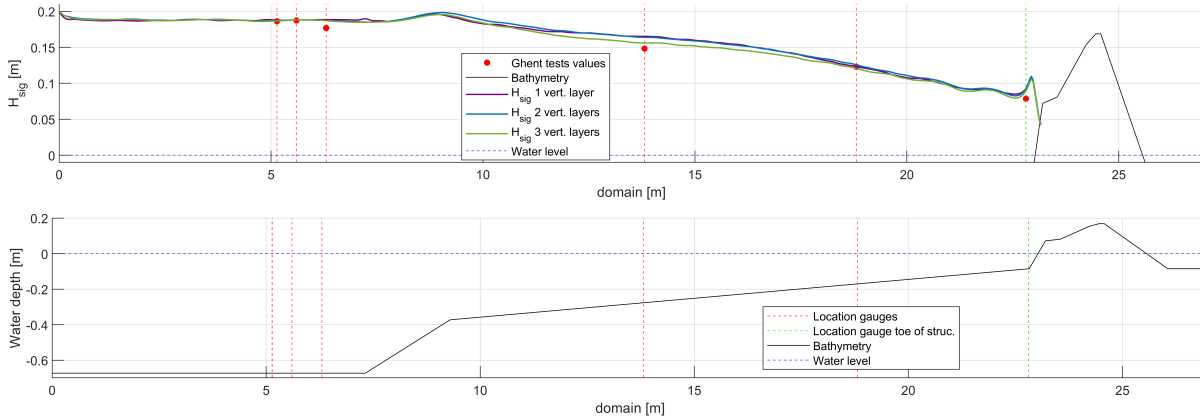

Figure A.5: H_{sig}=H_{m0} along the domain for a different number of vertical layers.

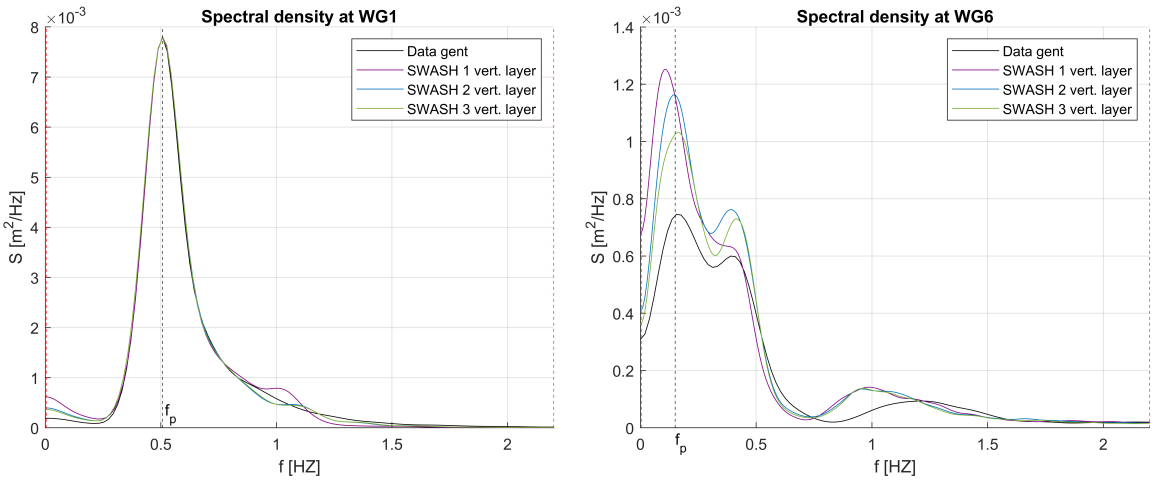

(a) WG5 (b) WG6

Figure A.6: Differences in energy density spectrum with the use of different vertical layers in SWASH

Number of grid cells

As explained in Section A.1.3, the SWASH manual (Zijlema et al., 2011) advices to use a minimum number grid cells per wave length in the model, but not necessarily a maximum. However, during the calibration, numerical 'wiggles' occurred when the number of grid cells per wave length was relatively high. Although the model was able to calculate the wave height in the domain still within tolerance limits, non-linearities increased and thus the wave spectrum at all locations showed more and more deviations. These inconsistencies increased when the structure was eventually implemented in later model runs.

See Figure A.5 and Figure A.7 for clear difference in numerical stability as is seen by 'wiggles'. In Figure A.7 the same exact input parameters are used for both model runs, but the number of grid cells was different.

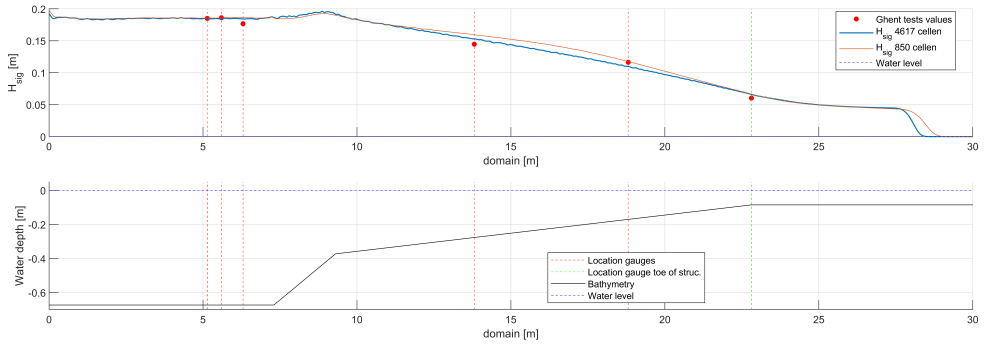

Figure A.7: Significant wave height over the domain from SWASH results for different number of grid cells

A.2. Input file SWASH

```
$*************MODEL INPUT***********************************
$
MODE NONST ONED
SET LEVEL 0.000
SET SEED 1
$SET BACKVISC 0.0001
$SET BACK MET DOET HIJ HET NIET
$
CGRID REGular 0.0 0 0 32.3850 0.000 850 0
$
VERT 3
$
INPGRID BOTTOM REGular 0.0 0 0 850 0 0.0381 0
READINP BOTTOM -1. '../data_punten/glad_talud_recht851.bot' 4 0 FREE
$
INPGRID FRICTION REGular 0.0 0 0 850 0 0.0381 0
READINP FRICTION 1. '../data_punten/roughfr851.dat' 4 0 FREE
$
INIT zero
$
BOU SHAP JON 3.3
BOU SIDE W BTYPE WEAK HYPER ADDBoundwave CON SPECT 0.191 2
BOU SIDE E CCW BTYPE RADIATION
SPON RI 5
$
FRIC LOGlaw ROUGH
VISC Vertical KEPS
VISC HOR CON
Break
$
NONHYDROSTATIC BOX
DISCRET UPW MOM
TIMEI 0.1 0.5
$
$************* OUTPUT ***************************************
$
POINTS 'GAUGE' FILE '../data_punten/wg_gent.wvg'
TABLE 'GAUGE' NOHEAD '2b_302_v2_1D.tbl' XP YP DIST TSEC DEPTH BOTLEV WATLEV SETUP HSIG OUTPUT 000000.000 0.025
SEC

POINTS 'LAYER' FILE '../data_punten/speed_gaug.lay'
TABLE 'LAYER' NOHEAD '2b_302_v2_OV.ltn' TSEC DIST BOTLEV WATLEV OUTPUT 000000.000 0.025 SEC
TABLE 'LAYER' NOHEAD '2b_302_v2_OV.lsp' TSEC DIST BOTLEV VEL OUTPUT 000000.000 0.025 SEC

BLOCK 'COMPGRID' NOHEAD '2b_302_v2_1D.mat' XP YP BOTLEV SETUP HSIG

$ wave parameters below are an indication, they have to be calculated based on .tbl
QUANT HSIG dur 40 min
QUANT SETUP dur 40 min
$
TEST 1 0
COMPUTE 000000.000 0.00010 SEC 002000.000
STOP
```

Figure A.8: SWASH input file example

B
Results SWASH

In this chapter all the results are given. For each of the SWASH model runs the significant wave height (H_s) over the spatial domain, the wave height exceedance at certain locations ($H_{2\%}$) and the energy density spectrum is plotted for both the deep water section and at the toe of the structure.

B.1. Cross-section 2b

B.1.1. Incident wave conditions

Model run	Unit	1	2	3	4	5	6	7
H_{m0}	[m]	4.63	4.59	4.65	4.61	4.64	4.63	4.62
$T_{m-1,0}$	[s]	9.836	9.741	9.728	9.862	9.717	9.735	9.704
$H_{2\%}$	[m]	6.075	6.100	6.150	6.225	5.900	6.075	5.950
H_{max}	[m]	8.175	8.475	8.650	7.450	7.725	8.000	8.275
q_{SWASH}	[l/s/m]	0.1571	0.0119	0.0158	0.1591	0.0394	0.0535	0.1318

Table B.1: Average overtopping volumes for different seed numbers in SWASH relative to wave conditions at deep water (WG1). Bathymetry without structure

Model run	Unit	1	2	3	4	5	6	7
H_{m0}	[m]	1.55	1.53	1.51	1.54	1.51	1.52	1.53
$T_{m-1,0}$	[s]	16.48	15.37	15.24	16.25	15.34	15.17	15.58
$H_{2\%}$	[m]	1.900	1.850	1.875	1.900	1.850	1.875	1.900
H_{max}	[m]	2.400	2.125	2.400	2.200	2.200	2.225	2.375
q_{SWASH}	[l/s/m]	0.1571	0.0119	0.0158	0.1591	0.0394	0.0535	0.1318

Table B.2: Average overtopping volumes for different seed numbers in SWASH relative to wave conditions at the toe of the structure (WG6). Bathymetry without structure

Influence seed number on spectrum
Different model runs with different seed numbers were modelled to analyse the large differences in wave overtopping at the crest of structure. It turned out that the seed numbers could lead to major differences in wave conditions at the toe of the structure, see Section 5.3.1. Figure B.1 shows the difference in wave spectrum for the model runs with same boundary conditions, but different seed numbers.

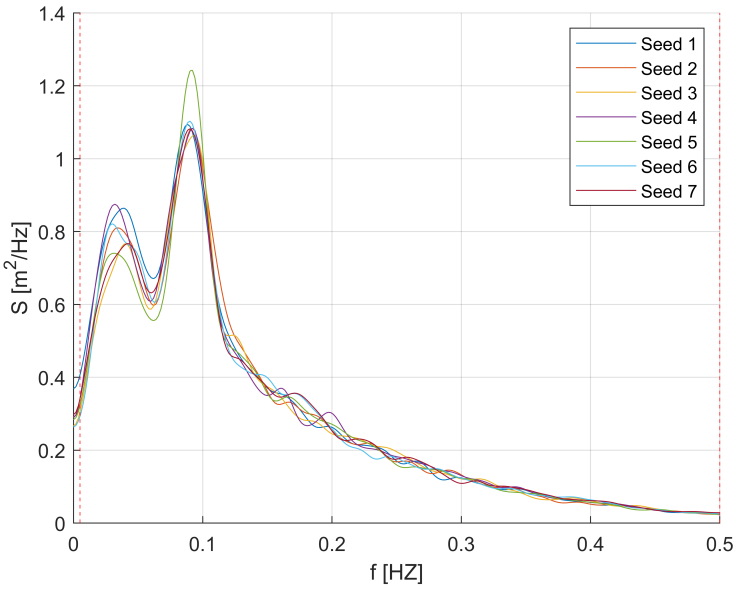

Figure B.1: This figure shows the difference of a different seed number on the wave spectrum, all other boundary conditions are kept the same

B.1.2. Wave analysis with structure

Model run	Unit	1	2	3	4	5	6	7
H_{m0}	[m]	4.64	4.63	4.69	4.65	4.68	4.67	4.68
$T_{m-1,0}$	[s]	10.275	10.096	10.059	10.268	10.006	10.082	10.012
$H_{2\%}$	[m]	6.050	6.075	6.275	6.275	5.950	6.100	5.993
H_{max}	[m]	8.30	8.600	8.575	8.100	8.125	8.125	8.490
q_{SWASH}	[l/s/m]	0.1571	0.0119	0.0158	0.1591	0.0394	0.0535	0.0821

Table B.3: Average overtopping volumes for different seed numbers in SWASH relative to wave conditions at deep water (WG1). Bathymetry with structure

Model run	Unit	1	2	3	4	5	6	7
H_{m0}	[m]	2.24	2.18	2.13	2.22	2.15	2.16	2.18
$T_{m-1,0}$	[s]	25.45	24.60	24.32	25.73	24.10	24.09	24.81
$H_{2\%}$	[m]	2.70	2.63	2.60	2.68	2.58	2.45	2.60
H_{max}	[m]	3.40	3.225	3.600	3.200	3.300	3.250	3.398
q_{SWASH}	[l/s/m]	0.1571	0.0119	0.0158	0.1591	0.0394	0.0535	0.0825

Table B.4: Average overtopping volumes for different seed numbers in SWASH relative to wave conditions at the toe of the structure (WG6). Bathymetry with structure

Wave Height	Unit	1	2	3	4	5	6	7	8
H_{Ghent}	[m]	2.72	2.79	2.89	2.97	3.03	3.08	3.12	3.25
H_{SWASH}	[m]	2.91	2.92	2.95	2.97	3.03	3.15	3.21	3.32

Table B.5: Ten largest waves measured during the physical experiments and SWASH simulations

Energy density spectrum in domain

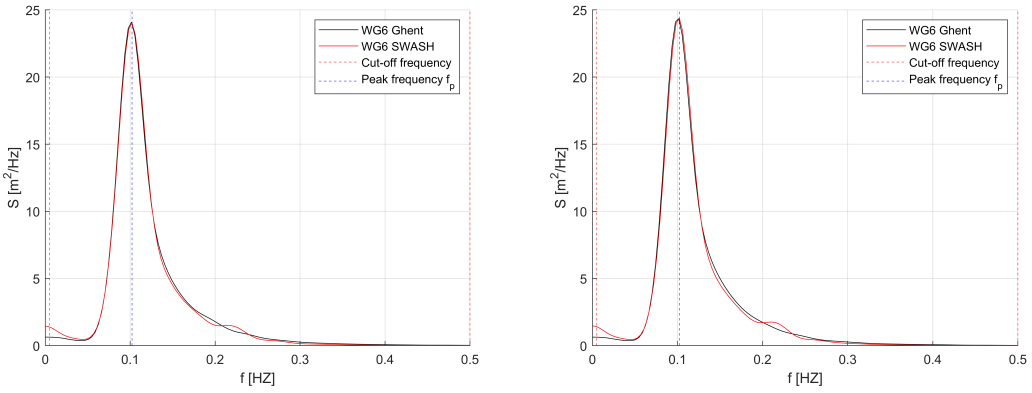

(a) WG1 (b) WG2

Figure B.2: Wave spectra in the domain from SWASH simulations for different surface elevation gauges compared to physcial experiments in Ghent. Again cut-off frequency same as Ghent.

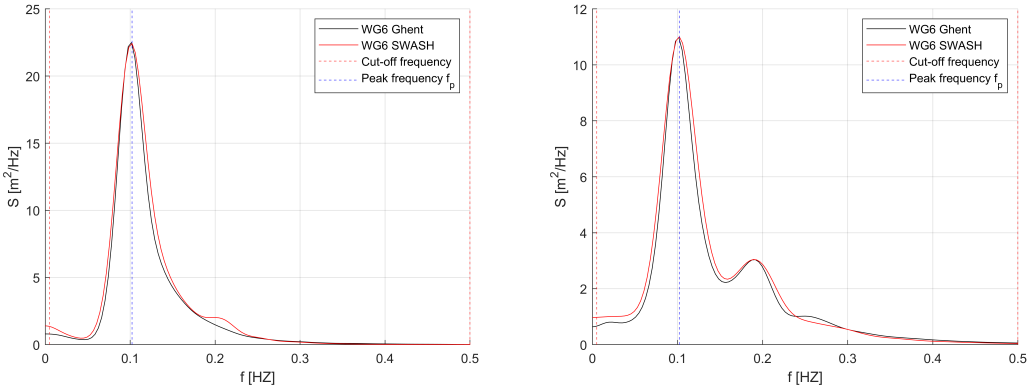

(a) WG3 (b) WG4

Figure B.3: Wave spectra in the domain from SWASH simulations for different surface elevation gauges compared to physcial experiments in Ghent. Again cut-off frequency same as Ghent.

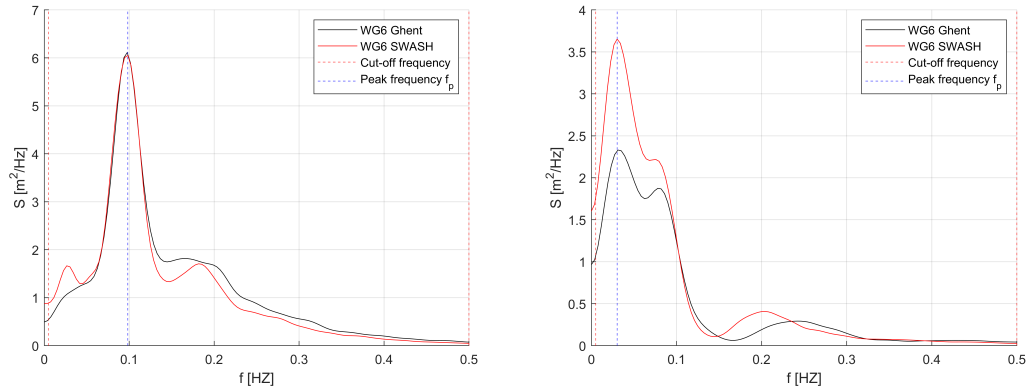

(a) WG5 (b) WG6

Figure B.4: Wave spectra in the domain from SWASH simulations for different surface elevation gauges compared to physcial experiments in Ghent. Again cut-off frequency same as Ghent.

Influence horizontal viscosity setting SWASH

	Ghent	SWASH horizontal viscosity off	SWASH constant horizontal viscosity
H_{m0}	1.97	2.24	2.17
Difference [%]	-	13	9.7
$T_{m-1,0}$	21.27	24.45	27.1
Difference [%]	-	14	24

Table B.6: SWASH horizontal viscosity setting sensitivity on wave conditions at toe of the structure (WG6) compared to the physical experiment in Ghent.

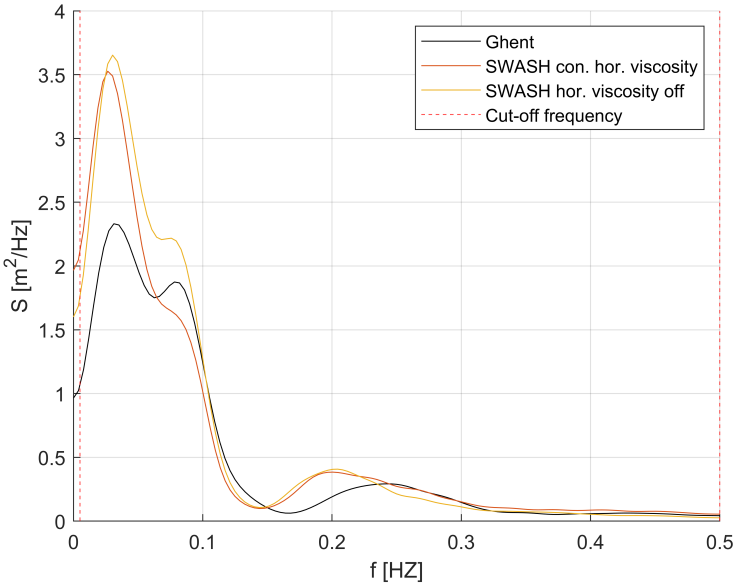

Figure B.5: This figure shows the difference of the viscosity setting in SWASH, using the default setting in SWASH, a constant horizontal viscosity and turning the horizontal viscosity setting off.

Reflection

The method used in this these to separate the incident and reflective wave height is based on linear wave theory. Zelt and Skjelbreia (1993) presented a method to decompose one dimensional wave fields into left and right-travelling components using an arbitrary number of wave gauges. Since the waves near the toe of the structure are affected by breaking and thus non-linearity's, the wave conditions in deep water are used to asses the reflection coefficient of the structure. The reflection coefficient K_r is calculated with the following formula:

$$K_r = \frac{\sqrt{m_{0r}}}{\sqrt{m_{0i}}} = \frac{H_r}{H_i} \tag{B.1}$$

An example of a decomposed wave signal from the surface elevation measurement in SWASH is given in figure B.6

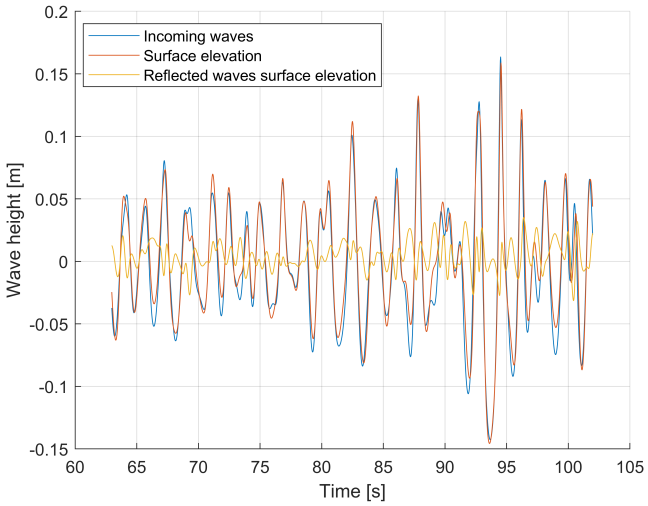

Figure B.6: Wave reflection along the domain, zoomed in.

C
EurOtop calculations

The average wave overtopping discharge at the crest of the structure is determined with Equation C.1, according to the EurOtop Manual (2018).

$$\frac{q}{\sqrt{gH_{m0}^3}} = 10^{-0.79} \exp\left(-\frac{R_c}{H_{m0}\gamma_f\gamma_\beta\gamma_b\left(0.33 + 0.022\xi_{\mathrm{m-1,0}}\right)}\right) \tag{C.1}$$

C.1. Equivalent slope calculation

If the slope of the structure consists of a varying slope angle/berm, a characteristic slope is required to be used in the breaker parameter $\xi_{m-1,0}$ to determine wave run-up or wave overtopping (The EurOtop Manual, 2018). Theoretically, the run-up process is affected by the change in slope angle from the breaking point to the maximum wave run-up height. Therefore, the EurOtop Manual (2018) proposes to determine the characteristic slope from the point of wave breaking to the maximum wave run-up height. It is an iterative solution because the wave run-up height Ru2% is unknown. For the breaking limit a point on the slope must be set which is 1.5 times the significant wave height H_{m0} below the still water line. Also a point on the slope 1.5 times H_{m0} above water as a first estimate to calculate the characteristic slope and to exclude the berm.
Thereafter, the wave run-up height from the first estimate is used to determine the average slope angle. The $R_{2\%}$, wave run-up level measured vertically from the still water line, which is exceeded by 2% of the number of incident waves (The EurOtop Manual, 2018). During the calculation for this case study, this $R_{2\%}$ was calculated higher than the height of the crest of the structure. Therefore, the maximum $R_{2\%}$ is set at the height of the crest. Figure C.3 shows an overview of the parameters.

First estimate:

$$\tan\alpha = \frac{3 \cdot H_{m0}}{L_{\mathrm{Slope}} - B} \tag{C.2}$$

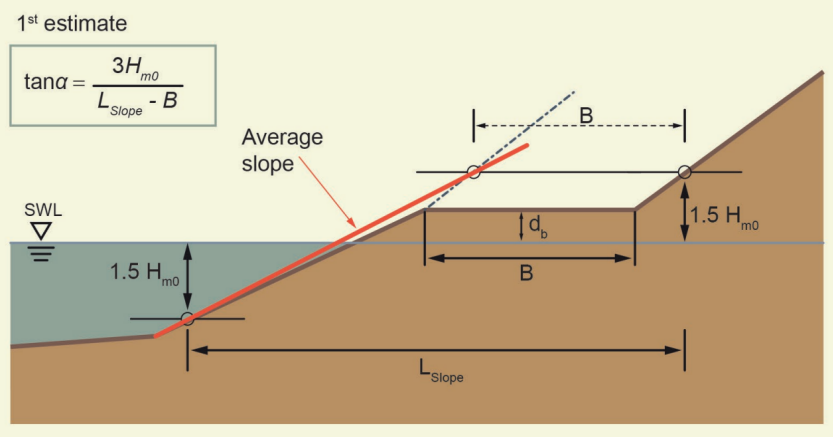

Figure C.1: Determination of the average slope (1st estimate), EurOtop Manual (2018)

Second estimate:

$$\tan\alpha = \frac{\left(1.5 \cdot H_{m0} + R_{u2\%(\text{ from 1st estimate })}\right)}{L_{\mathrm{Slope}} - B} \tag{C.3}$$

For a shallow foreshore, part of the slope of the foreshore may be included in the slope of the seawall (The EurOtop Manual, 2018). This only applies if the water depth on the toe is less than the significant

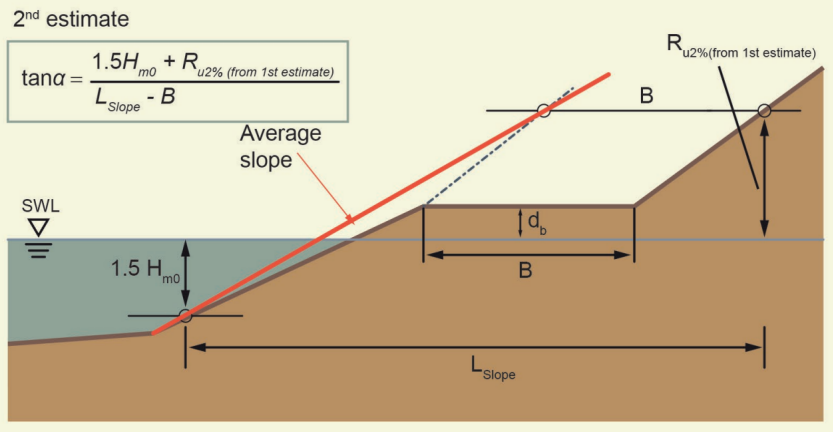

Figure C.2: Determination of the average slope (2nd estimate), EurOtop Manual (2018)

wave height in deep water, which also influences the Irribaren parameter. The representative slope can be calculated according to Equation C.4. The slope angle $\alpha_{seadefense}$ has been determined with Equation C.3

$$\tan\left(\alpha_{representative}\right) = \frac{\left(1.5H_{m0} + R_{u2\%}\right)}{(1.5H_{m0} - h) * \cot\left(\alpha_{foreshore}\right) + (h + R_{u2\%}) * \cot\left(\alpha_{seadefense}\right)} \tag{C.4}$$

With Equation C.4 an the adjusted breaker parameter $\xi_{m-1,0}$ is calculated, which is used in Equation C.1 to determine the average wave overtopping at the crest of the structure.
In Table C.1 an overview is given for the input parameters used to calculate the average wave overtopping with formula C.1 according to the EurOtop Manual (2018). The calculation of the berm influence factor is described below.

H_{m0} [m]	$T_{m-1,0}$ [s]	$\xi_{m-1,0}$ [-]	ξ_{adjust} [-]	R_c [m]	γ_f [-]	γ_β [-]	γ_b [-]
1.51	16.68	8.48	3.26	4.25	0.75-0.9	1	0.86

Table C.1: Overview important input parameters for EurOtop Manual (2018) calculations, full calculation can be found in Appendix C.

C.2. Berm influence factor

The berm influence factor can be determined with Equation C.6. Figure C.3 shows the schematization of the parameters used to calculate the berm factor. Table C.2 gives an overview of the important parameters.
To calculate the influence factor γ_b, the following formula is used in the EurOtop Manual (2018).

$$\gamma_b = 1 - r_B(1 - r_{db}) \quad for: 0.6 \leq \gamma_b \leq 1.0 \tag{C.5}$$

For this situation with a berm above the SWL:

$$r_{db} = 0.5 - 0.5 * \cos(\pi \frac{d_b}{R_{u2\%}}) \tag{C.6}$$

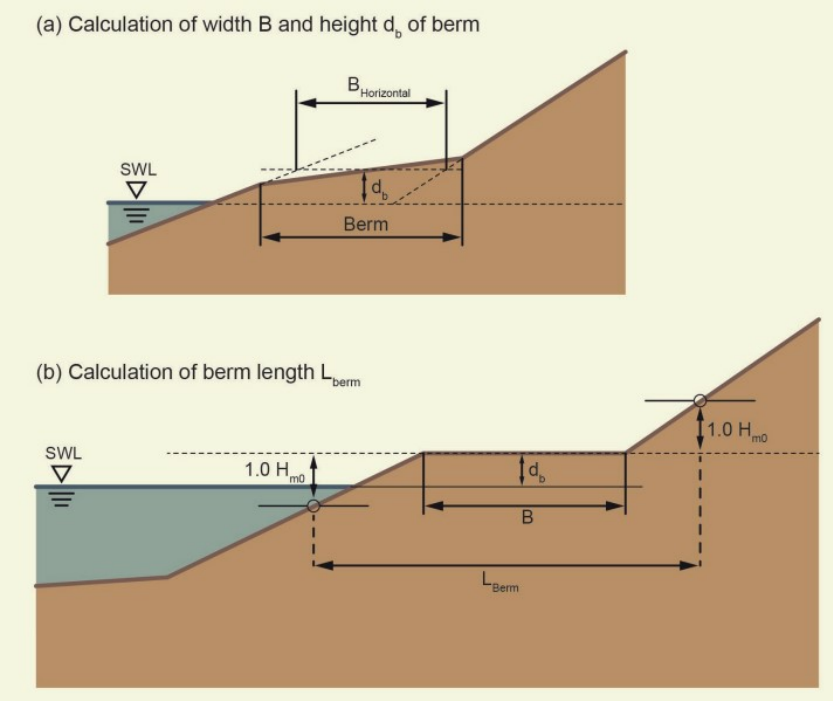

Figure C.3: Calculation of the effective horizontal berm and characteristic berm length L_{berm}, EurOtop Manual (2018)

H_{m0}	d_b [-]	Berm [m]	$B_{horizontal}$ [m]	L_{slope} [m]
1.51	1.95	8.9	5.57	35.25

Table C.2: Overview important input parameters for EurOtop Manual (2018) calculations, prototype dimensions

Filling in the equations above, the berm influence factor γ_b for this case study is calculated to be:

$$\gamma_b = 0.86 \text{ [-]}$$

C.3. Stair case influence factor determination

The first to relate to structural properties of a coastal sea defence structure were van Steeg et al. (2018). They developed an empirical relation for the preliminary design fase, since they discovered a wide spreading of overtopping rates. The fit through the data as given in Figure C.4 is described by Eq. C.7

$$\gamma_f = -0.170 \cdot \ln\left(\frac{-\cos\alpha \cdot h_{\text{stair}}}{H_{m0}} \cdot \ln\left(\frac{q}{\sqrt{g \cdot H_{m0}^3}}\right)\right) + 0.650 \tag{C.7}$$

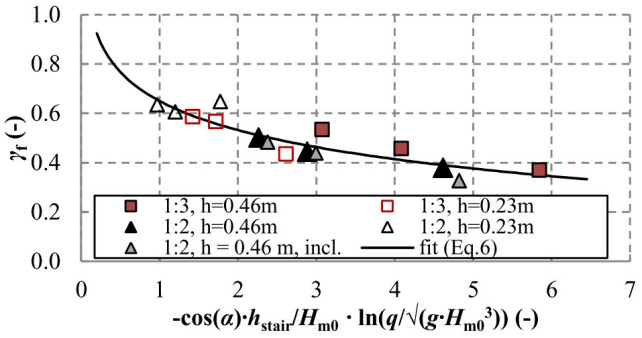

Figure C.4: Influence factor for roughness γ_f as function of dimensionless parameter (van Steeg et al., 2018)

From this study it was concluded that: The roughness influence factor isn't a fixed value, but depends on other multiple parameters such as the local wave height, overtopping volumes and the dimensionless step height" (van Steeg et al., 2018)

Kerpen et al. (2019) wrote the first systematic comparison of the influence of stepped revetments to reduce wave overtopping. The objective was to derive a reduction coefficient for the roughness of a stepped revetment, considering a wider range of of hydraulic- and structure related parameters. For example, breaking and non-breaking wave conditions, slope gradients and step heights much smaller and much larger than the spectral significant wave height (Kerpen et al., 2019).

$$\gamma_f = 1.55 - 0.55\,\text{atan}\left[12\left(\frac{k_h}{H_{m0}} + 0.07\right)^{1.4}\right] + 0.35 \times \text{atan}\left[0.6\left(\frac{k_h}{H_{m0}} - 3.5\right)\right] \tag{C.8}$$

The function describes the relation between the reduction coefficient for roughness of a stepped revetment and the corresponding step ratio with a goodness of fit of R^2 = 0.82, a root mean square error of RMSE = 0.059 and a standard deviation σ = 0.022 (Kerpen et al., 2019).

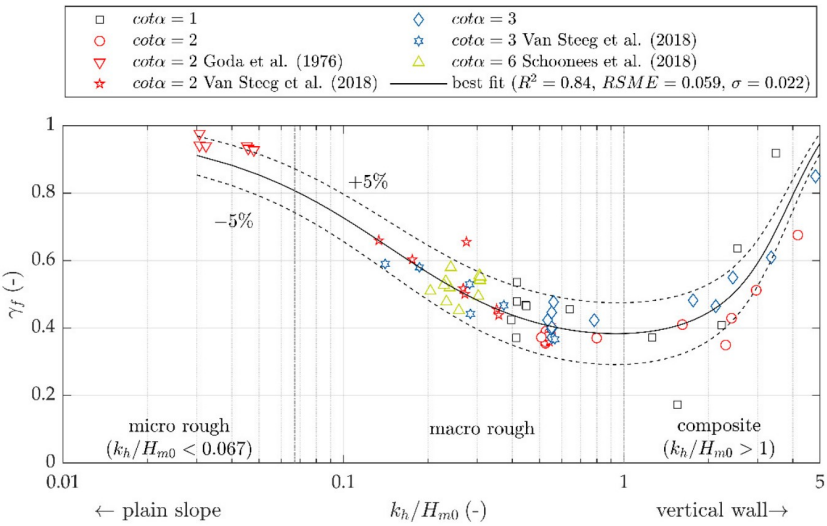

Figure C.5: Roughness reduction factor γ_y vs. the step ratio (kh/Hm0) for varying slopes (1 ≤ cotα ≤ 6) including a best fit regression line and the 90% confidence band. (Kerpen et al., 2019)

Schoonees et al. (2021) continued with full-scale experiments and analysed individual overtopping events. The following formula was proposed, which is also displayed in Figure C.6

$$\gamma_f = 1 - 0.55 \cdot \tanh\left[-31.07 \cdot \ln\left(q_{\gamma_f=1}/\sqrt{g \cdot H_{m0}^3}\right) \cdot \cos\alpha \cdot S_h/L_{m-1,0}\right] \quad \text{(C.9)}$$

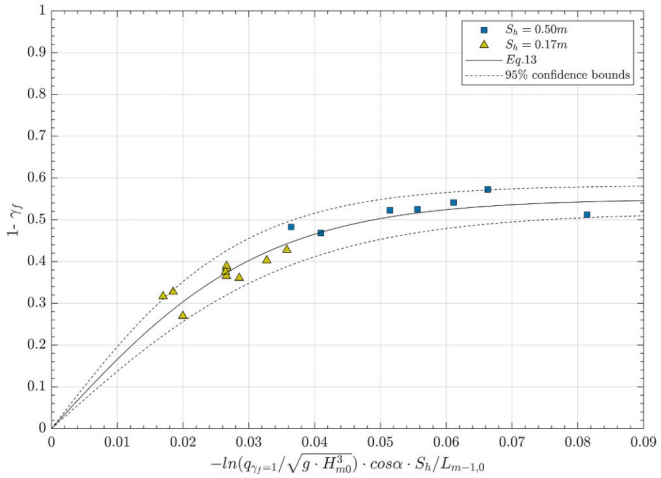

Figure C.6: Empirical formula for estimating the roughness factor of stepped revetments. (Schoonees et al., 2021)

Schoonees et al. (2021) also concluded that the roughness factor is not constant value, but it a function of the hydraulic conditions in front of the structure and the geometry of stepped revetment. The influence of the wave period, wave height and wave steepness is displayed in Figure C.7. Also, the influence of the dimensionless step height, relative overtopping rate and ratio of characteristic step height to wavelength on the slope roughness are displayed from (Schoonees et al., 2021). These are extensively discussed in Section 2.3.2.

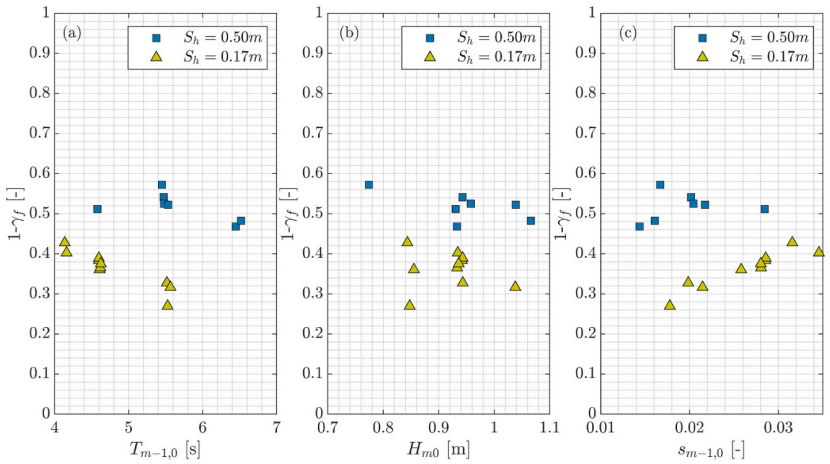

Figure C.7: The influence of (a) wave period, (b) wave height and (c) wave steepness on the slope roughness (Schoonees et al., 2021)

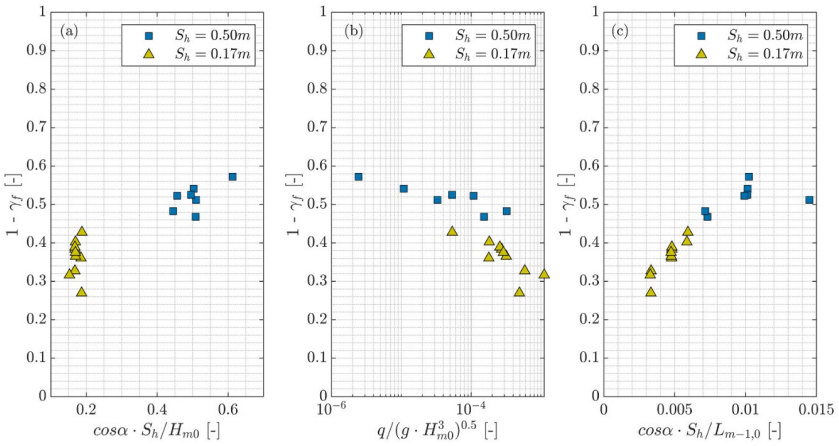

Figure C.8: The influence of (a) dimensionless step height, (b) relative overtopping rate and (c) ratio of characteristic step height to wavelength on the slope roughness(Schoonees et al., 2021)

D
Matlab Scripts

This gives an overview with the Matlab script that are used to process the data for this thesis.

Script	Function of script	Author
Load_Table	Load data from SWASH in Matlab	A. Kaji, Witteveen+Bos
SpectralAnalysis	Perform spectral analysis with surface elevations	A. Kaji, Witteveen+Bos
CalculateOvertoppingSwash_v3	Calculate overtopping discharges at point of interest	A. Kaji
postprocessing_overslag_SWASH	Postprocess overtopping discharges	SCHM28, Witteveen+Bos

E
Ghent data

E.1. Geometry

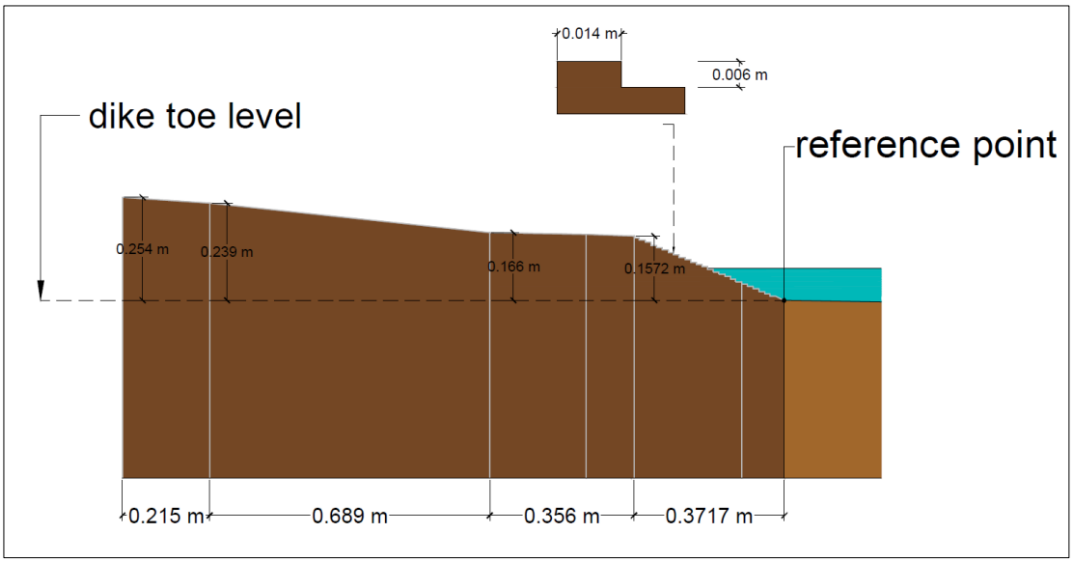

Figure E.1: Scale model of the coastal sea defence for cross section 2b (model dimensions).

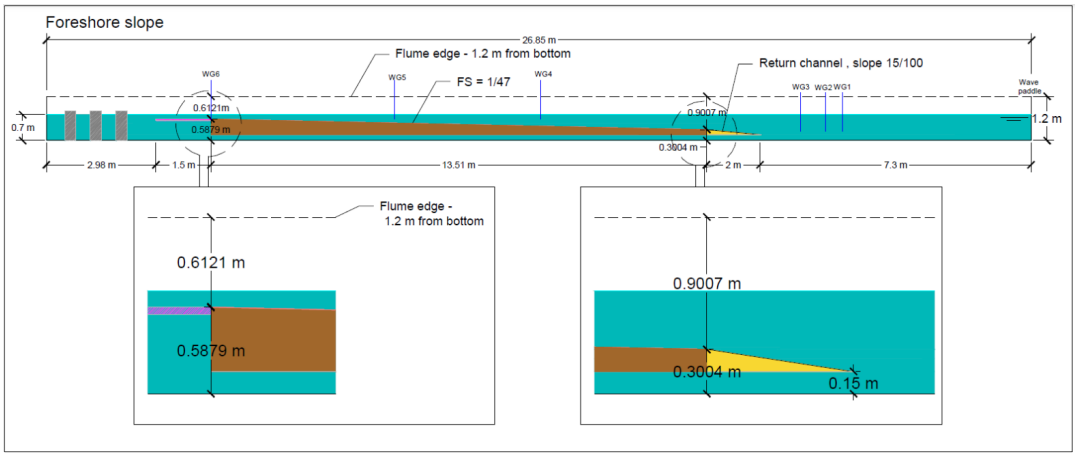

Figure E.2: Technical drawing of the model set-up for the wave calibration setup.

E.2. Wave conditions

The objective of the wave calibration tests is to achieve the target wave conditions within the predefined acceptable tolerances (+/- 3% for H_{m0}, +/- 5% for $T_{m-1,0}$, model dimensions) at the toe of the dike in the scale model. Therefore, the boundary conditions are different to obtain the same wave conditions at the toe of the structure. it was not possible to achieve the target tolerances for both parameters (H_{m0} and T_p). Thus, an alternative calibration approach, as approved by Flanders Hydraulics (Dieter Vanneste), is used . A new variable, Δq, defined as the discharge percentage difference between the target and measured wave conditions (at the toe), is introduced. The overtopping discharges for both the target and measured wave conditions are calculated using the EurOtop formulae, presented in Section 2.2. On this basis, the updated acceptance criterion for the calibration tests of cross-section 2b is a Δq tolerance of ±10 %

	Wave conditions Offshore				Wave conditions toe				Tolerance			
Test ID	Seed	$H_{m0,o}$ (m)	T_p (s)	Water level (m)	$H_{m0,t}$ (m)	$T_{m-1,0,t}$	h_{total} (m)	$q(m^3/s/m)$	$\Delta H_{m0,t}$ (±3%)	$\Delta T_{m-1,0,t}$ (±5%)	Δ h (±2 mm)	Δ q (±10%)
					Target = 0.064 m	Target= 3.028 s	Target = 0.084 m	Target = 1.552E-05				
CS2b-CAL10	100	0.180	2.000	0.673	0.061	3.238	0.0899	1.682E-05	-4.016%	6.935%	0.006	8.4
CS2b-CAL16	788169	0.180	2.000	0.673	0.060	3.333	0.0895	1.422E-05	-6.500%	10.073%	0.006	-8.4
CS2b-CAL19	48754	0.200	2.000	0.673	0.060	3.339	0.0905	1.593E-05	-5.672%	10.271%	0.007	2.6
CS2b-CAL20	9658	0.180	2.000	0.673	0.060	3.289	0.0898	1.442E-05	-6.406%	8.620%	0.006	-7.1
CS2b-CAL23	87333	0.200	2.000	0.673	0.060	3.347	0.0905	1.475E-05	-6.859%	10.535%	0.007	-5.0
CS2b-CAL27	683325	0.190	2.000	0.673	0.060	3.286	0.0903	1.451E-05	-6.734%	8.520%	0.006	-6.6
CS2b-CAL28	189	0.180	2.000	0.673	0.060	3.301	0.0897	1.477E-05	-6.000%	9.016%	0.006	-4.8
CS2b-CAL29	14569	0.190	2.000	0.673	0.060	3.381	0.0903	1.597E-05	-5.594%	11.658%	0.006	2.9

Figure E.3: Calibration tests cross section 2b.

E.3. Overtopping discharges

Test ID	Seed	Total Volume in reservoir (l)	q ($m^3/s/m$) scaled	q (l/s/m) prototype
CS2b-O1	100	0.165	3.90571E-07	**0.0488**
CS2b-O2	788169	0.075	1.77530E-07	**0.0222**
CS2b-O3	48754	0.145	3.43237E-07	**0.0429**
CS2b-O4	9658	0.340	8.04781E-07	**0.1006**
CS2b-O5	87333	0.150	3.55069E-07	**0.0444**
CS2b-O6	683325	0.265	6.27304E-07	**0.0784**
CS2b-O7	189	0.020	4.73419E-08	**0.0059**
CS2b-O8	14569	0.075	1.77543E-07	**0.0222**
CS2b-O9	100 (Overload)	0.275	6.50959E-07	**0.0814**

Figure E.4: Measured overtopping discharge for cross-section 2b.